Hindawi
Journal of Nanotechnology
Volume 2022, Article ID 2187932, 51 pages
https://doi.org/10.1155/2022/2187932

Review Article

A Perspective Review on Thermal Conductivity of Hybrid Nanofluids and Their Application in Automobile Radiator Cooling

Wisdom Etabiese Ukueje,[1] **Fidelis Ibiang Abam**,[2] **and Anthony Obi**[1]

[1]*Department of Mechanical Engineering, Energy, Exergy, and Environment Research Group (EEERG), Michael Okpara University of Agriculture, Umudike, P.M.B. 7267, Umuahia, Nigeria*
[2]*Africa Centre of Excellence for Sustainable Power and Energy Development, University of Nigeria, Nsukka, Nigeria*

Correspondence should be addressed to Fidelis Ibiang Abam; abamfidelis@mouau.edu.ng

Received 14 October 2021; Accepted 11 April 2022; Published 30 May 2022

Academic Editor: Marco Rossi

Hybrid nanofluids developed with the fusion or suspension of two or more different nanoparticles in a mixture as a novel heat transfer fluid are currently of interest to researchers due to their proven better measured thermal conductivities. Several reviewed articles exist on the thermal conductivity of hybrid nanofluids, a vital property for which the heat transfer rate is directly dependent. This review aims to understand the current developments in hybrid nanofluids and their applications. An extensive literature survey was carried out of heuristic-based articles published in the last 15 years. The review reiterates topical research on the preparation methods and ways to improve the stability of readied fluid, thermophysical properties of mixture nanofluids, and some empirical correlations developed for estimating thermal conductivity. Hybrid nanofluid studies on heat transfer performance in automobile radiator cooling systems were also obtained and discussed. The review's significant findings include the following: (1) hybrid nanofluids produce a noticeable thermal conductivity enhancement and a relatively higher heat transfer coefficient than mono nanofluids and regular liquids. Furthermore, through the uniform dispersion and stable suspension of nanoparticles in the host liquids, the maximum possible thermal augmentation can be obtained at the lowest possible concentrations (by <0.1% by volume). (2) An automobile radiator's overall heat transfer accomplishment can thus be boosted by using a mixture of nanofluids as conventional coolants. Up-to-date literature results on the thermal conductivity enhancement of mixture fluids are also presented in this study. Nonetheless, some of the barriers and challenges acknowledged in this work must be addressed for its complete deployment in modern applications.

1. Introduction

In a lecture titled, "There's Plenty of Room at the Bottom" at the California Institute of Technology (Caltech) in 1959, Richard Feynman advocated that man would soon possess the ability to transform matter at the atomic scale. To illustrate miniaturization's technological potential, he cited the example of storing all 24 volumes of the Encyclopædia Britannica on the head of a pin. This talk, many years later, inspired the conceptual foundations of nanotechnology. But the word "nanotechnology" was first used in 1974 by the Japanese scientist Norio Tanigushi [1] of the Tokyo University of Science when discussing nanotechnology and the possibility of manufacturing materials at the nanometric scale (i.e., one-billionth or 10^{-9} of a meter or about the size of a molecule, Figure 1). Thus, Tanigushi gave a name to the infinitesimally small technologies that would soon experience rapid development in the industry [1]. This discovery has sparked further research and diverse applications in every human endeavour, including engineering.

In thermal systems, liquid materials such as water, organic liquids, and oil have naturally been employed as heat transfer fluids. However, these fluids' performance is usually limited due to the smaller available surface-to-volume ratio for heat transfer to occur. Therefore, research has sought a way to improve the thermal performance of these materials. Nanoparticles in the range of 1–100 nm have been used to manipulate liquids to create nanofluids with improved

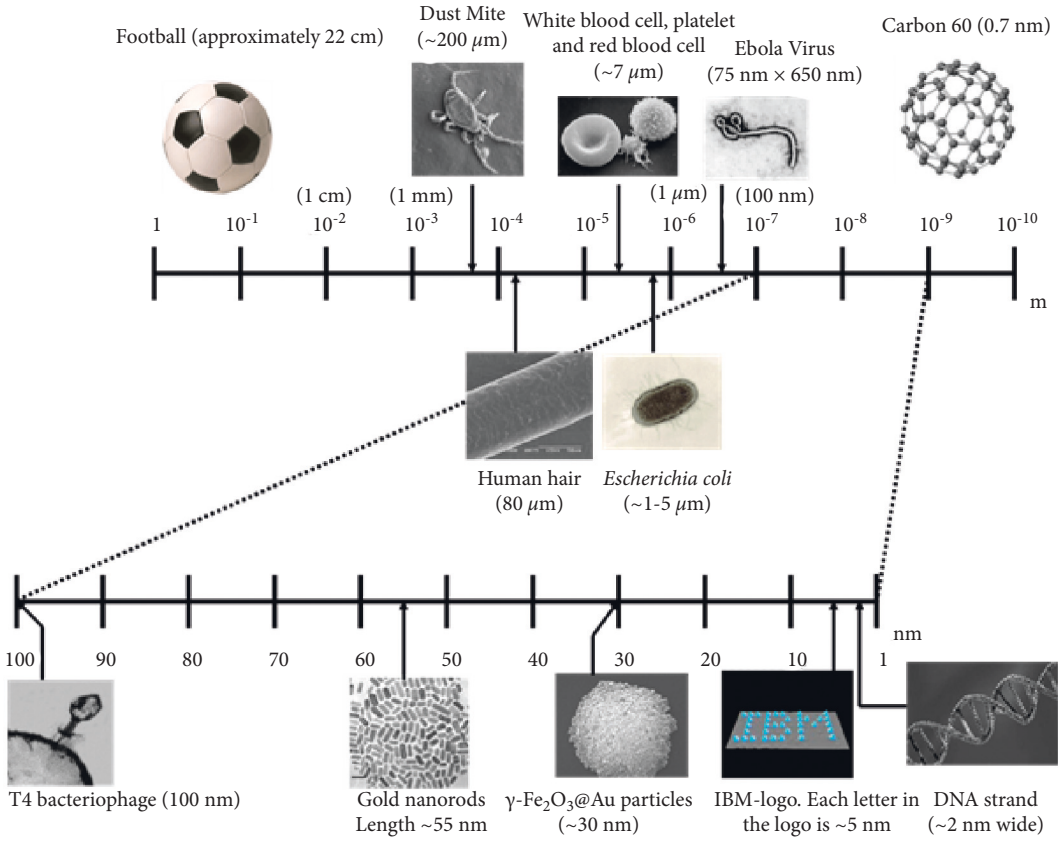

FIGURE 1: Picture showing the nanoscale in context. The length scale at the top ranges from 1 m to 10^{-10} m. The section from 10^{-7} m (100 nm) to 10^{-9} m (1 nm) is expanded on the length scale beneath. The typical length scale of interest for nanoscience is from 100 nm down to the atomic scale.

quantum mechanical effects. This delivers an incredible velocity for heat transfer to occur at an elevated temperature [2]. However, nanofluids can be a nanomaterial mixture (Figure 2), commonly suspended in a building base liquid to form a hybrid nanofluid.

Again, liquid suspended by ultrafine unit nanometer-sized metallic or nonmetallic solid particles (Figure 3) is also referred to as nanofluids, a term instituted by Choi and Eastman in 1995 [3]. Hence, solid nanoparticles with high thermal conductivity have been used as additives to create hybrid nanofluids [4]. Another fascinating concept of interest is "Nanofluidics," the study of fluid motion through small structures, an idea that involves the investigation of the behavior, scheming, and control of liquids that are restricted to nanometer-sized structures. It is the science, innovation, and appliance of transport phenomena and liquid streams in channels. In contrast, nanofluids are a class of fluid containing nanoparticles. Moreover, nanofluidics and nanofluids can present unique physical behaviors not seen in microfluidics and microfluids (such as acoustic properties, higher thermal conductivity, increased viscosity, and distinct rheological). These features have made them potentially valuable in diverse applications.

The nanofluids' fractions for achieving experimental results vary from a virtually vanishing value of 0.0001–10%. Researchers use graphene as a typical example of solid nanoparticles, which shows thermal conductivity in an array of 2000–5000 W/m K [5] or more. Although metals are initially thought to have high thermal conductivities ranging from 10 to 100 W/m K [6], these values are less than the thermal conductivity of carbon nanotubes, which ranges from 1800 to 4000 W/m K [6, 7] (Figure 4). Materials like these tend to reinforce the positive aspects of one another. This new class of working fluids with enhanced thermophysical properties contains two or more distinct solid particles in a base fluid (water, ethylene glycol (EG), water and ethylene glycol (EG) mixture [8], water, ethylene glycol (EG), oil, and acetone [9]), which provided researchers with another breakthrough in the quest for enhanced energized transmitting fluid.

Turcu et al. [10] were the pioneering investigators in the study of hybrid particulate blends of nanocomposites, particularly multiwalled carbon nanotubes (MWCNTs) on Fe_2O_3 magnet nanoparticles and two different polypyrene-carbon nanotube (PPY-CNT) hybrids of the nanocomposite. Many other studies followed, expanding the science of mono and hybrid nanofluids. Recently, Akhgar et al. [11] developed disparate artificial neural networks (ANNs) to predict the thermal conductivity of MWCNT-TiO_2/ethylene glycol mixture nanofluid and inferred that ANN yields could thus predict the empirical outcomes better than the correlation method. Shahsavar et al. [12], using an artificial neural

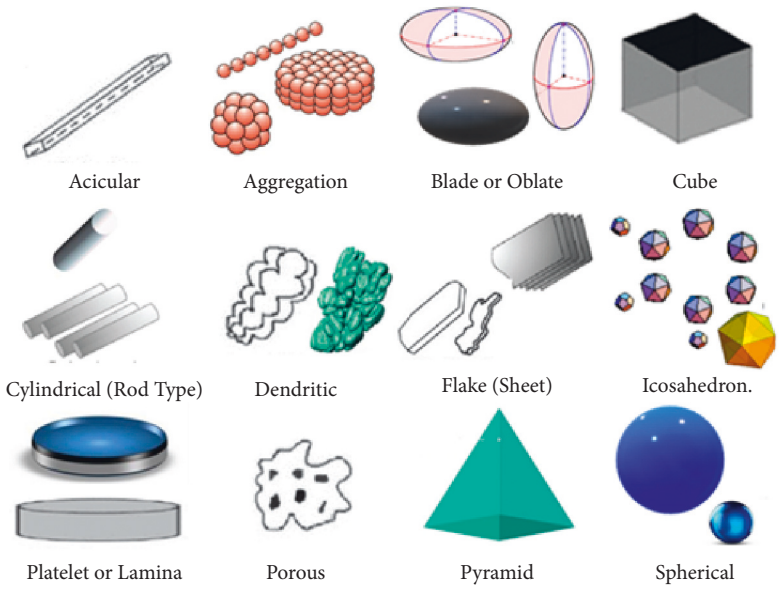

Figure 2: Some of the diverse particle shapes and geometries of nanoparticles.

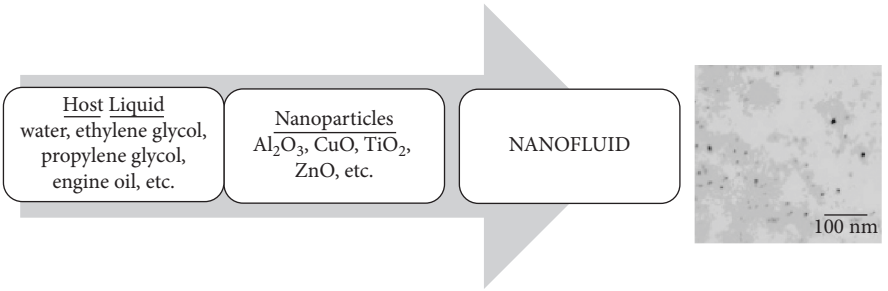

Figure 3: Schematic description of a nanofluid: base fluid in combination with nanoparticles.

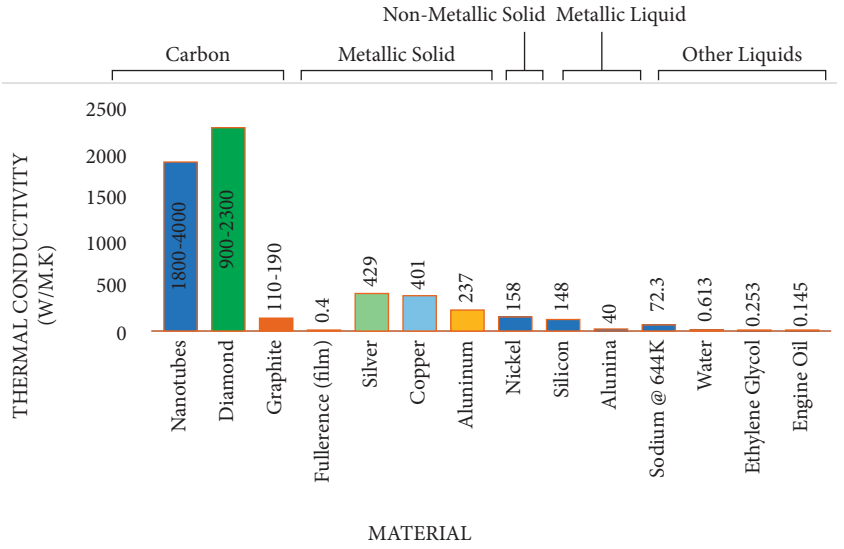

Figure 4: Thermal conductivities of various solid liquids at 300 K except stated otherwise.

network (ANN) algorithm, measured thermal conductivity and viscosity for molten paraffin-based nanofluid accommodating Al_2O_3 nanoparticles. Using experimental data and ANN modeling, Rostamian et al. [13] predicted the thermal conductivity of CuO-SWCNTs nanofluid. An analogous report with an increase in thermal conductivity was also

presented by Rostami et al. [14], Safaei et al. [15], Tian et al. [16], and Ji et al. [17] when they considered MWCNT-CuO/water, ZnO-TiO_2/EG, GO-Al_2O_3/water-EG, and TiO_2-Ag mixture nanofluid, respectively. Toghraie et al. [18] also designed an artificial neural network to envisage the viscosity of Ag/EG nanofluid for sundry temperatures and a solid fraction of nanoparticles. Komeilibirjandi et al. [19] engaged the group method of data handling (GMDH) ANN algorithm in estimating the thermal conductivity of nanofluids containing CuO nanoparticles in water, ethylene glycol, and engine oil as accommodating fluids. They concluded that using the GMDH ANN resulted in better accuracy. In a similar vein, Maleki et al. [20] deployed three approaches, including multivariate adaptive regression spline (MARS) and artificial neural network (ANN) with Levenberg–Marquardt, and GMDH, to determine the thermal conductivity of nanofluids containing ZnO particles in the water-EG mixture, EG, and water-propylene glycol as the host liquid. The authors confirmed that using the ANN with Levenberg–Marquardt for training gives the best results. Peng et al. [21] reported that the ANN-supported models agreed with the empirical results when used to decide the thermal conductivity of Al_2O_3-Cu/EG of equal volume ratio (50 : 50). Giwa et al. [22] analyzed the effect of base liquid, temperature, and volume fraction on electrical conductivity and effective viscosity of the two types of hybridized ferrofluids (Al_2O_3-Fe_2O_3/DW and Al_2O_3-Fe_2O_3/EG-DW) using the ANN and ANFIS soft computing techniques. The study concluded that hybridized ferrofluids may not be suitable for engineering, since model results show low viscosity compared with monoparticle ferrofluids and nanofluids. Bagherzadeh et al. [23] developed an "enhanced artificial neural network" (EANN) based on the novel generated hybridized nanocomposite of F-MWCNTs-Fe_3O_4/EG, representing functionalized multiwalled carbon nanotubes merged with Fe_3O_4 nanoparticles, spread in ethylene glycol (EG) as the working fluid. The proposed new sensitivity analysis result was thus confirmed to have been correct and precise; it also requires less computational time and cost. Safdari Shadloo [24] applied the least-square support vector machine (LS-SVM), another artificial intelligence approach, to predict nanofluids' convective heat transfer coefficient through circular pipes. The smart modeling results established that the convection heat transfer coefficient (HTC) increases via increasing dilution of nanoparticles up to the maximum value and undergoes a descending trend. The proposed intelligent paradigm accelerates the evaluation procedure of convection HTC of nanofluid flow within a circular pipe.

Furthermore, Saeedi et al. [25] in their study considered the rheological behavior of CeO_2-ethylene glycol (EG) nanofluid and reckoned that the mathematical correlation obtained was a suitable evaluation model for dynamic viscosity. Goodarzi et al. [26] assessed the dynamic viscosity of the ZnO-MWCNTs/engine oil mixture nanolubricant based on differences in temperature and solid volume fraction and confirmed Newtonian behavior at all concentrations and temperatures. Comparable work based on the effect of nanoparticles was also performed by Khodadadi et al. [27] for MgO-water nanofluid. Ruhani et al. [28] investigated the rheological behavior of Newtonian hybridized nanofluid, ZnO-Ag (50%–50%)/water, while taking experimental data into account. Afshari et al. [29] also investigated the rheological behavior of hybridized nanocomposite considering Al_2O_3-MWCNT/water/EG (80%:20%). The investigation in [28, 29] shows that viscosity mostly upsurges with increased volume concentration. A comparable result was thus published by Zadeh and Toghraie [30], when they investigated experimentally, the dynamic viscosity of Ag-EG nanofluid with a new model developed. Keyvani et al. [31] reported that the thermal conductivity of CeO_2/EG nanofluid using curve-fitting with two-variable correlation was enhanced with growing temperature and particle loading. Akhgar and Toghraie [32] completed an experimental study on the stability and thermal conductivity of water-ethylene glycol/TiO_2-MWCNTs hybridized nanoliquid and reported that the thermal conductivity of the prepared fluid can surge by a most of 38.7%. Furthermore, Moradi et al. [33] looked at MWCNT-water nanofluid stream and heat transference in a double pipe heat exchanger by means of permeable media. Arasteh et al. [34] considered ideal geometries arrangements of a heat sink partially loaded with multilayered permeable media employing hybridized solid-liquid composite (water-graphene nanoplatelet/platinum). Gholami et al. [35] modeled the effect of rib profile on the performance of a laminar stream of oil/MWCNT nanofluid in a rectangular microchannel. Barnoon et al. [36] modeled MHD mixed convection and entropy initiation in a lid-driven cavity with spinning cylinders occupied by a nanofluid.

However, despite these materials' extraordinary characteristics, as evidenced by published research, they are still in their early stage of advancement in research application, especially in automobile radiator cooling. To the authors' best knowledge, no review article has yet been published on this subject. So, the current review will provide a comprehensive overview of thermal enhancement for different hybrid nanofluids as they apply to automobile radiator cooling. This is the novelty of the present review. The current study also provides a further overview of different hybrid nanofluids and some methods of preparation, characteristics, and thermal properties of hybrid nanofluids. Nevertheless, the core focus of this review study is to elaborate on the thermal conductivity of hybrid nanofluids, a vital property since heat transfer rate, which is essential for the design and control of engineering processes, is clearly dependent on it, while also showcasing new blends of hybrid nanoparticles and looking at some empirical correlations presented in the literature, to predict the thermal conductivity of hybrid nanofluids and the status of ongoing research works permitting the use of hybrid nanofluids besides present challenges, and it is the authors' prospect that this review will be useful by giving relevant information (by serving as a minidatabase) to researchers, which will ease their judgment when choice and amalgamation of nanoparticles and base liquids are so required for thermal conductivity improvement and mixture fluid use. Finally, applications of hybrid nanofluids in today's automobile radiator cooling systems were also considered in the last section of the work.

1.1. Review Methodology. The review deals with the innovations around nanotechnology, focusing on thermal conductivity and identifying challenges limiting nanotechnology development. First, studies on the thermal conductivity of various mixture nanofluids are represented and followed by the investigation on the application of the referenced hybrid nanofluids in the auto radiator cooling system. An extensive literature survey was, however, carried out from a list of compiled heuristic or evidence-based articles in scholarly, peer-reviewed journals, conference proceedings, expert reports, papers, and chapters of books, for the past 15 years (with nanoparticles, hybrid nanofluids, thermal conductivity, automobile, cooling, and radiator as keywords) and reviewed in terms of results gotten from theoretical and experimental works on the thermal conductivity of hybrid nanofluids, preparation methods, performance characteristics, and variables to discuss and address the research questions. The research methodology adopted for this review is nevertheless divided into six generic steps as shown in Figure 5, considering the focal aspects: nanoparticles, nanofluids hybrid formulation, thermophysical properties, and nanofluids applications for auto cooling, as will be nevertheless detailed in the following subsequent sections.

Information obtained from literature is thus categorized into segments as stated in the contents. Section 2 presents and discusses the preparation/formulation procedures of hybrid nanofluids; this is followed by a review of recent analytical, artificial intelligence (AI), or machine learning approaches and experimental examinations with mixture nanofluids covered in Section 3. Methods implemented to evaluate the thermophysical properties of mixture nanofluids and correlations to estimate the thermal conductivity for hybrid nanofluids are also established in Section 4. Hybrid nanofluid use for auto cooling and the future prediction of nanofluid in new technological systems are thus discussed in Section 5. Finally, a sum-up will then be furnished in Section 6.

2. Preparation of Hybrid Nanofluids

Thermal decomposition pathways [37], microwave [38], irradiation, chemical reduction [39], laser [40], and gas-evaporation method [41] have all been used to prepare nanofluids, as shown in Figure 6. According to Das [42], nanocomposites are chiefly grouped into three classes, as shown in Figure 7. Al_2O_3 is perhaps the most well-known nanomolecule material used in nanoliquid for enhanced heat transfer. There are various reasons behind the Al_2O_3 nanomolecule being generally used in nanofluid investigations. First, they are low-cost metal oxides, particularly Al_2O_3, enabling large-scale manufacturing and making them economically accessible. Second, unlike many metallic nanoparticles, it is a ceramic nanoparticle that is not susceptible to surface oxidation and is simpler to combine into liquid due to its hydrophilic surface properties. Third, although the thermal conductivity of Al_2O_3 is not as high compared to other metal oxide materials such as CuO, MgO, and ZnO, it is two orders of magnitude higher than that of conventional heat transmission fluids. But Al_2O_3 is, however, chemically stable with enhanced mechanical strength. It is also applicable for electrical insulation. Suresh et al. [43] recognized that the Cu nanoparticles show modest dispersion stability but high thermal conductivity and reactivity.

In contrast, alumina (Al_2O_3) nanoparticles have dispersion and chemical inertness but exhibit low thermal conductivity. Hence, Siddiqui et al. [44] combined three samples of Al_3O_2-Cu hybrid nanofluid with different Cu and Al_2O_3 ratios to attain a significant enhancement in thermal conductivity and relatively better stability. Metal oxides are also blended in double and multiple forms to achieve the stability of hybrid nanofluids. Ramadhan et al. [45] activated trihybrid nanofluids by blending three metal oxides, Al_2O_3, TiO_2, and SiO_2, in a water-ethylene glycol (EG) mixture. They signaled that good stability was nevertheless achieved after 10 h of sonication. The amalgamation of double and multiple metals at the nanoscale level proffers an effective means to fine-tune the chemical and physical properties of nanoparticles, either by aiding hybridized chemical, electronic, and magnetic interfaces between metal components or by using hybridized chemical, electronic, and magnetic interfaces that combine various properties connected with each pure component. Again, the cost of a metallic nanoparticle is the core limiting factor behind its extensive industrial applicability. Chakraborty et al. [46] synthesized Cu-Al layered double hydroxide (LDH), i.e., Cu-Al LDH-water hybridized fluid using the coprecipitation technique and recorded a 16.07% rise in thermal conductivity measure for 0.8 vol% of nanofluid.

However, three kinds of host fluids are commonly used to set up the mixture arrangement of hybrid solutions [47]: water and ethylene glycol (EG) for hybrid nanofluids and oil-based liquids, and oil for hybrid solutions nano-lubricants. The formulation or making of hybrid nanofluids is known as "single or one-step" or "two-step" procedures. The two-step method is the most widely employed method for preparing nanofluids. This is because it is the most economical method available for the large-scale production of nanofluids. The choice and combination of nanoparticles in the right proportions and their readiness for use is one of the main tasks involved in hybrid nanofluid preparation. The proper or right selection and preparation of nanomaterials pave the pathway for attaining enhanced thermal conductivity [48]. Preparation may entail single particles in a unitary fluid (mono nanofluid), single particles in a dual or binary fluid (biliquid nanofluid), or single particles in a ternary fluid (triliquid nanofluid). Hybrid nanofluids are easily produced by blending two (or more than two) distinct types of nanoparticles into a building-based fluid.

The one-step or single-step technique (Figure 8) for nanofluid preparation is more reliable, following the challenges faced in preparing a stable nanofluid by using the two-step method.

Although some researchers like Han and Rhi [50] made Ag-Al_2O_3/H_2O with the one-step method, Bhosale and Borse [51] also prepared Al_2O_3-CuO/H_2O hybrid nanofluid

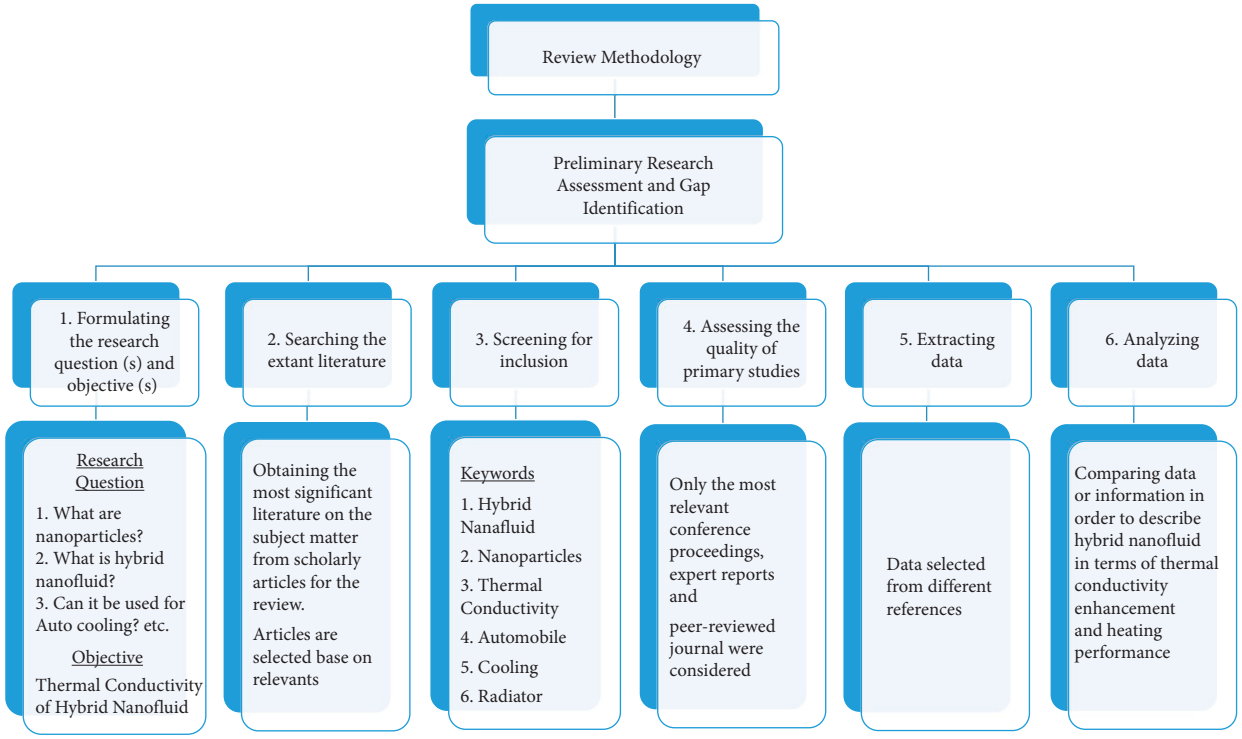

Figure 5: Schematic layout of the research review method.

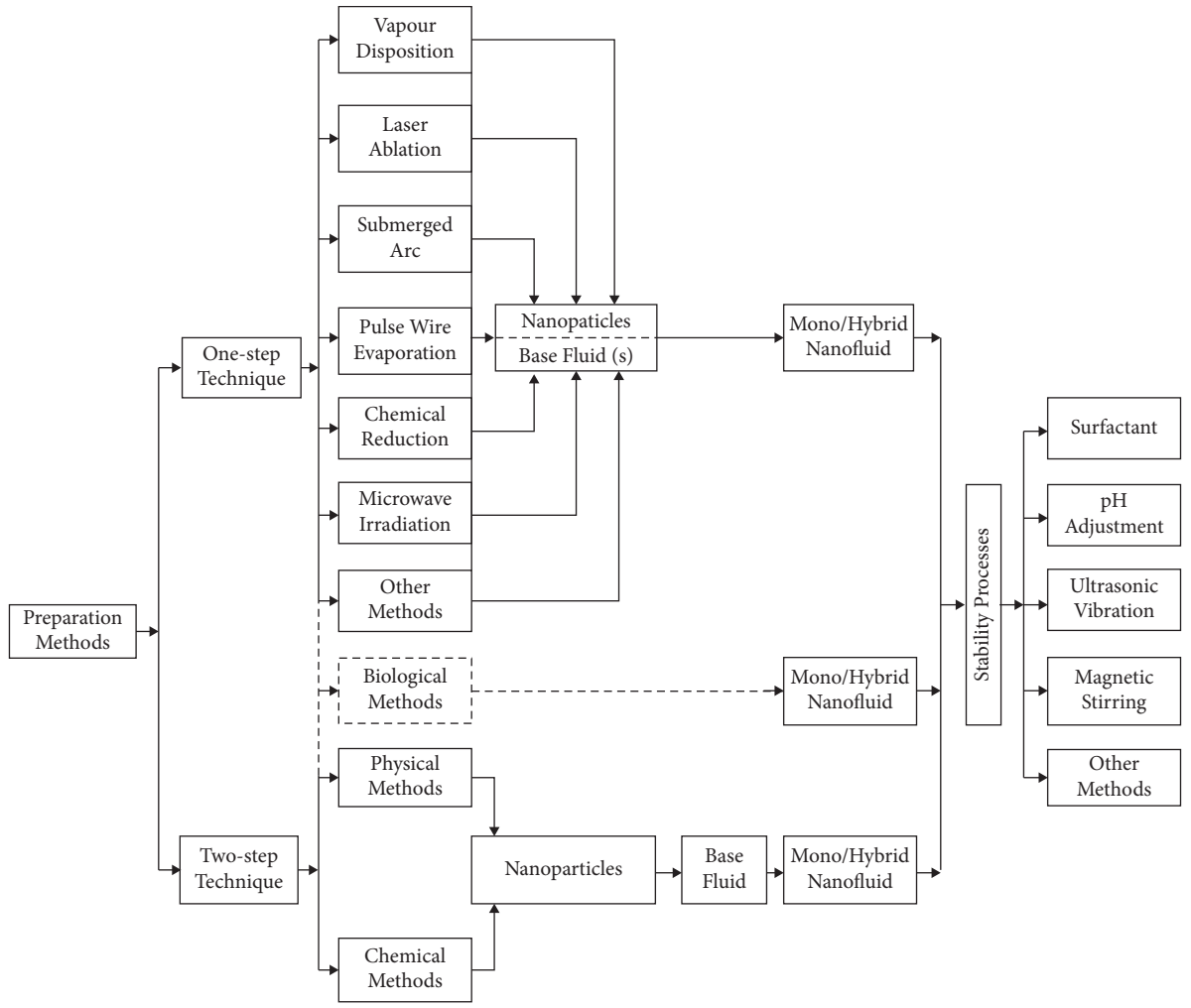

Figure 6: Schematic of various preparation processes of mono and hybrid nanofluids.

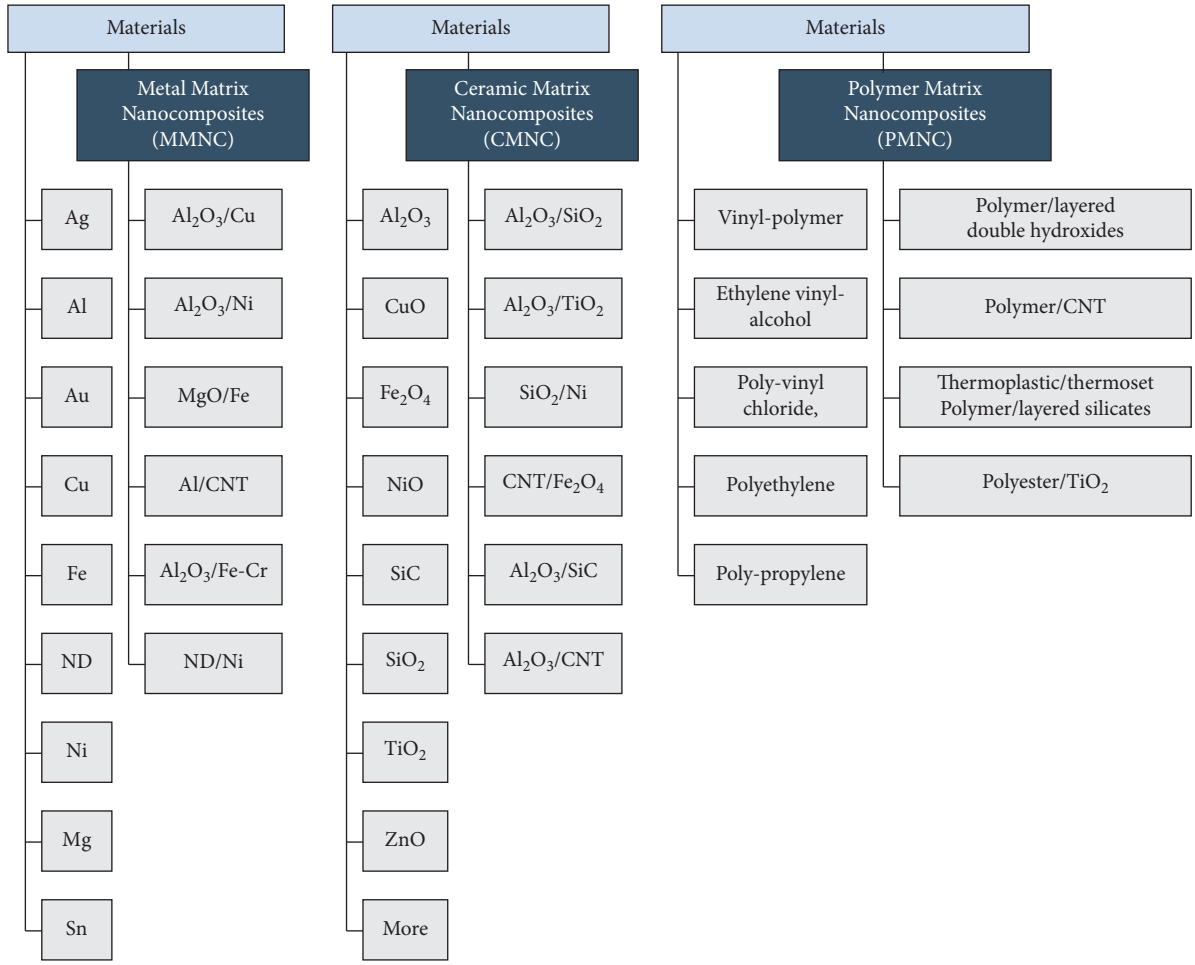

Figure 7: Classification of materials and nanocomposites.

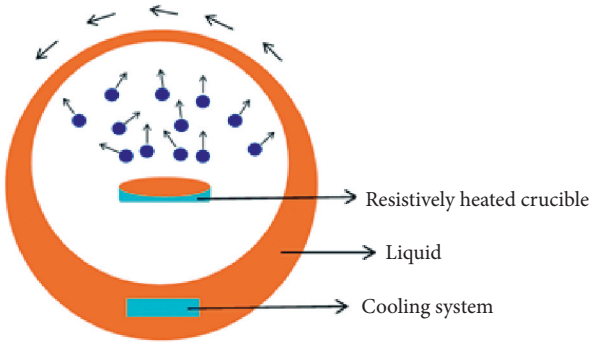

Figure 8: Schematic diagram of the nanofluid production system designed for direct evaporation/condensation of metallic vapour into low-vapour pressure liquids [49].

using this method (Table 1); this technique is, however, credited to Akoh et al. [74] called the vacuum evaporation on running oil substrate (VEROS) method. The technique instantaneously makes use of any of the methods of chemical vapour condensation [49], chemical precipitation [75–77], or direct evaporation [49], before scattering the nanoparticles (single, double, or multiple) right into an accommodating fluid in one step. It is most suitable for preparing metallic nanofluids because of their high thermal conductivity to avoid oxidation. It is the most effective technique for synthesizing low-cost nanofluids [78, 79]. Unlike the two-step method, the processes of drying, storing, and transporting the nanoparticles before dispersing them are thus avoided. This thus reduces the agglomeration of the nanoparticles and offers an increase in the resultant fluids' stability.

Nevertheless, some significant drawbacks of this technique, apart from the relatively high production cost and the fact that limited quantities are usually produced, are that the use of low vapour pressure liquids (mainly with the direct evaporation technique) is essential. Again, the initial intent of this method was to produce nanoparticles. However, it is difficult to separate the particles from the fluids later to get dry nanoparticles. It is also observed that the residual reactants (impurities) are often left in nanofluids due to the incomplete reaction, which is difficult to remove [80]. Other improved nanoparticle production methods are presently being practiced as presented by some researchers (depending on material combination). These include the synthesis of metal nanoparticles in deionized water, using multibeam laser ablation in liquids (where the laser parameters will thus

Figure 9: Two-step preparation process of nanofluids (direct mixing of nanoparticles followed by addition of dispersant and ultrasonication).

Table 1: Some syntheses of hybrid nanofluids conducted by different researchers.

Hybrid nanofluid	Preparation	Observation	Reference
Polypyrrole (PPy)-Fe_3O_4/water	Two-step strategy chemical: hybridized magnetic nanocomposites	Controllable magnetic properties can thus be engendered.	Turcu et al. [10]
CNT-Au/water and CNT-Cu/water	Two-step strategy mechanical: metal addition to CNT water based nanofluid	The synergistic effect of the hybridized fluid appears not to have created a better thermal conductivity.	Jana et al. [52]
Cu/MWCNTs-EG/water	Two-step strategy chemical: hybridized nanoliquid-solid composite	Homogeneous distribution of Cu-decorated MWCNTs in base fluids.	Jha and Ramaprabhu [53]
Ag-MWNTs-EG/water/Au-MWNTs-EG/water/Pd-MWNTs-EG/water	Two-step strategy chemical: hybridized nanoliquid-solid composite	Improvement of thermal conductivity with temperature was observed.	Jha and Ramaprabhu [54]
Al_2O_3 + MEPCM	Two-step strategy mechanical: hybridized nanoliquid-solid composite	There is a significant enhancement in thermal conductivity compared to water.	Ho et al. [55]
Ag-Al_2O_3/water	One-step strategy: 2 mixed nanofluids	Hybrid nanofluids were effective compared with mono nanofluids.	Han and Rhi [50]
SiO_2-MWCNT/water	Two-step strategy chemical: hybridized nanoliquid-solid composite	4 weeks of stability of fluid with surfactants. Inadequate thermal conductivity results.	Baghbanzadeh et al. [56]
Al_2O_3-Cu/water	Two-step strategy chemical: hybridized nanoliquid-solid composite	A thermal conductivity enhancement of 12.11% was achieved.	Suresh et al. [57]
Al_2O_3-Cu/water	Two-step strategy: 2 particles mixed in water	Improvement of 13.56% in Nu at Re = 1730.	Momin [58]
Cu-TiO_2/water	Two-step strategy: hybridized nanoliquid-solid composite	Thermal conductivity of Nu increases by 52%, 49%, and 68%, respectively.	Madhesh and Kalaiselvam [59]
γ-Al_2O_3-MWCNT/water	Two-step strategy: hybridized nanoliquid-solid composite	Thermal conductivity enrichment of about 14.75% was achieved.	Abbasi et al. [60]
Ag-MWCNT/water	One-step strategy thermal: hybridized nanoliquid-solid composite	MWCNT nanofluids are 14.5% less thermally conductive than Ag/MWNT hybrid nanofluids.	Munkhbayar et al. [61]
Cu/Cu_2O-water	Two-step strategy-mechanical: hybridized nanoliquid-solid composite	Thermal conductivity enhancement was observed.	Nine et al. [62]

Table 1: Continued.

Hybrid nanofluid	Preparation	Observation	Reference
MWCNT-Fe_2O_3/water	Two-step strategy-mechanical: 2 nanoparticles dissolved in water	Thermal conductivity is increased by 28%.	Chen et al. [63]
MWCNT-Fe_2O_3/water	Two-step strategy: hybridized nanoliquid-solid composite	Thermal conductivity is enhanced by 29%.	Sundar et al. [64]
$Fe_2O_3 + SiO_2$-MWCNT/water	Two-step strategy chemical: hybridized nanoliquid-solid composite	Thermal conductivity augmentation of 24.5% for 0.03% vol.	Theres Baby and Sundara [65]
Ag + MgO/water	Two-step strategy: hybrid nanocomposite	The thermal conductivity and viscosity of hybrids increase as the fraction of hybrids increases.	Esfe et al. [66]
Fe_3O_4-CNT/water	One-step strategy: 2 mixed nanofluids	In the presence of a magnetic field, the temperature had a negative effect on the thermal conductivity. This was for 0.9% FF + 1.35% CNT.	Shahsavar et al. [67]
Cu-Pd	One-step strategy: hybridized nanoliquid-solid composite	Maximum thermal conductivity improvement (18.79%) was observed for Cu/Pd at 20 : 1 molar ratio and at 80°C.	Jaiswal et al. [68]
SiC/SiO_2-water/EG	Two-step strategy: 2 nanoparticles dissolved in water and EG	Thermal conductivity and viscosity enhancement of nanofluid over the base liquid.	Nikkam et al. [69]
Al_2O_3-TiO_2/water	Two-step strategy: 2 nanoparticles dissolved in distilled water	The wettability of hybrid nanofluids improves with increasing volume fraction.	Septiadi et al. [70]
Al_2O_3-TiO_2-SiO_2/water/EG	Two-step strategy: 3 particles mixed and spread in water/EG	Formation of a stable solution.	Ramadhan et al. [45]
TiO_2-Al_2O_3/water/EG	Two-step strategy mechanical: 2 particles mixed in water and EG	Improved heat transfer efficiency of the hybridized fluids with a volume fraction above 0.04%.	Urmi et al. [71]
MgO-ZnO/deionized water (DIW)	Two-step strategy: 2 particles hybridized in water	The stability and morphology of the hybridized fluids were confirmed to be satisfactory.	Giwa et al. [72]
Cu-COOH-MWCNT//water	Two-step strategy: 2 particles mixed in water	Enhanced heat transfer capability was registered.	Gupta et al. [73]

control the nanoparticle size and distribution) [81, 82]. Another is the submerged arc nanoparticle synthesis system (SANSS) [83, 84] [85]. In the two-step formulation technique, the nanofluid preparation is normally separated from the nanoparticles' synthesis, hence the two-step (Figure 9). The method begins with producing nanoparticles by chemical, mechanical, or physical processes (e.g., evaporation and inert gas condensation processing) [86]. It then proceeds to scatter them into the host fluid. In the initial stage (first step), nanomaterials are usually synthesized and acquired as powders, which are then introduced to the accommodating liquid in a subsequent advance (second step). The two-step process is generally applied to oxide nanofluids ("Kool–Aid" method) nanoparticles and is used to synthesize carbon nanotube-based nanofluids. The two-step system's major drawback is that the nanoparticles' structure clusters (which occurs during drying, storage, haulage, and redispersion of nanoparticles) during the nanofluid preparation, inhibiting the proper scattering of nanoparticles inside the base liquid. This phenomenon happens because of the strong van der Waals force among nanoparticles [87] and can negatively affect the nanofluid's thermal conductivity. Stabilizing the blend requires but is not limited to three primary methods:

(a) Surfactants-surface activators [88, 89]

(b) Changing the pH value [57] and

(c) Utilizing ultrasonic vibrations [90, 91]

Septiadi et al. [70] suspended two different metallic oxide particles, γ-alumina (Al_2O_3) and titanium dioxide (TiO_2), with the two-step method. The two-step method was also used for preparing trihybrid nanofluids by mixing three nanofluids (of nanoparticles Al_2O_3, TiO_2, and SiO_2), subjected to mixing and sonication-based processes by Ramadhan et al. [45] (Table 1).

The synthesis of hybrid nanoparticles has been practically carried out by employing two distinct approaches grouped into physical and chemical. However, biological methods are sometimes considered (Table 2). Physical methods are straightforward, and robust hybridization between nanoparticles is acquired by this pathway. Still, the control of the size of hybrid nanoparticles looks complex. The upsides of the physical process are rapidity in the preparation process, radiation employed as a reducing agent, and no hazardous chemicals engaged.

Nonetheless, the downsides are little yield and high energy expenditure, impurities, and inadequate or nonuniform distribution; individual nanoparticles stay, in some cases, discrete, particularly within the finished

Table 2: Summary of the method of preparation of hybrid nanofluids.

S/N	Techniques	Some hybrid nanoparticle syntheses by the method	Main advantages	Disadvantages
		(a) Chemical synthesis methods		
1	Chemical reduction (CR)	Au-Pd-Pt, Au/TiO_2, and Au-ZnO	Nanoparticles' size and concentration can be tuned by controlling the synthetic.	Inability of both pure noble metals (NM) nanoparticles and hybrid nanoparticles to mix properly.
2	Photoreduction (PR)	Pd/TiO_2, Ag/TiO_2, Au/TiO_2	Simplicity of steps and versatility of application.	Presence of impurities
3	Sol-gel	Au/SiO_2, CNT-Fe_3O_4, and silica-MWCNT	Obtaining a high surface area and stable surfaces thus improves adhesion between the substrate and the topcoat. Low processing temperature (energy saving). The aspect ratio. Precisely controlled in size and internal structure.	High cost of precursor. Long duration of the process. Relatively low yield.
4	Hydrothermal	Pt/TiO_2, Ag-ZnO	Ease in controlling the size and shape of nanoparticles.	High pressure and reaction temperature
5	Thermal decomposition	Pd-Fe_3O_4, Ag-TiO_2		High cost of equipment
6	Coprecipitation method	Au-Fe_2O_3, Au-NiO, Au-Co_3O_4, and Au-ZnO	Simple and effective.	It is inappropriate for the synthesis of a highly untainted, precise stoichiometric phase.
7	Sonochemical synthesis	Pd-CuO, Pd-TiO_2 Au-TiO_2	It is faster, safer, less complicated, and eco-friendly. Size distribution in narrow particles.	Still, the mechanism is not well understood
8	Seeding growth	Ag-Fe_3O_4	It is a very effective method, especially in the case of dumbbell-like hybrid nanoparticles.	
9	Electrodeposition (ED)	Ni-graphene, Ni-TiN, Pt-Ru, Ni-TiO_2, Ni-ZrO_2, Ni-AlN, Ni-Al_2O_3, and Ni-Si_3N_4	Process of rapid solidification. Cost-effectiveness and method adaptability. It is quick and has high purity. Low processing temperature (room temperature).	Low temperature can lead to poor crystallinity.
		(b) Physical fabrications of hybrid nanoparticles		
10	Laser-induced heating (laser ablation)	Ag-Al_2O_3, Cu-Cu_2O	Highly pure colloids are produced with unique surface characteristics and without any by-products.	It requires a great amount of energy. NP colloids is often low, hence difficult to implement them on an industrial scale. Lack of control of the size and shape of the particles.
11	Atom beam cosputtering	Au-ZnO, Au-Ag	High purity	It is difficult to control the morphology of the formed nanoparticles
12	Ion implantation	Au-TiO_2, Ag-TiO_2		Extensive energy requirement. High energy demands.
		(c) Biological fabrications of hybrid nanoparticles		
13	Microbial incubation and plants extract	Fe-Pt, Co-Pt, Co-Fe, and Cd-Se.	Good reproducibility and scalability, high yield, and low cost	Slow and laborious

Source: Mohapatra et al. [92]; Ali et al. [93].

nanostructure. Chemical blends (particularly the controllable nanostructures) will perform better than physical techniques. On the other hand, they can display undesirable properties because of compound species such as settling ligands and polymer shells. Chemical pathways are further grouped into a reduction of metal precursors and the

processing routes. The main advantage of the chemical process, as opposed to physical techniques, is high yield. Other benefits include ease of production. Although it is considered a less costly process, some of its procedures, such as "top-down" and "bottom-up" methods, are quite expensive. Hazardous chemicals as reducing agents make biological methods a viable option.

2.1. Stability of Nanoparticles and Hybrid Nanofluids. Stability is critical in achieving good heat transfer performance when considering nanofluid for use. Hybridized liquid also faces stability challenges, which may be greater for suspension of two different types of nanoparticles than for suspension of similar nanoparticles. The nanocomposite, on the other hand, is extremely stable in a variety of aqueous solvents without the use of a surfactant [94]. Table 3 provides the stability level of the related nanofluids with no stabilizing agent/surface functionalization. In addition, it addresses the inherent dispersibility of the nanoparticles in base liquids.

There is, however, no clear definition of a stable hybrid nanofluid. Notwithstanding, there is a broad knowledge of agreement to the fact that hybrid nanofluids are "stable" or that the stability of hybrid nanofluids is said to be if they stay as one unit for a lengthy period of time, typically in the order of a quarter or more from the date of preparation. This involves the preservation of specific nanostructure characteristics such as aggregation, composition, crystallinity, shape, size, and surface chemistry. The stability concern of the finished blend is one of the foremost challenges of mono and hybrid nanofluids as the synthesis of materials, and their right selection to prepare stable hybrid nanofluids is yet a subtle goal to achieve. Chopkar et al. [96] realized a thermal conductivity increase of about 200% by dispersing the nanocrystalline of $Al_{70}Cu_{30}$ at a particle volume fraction of 1.5% in ethylene-glycol (EG) base fluid. But for the stability hitch, more particle dispersion would have been possible and, relatively, the thermal conductivity enhancement too. Reports indicate that the thermal conductivity of mono nanofluids diminishes with time. Nonetheless, for hybrid nanofluids, this may vary since the stability characteristics of hybrid nanofluids are different based on the amalgamation structure of dissimilar dual materials such as nanocomposites and, again, the diverse attractions amongst the materials involved in the composite. Furthermore, for mono nanofluids, although a higher level of stability can nevertheless be achieved via the one-step method, stability of the particles can also be achieved with other well-established chemical and physical techniques. Researchers are taking advantage of incorporating these techniques (chemical use of double or multiple and right surfactants, particle functionalization, and pH modification; physical or mechanical means such as magnetic stirring, ultrasonication, homogenization, and ball milling) that are already in use for stability enhancement of mono nanofluids for stability measure of hybrid nanofluids. But the spread of diverse (double or multiple) materials in the host liquid creates another challenge for nanocomposite-based nanofluids because of the different particles' facial charges (+ve or −ve) variation. Furthermore, the proper pairing of nanoparticles and mixture ratio may bring about some level of stability. The electrokinetic properties of a nanofluid are directly related to its stability. Hence, pH adjustment promotes the stability of nanofluid due to strong repulsive forces. Suresh et al. [57] measured the pH of a water-based mixture nanofluid containing both Al_2O_3 and Cu. They recorded a value of about 6, far less than the distinct nanofluids containing Al_2O_3 and Cu. This ensures the stability of the ready hybrid nanofluid. So, a predictive model for pH of the mixture nanofluid will also be useful for estimating stability. Van Trinh et al. [97] reported that nanofluids can give good stability based on the functional groups attached to the surfaces of both graphene sheets and MWCNTs. Esfe et al. [66] achieved stability with water of Ag-MgO hybrid nanofluids of the size of 25 nm (Ag) and 40 nm (MgO) nanoparticles, after three hours of ultrasonication and with the use of low concentrations of cetyltrimethylammonium bromide (CTAB) additive surfactant. However, the dispersed nanoparticles were confirmed to have been steady for several days. The use of surfactants has its limitations, especially when fluid acts at a high temperature. This can affect bonding between the nanoparticle and the surfactant. Besides, there is no definite work today that has completely dealt with the steadiness or stability of hybrid nanofluids. Aureen Albert et al. [98] opine that the sedimentation velocity can nevertheless be reduced by the synergistic effect of cutting down the particle size, by the particle's density, or by increasing the viscosity of accommodating fluid. Although, the rising viscosity of hose liquid is not practical for heat transfer. It also increases the pumping power mandatory to pump the fluid. They had achieved PVA-CuO hybrid nanofluid stability when CuO nanoparticles were eventually enveloped by PVA, resulting in a nanocomposite with a lower density, preventing particle agglomeration. The report indicates that the resultant PVA-CuO hybrid nanofluid was stable for up to 1 year. Furthermore, to achieve stability of CNTs-based hybrid nanofluids, their surfaces are, however, reformed to hydrophilic nature. Nanoparticles react and behave differently to various base fluids. According to Shahsavar et al. [12], the accommodating liquid (one of the significant variables influencing nanofluids' performance) is further grouped into two classes: aqueous (i.e., water and ethylene glycol) and nonaqueous liquids (i.e., oil and liquid paraffin). Because watery (aqueous) base liquids contain polar bonds, nanoparticles with high surface polarity should be considered with aqueous liquid to avoid nanoparticle agglomeration. Subsequently, on account of nanoparticles with low surface polarity, nonaqueous base fluids ought to be considered for preparing efficient nanofluids. In addition, nonaqueous base fluids can, however, be used as base fluids for nonpolar nanoparticles.

2.2. Benefits of Hybrid Nanofluids over Single-Base Nanofluids. Hybrid nanofluids outperform conventional and modern thermofluids in terms of thermophysical and optothermal properties. They have been known to give perceptibly increased heat transfer characteristics. The numerous benefits of hybrid nanofluids remain the combined influence of

Table 3: Stability of nanoparticles in different fluids.

Without treatment	Water/water-soluble molecular liquid	Oil	Ionic liquid
Metallic	Poor	Moderate	Good
Ceramic	Moderate	Good	Very good
Carbon	Very poor	Poor	Moderate

Source: Ma and Banerjee [95].

nanomaterials, extensive advanced thermal conductivity, the positive impacts of individual suspension of every single dispersion, rectified heat transmission, and stability. A single type of nanoparticle possesses certain unique benefits owing to the characteristics of the suspended nanoparticle. However, it cannot improve all of the needed qualities of the base fluid. It may also not have all of the desirable traits for certain applications [70]. Applications of nanofluids in various domains necessitate fine-tuning of various properties in order to get the desired outcomes. Thus, by adopting hybrid nanofluids via picking the right combination of nanoparticles, one can manipulate the favorable attributes of each particle while making up for their weaknesses when used alone. So, by weighing and balancing the advantages and disadvantages of individual suspensions (Table 4), mixing two or more nanoparticles in a building base fluid (which increases the thermophysical properties) can cause significant changes in heat transfer and pressure drop characteristics. This can be attributed to a better aspect ratio, a more suitable thermal network, and especially to the synergistic influence of nanoparticles. This is one apparent advantage that the hybrid nanofluids have over unitary nanofluids.

Furthermore, when compared to single-type nanofluids, hybrid nanofluids offer a variety of chemical, physical, and thermal properties (i.e., better thermal characteristics and rheology at the same time) that a single-segment nanofluid does not exhibit [9]. They present better chemical stability, mechanical resistance, physical strength, electrical conductivity, and other properties than individual nanofluids. When nano-sized particles are appropriately distributed, hybrid nanoparticles offer a massive advantage due to their exponentially enormous effective thermal conductivity. In most cases, the drawback of the increased viscosity of the resulting liquids was overcome and better with a hybrid than with a mono nanofluid. In addition, the fluid flow in a typical nanofluid is widely known to allow for greater heat transfer. To make it even better, a mixed nanofluid is used. Hybrid nanofluids could achieve the same heat transfer performance as mono nanofluids. This can thus be done at a lower percentage of the particle volume [100]. The combined influence of Al_2O_3 nanoparticles and nanoparticles of microencapsulated phase change material (MEPCM) has demonstrated a remarkable improvement in terms of cooling effectiveness compared to mono (pure PCM) nanoparticles and water [101]. Due to their intriguing features, hybrid nanofluids have found a vital role in energy transfer applications that can be adjusted according to needs.

Furthermore, composite nanofluids also have some other advantages over mixture nanofluids. Table 4 provides the benefits and drawbacks of composite nanofluids.

3. Enhancement of the Thermal Conductivity of Nanofluid through Hybridization

Several literature pieces have nevertheless been published on the heat transfer capacities of novel nanofluid blends with solid nanoparticles as they develop. These materials' thermal conductivity reveals the capacity or potential of these blends to deliver a high heat exchange between the associated environments. Jana et al. [52] published the first article covering the thermal conductivity of hybrid nanofluids. In their studies, they achieved stability and higher thermal conductivity with nanofluids laced with solid carbon nanotubes (CNT), gold nanoparticles (AuNPs), and copper nanoparticles (CuNPs) with water as the host fluid. However, the thermal conductivity was not affected with further hybridization when more than one nano solid, such as CNT-CuNP and CNT-AuNP came together. This is due to the poor association between Cu nanoparticles and CNTs, which lowers the dispersion propensity of the two classes of nanomaterials, bringing about increased agglomeration [102]. Furthermore, to improve the dispersion quality of CNT in water, Gupta et al. [73] organized a stable metal/COOH-MWCNT hybridized nanofluids by adding Zn, Ag, Fe, and Cu nanoparticles with COOH-MWCNT. All the readied metal/COOH-MWCNT hybridized nanofluid showed enhanced thermal conductivity compared to water with Cu/COOH-MWCNT, which established the greatest thermal conductivity enhancement of 78.5%. Chakraborty et al. [46] looked at Cu-Al/water, Akram et al. [103] tried Ag-Au/water, while Gupta et al. [104] considered Zn-Fe_2SO_4/water in their experiments. An outstanding result, which was attributed to nanoparticle concentration, was obtained for the Ag-Au/water trial, while others [46, 104] yielded similar outcomes. Pourrajab et al. [105] were able to get a better result when they paired Cu-SAB-15 in distilled water (DW). Suresh et al. [57] in their test work with Al_2O_3-Cu hybrid particles observed that the thermal conductivity of Al_2O_3-Cu/water hybrid nanofluid rose linearly with an increment in the volume concentration of the nanoparticles. They attained a maximum enhancement value of 12.11% for a solid volume fraction ϕ of 2% as opposed to results obtained by Jana et al. [52]. The foremost reason for the increased thermal conductivity of Al_2O_3-Cu/water hybrid nanofluid could be traced back to the interaction between Al_2O_3 and Cu nanoparticles, since Cu nanoparticles are of higher thermal conductivity (Figure 4) to that of Al_2O_3 nanoparticles [102]. Suresh et al. [106] likewise estimated the thermal conductivity of 0.1% Al_2O_3-Cu/water hybrid nanofluids as 0.62 W/m K. It implied that by adding 0.1% hybrid nanomaterial, a 1.2% augmentation in thermal conductivity was, however, achieved. Similar analysis and

Table 4: Advantages and disadvantages of nanocomposite-dispersed nanofluid.

Advantages	Disadvantages
A hydrophilic nanocomposite can be created by coating hydrophilic material on hydrophobic material, which is not possible with a nanoparticle mixture.	Not readily or easily available.
Better stability in comparison with mixture-based hybrid nanofluid.	Uncontrollable shape and size of particles
The heat capacity of composite nanofluid may be higher than host liquid, which is not possible for mixture nanofluid.	Inadequate theoretical models are available.
Advance enhancement in thermal conductivity and heat transfer characteristics compared to monoparticle nanofluids.	There are only a few applications in the literature, but they can be used in any application where mono nanoparticle nanofluids are used.
Nanocomposite (metallic and oxide particles)-based hybrid nanofluids are marginally less expensive than metallic-based single-particle nanofluids with same performance ratings.	Augmentation of viscosity is slightly more as compared to mono nanoparticle nanofluids.
	In internal flow, pressure drop increases, which increases the pumping power slightly compared to single particle nanofluids.

Source: Kumar and Sarkar [99].

outcomes with Al_2O_3-Cu/water were equally reported by Mehryan et al. [107] and Siddiqui et al. [44]. Nevertheless, a better result was, however, obtained when Taherialekouhi et al. [108] carried out a comparable experiment with water-graphene oxide (GO) and aluminium oxide (Al_2O_3) nanoparticles (Table 5). Abbasi et al. [60] studied the thermal conductivity of hybrid nanofluids blended onto MWCNT-γ-Al_2O_3 nanoparticles. The hybrid nanofluids were formerly formulated with pure MWCNTs of an average particle size of 37 μm, functionalized MWCNTs of an average particle size of 804 nm, and functionalized MWCNTs of an average particle size of 335 nm. The experiment's outcome at room temperature showed that the functionalized groups had a substantial effect on the thermal conductivity of the solid-liquid composite. The results also indicated that the augmentation in thermal conductivity had gone up to 20.68% at a 0.1% volume fraction of the hybrid compared to the pure form. Nine et al. [109] synthesized and characterized water-based Al_2O_3-MWCNTs hybrid nanofluids in a weight proportion of 97.5 : 2.5 to 90 : 10 over a 1–6% weight concentration. The thermal conductivity of the solid-liquid composite was compared with that of base Al_2O_3/water nanofluids. The overall outcome demonstrated that Al_2O_3-MWCNTs water base hybrid nanofluids gave a higher thermal conductivity compared to Al_2O_3/water nanofluids. It was also observed that hybrid nanofluid containing cylindrical particles displayed higher enhancement than those containing spherical particles in hybrid nanofluid. Esfe et al. [110] in their work contemplated the impact of temperature and volume concentration of nanoparticles on the thermal conductivity of CNTs-Al_2O_3/water nanofluids. The outcomes demonstrated that the thermal conductivity of CNTs-Al_2O_3/water nanofluid increased with temperature and solid volume fraction. Comparable work was also reported by Devarajan et al. [111]. Taherialekouhi et al. [108] considered the pair of GO-Al_2O_3/water hybridized nanofluid in their experimentation, and a better result was further obtained. In another study, Ho et al. [55] prepared a hybrid water-based suspension of Al_2O_3 nanoparticles and microencapsulated phase change material (MEPCM) particles, and the results after the experimental investigation indicated that at set limits of 30°C for different PCM suspensions (ω_{pcm} = 0%, 2.0%, 5.0%, and 10 wt%) and several mass concentration of Al_2O_3 nanoparticles, the hybrid nanofluids exhibited a higher thermal conductivity as the mass concentrations of nanoparticles increased compared with the PCM suspension. The improvement in thermal conductivity was because alumina had a much higher thermal conductivity (Figure 4) than n-eicosane particles. Similar results were obtained in terms of thermal conductivity enhancement with pure water and Al_2O_3-SiO_2 [112], Al_2O_3-TiO_2 [113, 114], Al_2O_3-TiO_2 and Al_2O_3-SiO_2 [115], Al_2O_3-ZnO [116], Al_2O_3-CeO_2 [117], and Al_2O_3-Ag [118] (Table 5). Similar to the case of Jana et al. [52], experimental work was also carried out for three mass concentrations (0.1, 0.5, and 1.0%) of nanoparticles at two different room temperatures of 27°C and 40°C correspondingly to check for the thermal conductivity of nanofluids based on multiwall carbon nanotube (MWCNT) and silica (SiO_2) nanoparticles along with that of hybrid nanofluids SiO_2-MWCNT/water in two proportions of 80% SiO_2–20% MWCNT and 50% SiO_2–50% MWCNT by Baghbanzadeh et al. [56]. The trial test results disclosed that the values of the hybrid nanofluids' thermal conductivity were within the range of the values of the thermal conductivities of most nanofluids. Safi et al. [119] achieved a thermal conductivity enhancement of 12.1% for a specimen with 0.08% weight percentage of MWNT-TiO_2 compared to distilled water (DW) at 36°C and 13.71% at 52°C. The results obtained by Jana et al. [52], juxtaposed with Suresh et al. [57] using Cu metal are similar to the cases of Baghbanzadeh et al. [56] and Safi et al. [119] using ceramic matrix. Higher thermal conductivity was also reached when Karimipour [120], Zadkhast et al. [121], and Verma et al. [122] considered CuO-MWCNT dispersed in pure water. Senthilraja et al. [123] conducted a study to ascertain the thermal conductivity of Al_2O_3/water, CuO/water, and CuO-Al_2O_3/water nanofluids. Thermal conductivity was then measured in terms of temperature and volume concentration. The maximum enhancement in thermal conductivity displayed by Al_2O_3/water, CuO/water, and CuO-Al_2O_3/water nanofluids at 0.2% concentration and a temperature of 60°C was 6.1%, 8%, and 9.8%, respectively. Ramachandran et al. [124]

Table 5: Summary of results from published literature on thermal conductivity of various hybrid nanofluids.

S/N	References authors	Thermal conductivity (TC) of hybrid composite element (W m^{-1} K^{-1})			Observation summary			
		Material/base fluid	TC (K (W/m K))	Source	hnf with increased TC	ϕ (%)	T (°C)	Max % rise
1	Jana et al. [52]	CNTs	~3000	[52]	CNT-CuNP/water			No effect on TC
		Cu	400	[52]				
		Au	318	[52]	CNT-AuNP/water			
		Distilled water (DW)	0.597	[112]				
		COOH-functionalized MWCNT	1500–3000	[121]				
2	Gupta et al. [73]	Cu	401	[4]	MWCNT-Cu/water			78.5
		Ag	429	[3]				
		Zn	116	[296]				
		Fe	83.5	[4]				
		Distilled water (DW)	0.597	[112]				
3	Chakraborty et al. [46]	Cu	401	[4]	Cu-Al/W	0.80		16.07
		Al	237	[4]				
		Distilled water (DW)	0.597	[112]				
4	Akram et al. [103]	Ag	429	[103]	Ag-Au/water	0.6–2.0		71.53
		Au	318	[103]				
		Water	0.613	[103]				
5	Gupta et al. [104]	Zn	116	[296]	Zn-Fe_2O_4/water	0.50		11.80
		Fe_2O_4	9.7	[297]				
		Distilled water (DW)	0.597	[112]				
6	Pourrajab et al. [105]	Cu	401	[4]	Cu-SAB-15/water	0.08	50	24.24
		SAB-15	0.2-0.3	[298]				
		Distilled water (DW)	0.613	[4]				
7	Suresh et al. [57]	Cu	401	[4]	Cu-Al_2O_3/water	0.20		12.11
		Al_2O_3	40	[4]				
		Distilled water (DW)	0.611	[57]				
8	Suresh et al. [106]	Cu	401	[4]	Cu-Al_2O_3/water	0.10		1.20
		Al_2O_3	40	[4]				
		Distilled water (DW)	0.597	[112]				
9	Mehryan et al. [107]	Cu	401	[4]	Cu-Al_2O_3/water	2.00		1.20
		Al_2O_3	40	[4]				
		Deionized (DI) water	0.613	[4]				
10	Siddiqui et al. [44]	Cu	401	[4]	Cu-Al_2O_3/water			
		Al_2O_3	40	[4]				
		Deionized (DI) water	0.606	[44]				
11	Abbasi et al. [60]	MWCNT-γ	3000	[4]	MWCNT-γ-Al_2O_3/water	0.10	25	20.68
		Al_2O_3	40	[4]				
		Deionized (DI) water	0.613	[4]				
12	Nine et al. [109]	MWCNTs	~3000	[4]	MWCNT-Al_2O_3/water			
		Al_2O_3	40	[4]				
		Distilled water (DW)	0.597	[112]				
13	Esfe et al. [110]	CNTs	3000	[110]	CNT-Al_2O_3/water			
		Al_2O_3	40	[110]				
		Distilled water (DW)	0.597	[112]				
14	Devarajan et al. [111]	CNT	3007.4	[111]	CNT-Al_2O_3/water	2.00	60	20.00
		Al_2O_3	40	[111]				
		Deionized (DI) water	0.613	[4]				
15	Taherialekouhi et al. [108]	GO	1000	[156]	GO-Al_2O_3/water	1.00	50	39.30
		Al_2O_3	40	[4]				
		Distilled water (DW)	0.597	[112]				
16	Moghadam et al. [261]	GO	1000	[156]	GO-TO_2/water	01.00	50	32.80
		TiO_2	8.4	[222]				
		Distilled water (DW)	0.597	[112]				
17	Singh et al. [299]	GO	2000	[299]	GO-CuO/water	0.30	60	30.00
		CuO	33	[299]				
		Distilled water (DW)	0.597	[112]				

Table 5: Continued.

S/N	References authors	Thermal conductivity (TC) of hybrid composite element (W m^{-1} K^{-1})			Observation summary			
		Material/base fluid	TC (K (W/m K))	Source	hnf with increased TC	ϕ (%)	T (°C)	Max % rise
18	Zayan et al. [300]	GO	1000	[300]	rGO-TiO_2-Ag	0.05	25–50	66.00
		rGO	1000	[301]				
		Ag	429	[3]				
		TiO_2	8.4	[222]	GO-TiO_2-Ag	0.05	25–50	83.00
		Deionized (DI) water	0.613	[4]				
19	Ho et al. [55]	Al_2O_3	40	[4]	Al_2O_3-MEPCM/water	10.00		13.00
		MEPCM	0.15–0.35	[101]				
		Distilled water (DW)	0.597	[112]				
20	Moldoveanu et al. [112]	Al_2O_3	40	[4]	Al_2O_3-SiO_2/water			23.61
		SiO_2	1.4–12	[88, 302]				
		Distilled water (DW)	0.586	[112]				
21	Septiadi et al. [70]	Al_2O_3	40	[4]	Al_2O_3-TiO_2/water	0.70		32.50
		TiO_2	8.4	[222]				
		Distilled water (DW)	0.586	[113]				
22	Moldoveanu et al. [113]	Al_2O_3	40	[4]	Al_2O_3-TiO_2/water		25	19.20
		TiO_2	8.4	[222]				
		Distilled water (DW)	0.586	[113]				
23	Wanatasanapan et al. [114]	Al_2O_3	40	[4]	Al_2O_3-TiO_2/water	1.00	70	71.00
		TiO_2	8.4	[265]				
		Deionized (DI) water	0.606	[219]				
24	Minea [115]	Al_2O_3	40	[115]	Al_2O_3-SiO_2/water			12.00
		SiO_2	1.2	[115]				
		TiO_2	8.4	[115]	Al_2O_3-TiO_2/water			
		Pure water	0.613	[4]				
25	Wole–Osho et al. [114]	Al_2O_3	40	[4]	Al_2O_3-ZnO/water	1.67	65	40.00
		ZnO	29	[303]				
		Distilled water (DW)	0.597	[112]				
26	Kamel et al. [117]	Al_2O_3	40	[4]	Al_2O_3-CeO_2/water	0.50	50	8.80
		CeO_2	12–14.1	[304]				
		Deionized (DI) water	0.606	[219]				
27	Aparna et al. [118]	Ag	429	[3]	Ag-Al_2O_3/water	0.10	53	23.82
		Al_2O_3	40	[4]				
		Distilled water (DW)	0.597	[112]				
28	Khan [305]	Ag	419	[305]	Ag-TiO_2/water	0.10	31	12.20
		TiO_2	12	[305]				
		Distilled water (DW)	0.597	[112]				
29	Khan [259]	Ag	419	[305]	Ag-TiO_2/water	0.4	60	18.47
		TiO_2	12	[305]				
		Distilled water (DW)	0.597	[112]				
30	Baghbanzadeh et al. [56]	MWcNTs	~3000	[4]	MWcNT-SiO_2/water			nf = hnf
		SiO_2	1.38	[56]				
		Distilled water (DW)	0.6	[56]				
31	Safi et al. [119]	MWCNT	~3000	[4]	MWCNT-TiO_2/water	0.08	52	13.71
		TiO_2	8.4	[265]				
		Distilled water (DW)	0.597	[112]				
32	Karimipour et al. [120]	MWCNT	~3000	[4]	MWCNT-CuO/water	1.00	50	37.05
		CuO	76.5	[4]				
		Distilled water (DW)	0.6	[120]				
33	Rostami et al. [14]	MWCNT	~3000	[4]	MWCNT-CuO/water	0.60	50	30.38
		CuO	76.5	[4]				
		Water	0.613	[4]				
34	Zadkhast et al. [121]	COOH-MWCNT	1500–3000	[121]	MWCNT-CuO/water	0.60	50	30.38
		CuO	32.9	[121]				
		Pure water	0.613	[4]				

Table 5: Continued.

S/N	References authors	Thermal conductivity (TC) of hybrid composite element (W m^{-1} K^{-1})			Observation summary			
		Material/base fluid	TC (K (W/m K))	Source	hnf with increased TC	ϕ (%)	T (°C)	Max % rise
35	Verma et al. [122]	MWCNT	~3000	[4]	MWCNT-CuO/water	1.00		20.82
		CuO	76.5	[4]				
		MgO	48	[237]				
		Pure water	0.613	[4]				
36	Senthilraja et al. [123]	CuO	32.9	[123]	$CuO-Al_2O_3$/water	0.20	60	9.80
		Al_2O_3	30	[123]				
		Distilled water (DW)	0.597	[112]				
37	Yarmand et al. [91]	GNP	~3000	[4]	GNP-Ag/water	0.10	50	22.22
		Ag	429	[3]				
		Distilled water (DW)	0.597	[112]				
38	Megatif et al. [125]	CNT	~2000–4000	[6]	$CNT-TiO_2$/water	0.20	25	20.50
		TiO_2	8.4	[265]				
		Distilled water (DW)	0.597	[112]				
39	Dalkılıç et al. [126]	CNT	25	[126]	$CNT-SiO_2$/water	1.00	60	26.29
		SiO_2	1.4	[126]				
		Distilled water (DW)	0.597	[112]				
40	Sundar et al. [127]	Nanodiamond	3300	[265]	ND-Ni/water	3.00	60	29.39
		Ni	53.3	[306]				
		Distilled water (DW)	0.597	[112]				
41	Ramachandran et al. [124]	CuO	76.5	[4]	$CuO-Al_2O_3$/water	0.10		79.35
		Al_2O_3	40	[4]				
		Deionized (DI) water	0.606	[219]				
42	Mousavi et al. [307]	CuO	69	[128]	CuO/MgO/TiO_2/water	0.10	50	78.60
		TiO_2	5.41	[128]				
		MgO	5.11	[128]				
		Distilled water (DW)	0.597	[112]				
43	Mousavi et al. [128]	TiO_2	5.407	[128]	MgO-TiO_2/water	0.30	60	21.80
		MgO	5.112	[128]				
		Distilled water (DW)	0.597	[112]				
44	Esfe et al. [66]	Ag	429	[3]	Ag-MgO/water			
		MgO	48	[237]				
		Distilled water (DW)	0.597	[112]				
45	Batmunkh et al. [129]	Ag	429	[3]	Ag-TiO_2/water	1.00	25	1.00
		TiO_2	8.4	[265]				
		Distilled water (DW)	0.597	[112]				
46	Madhesh and Kalaiselvam [59]	Cu	401	[4]	Cu-TiO_2/water	1.00	80	
		TiO_2	8.4	[265]				
		Deionized distilled water	0.613	[4]				
47	Madhesh et al. [130]	Cu	401	[4]	Cu-TiO_2/water			
		TiO_2	8.4	[265]				
		Deionized distilled water	0.613	[4]				
48	Nine et al. [62]	Cu	401	[4]	Cu-Cu_2O/water			
		Cu_2O	4.5	[308]				
		Deionized (DI) water	0.606	[219]				
49	Ranga Babu et al. [131]	Cu	401	[4]	Cu-Cu_2O/water			17.52
		Cu_2O	4.5	[308]				
		Water	0.606	[219]				
50	Aureen et al. [98]	CuO	76.5	[4]	CuO-PVA/water			
		Polyvinyl alcohol (PVA)	0.31	[309]				
		Deionized (DI) water	0.606	[219]				
51	Theres Baby and Sundara, [65]	MWNT	~3000	[4]	MWNT-Fe_2O_3/water	0.03		24.50
		Fe_2O_3	7	[303]				
		SiO_2	1.4–12	[88, 302]				
		Deionized (DI) water	0.606	[219]				

Table 5: Continued.

S/N	References authors	Thermal conductivity (TC) of hybrid composite element (W m^{-1} K^{-1})			Observation summary			
		Material/base fluid	TC (K (W/m K))	Source	hnf with increased TC	ϕ (%)	T (°C)	Max % rise
		CNT	~2000–4000	[6]				
52	Shahsavar et al. [132]	Fe_3O_4	9.7	[236]	CNT-Fe_2O_3/water		55	34.26
		Water	0.613	[4]				
		CNT	~2000–4000	[6]				
53	Shahsavar et al. [67]	Fe_3O_4	9.7	[236]	CNT-Fe_2O_3/water		25	151.31
		Deionized (DI) water	0.606	[220]				
		CNT	~2000–4000	[6]				
54	Shahsavar et al. [133]	Fe_3O_4	9.7	[236]	CNT-Fe_2O_3/water		55	44.60
		Deionized (DI) water	0.606	[220]				
		CNT	~2000–4000	[6]				
55	Shahsavar and Bahiraei [134]	Fe_3O_4	9.7	[236]	CNT-Fe_2O_3/water			
		Water	0.613	[4]				
		CNTs	~2000–4000	[6]				
56	Syam Sundar et al. [135]	Fe_3O_4	9.7	[236]	CNT-Fe_2O_3/water	0.30	60	29.00
		Water	0.613	[4]				
		MWCNTs	~3000	[4]				
57	Chen et al. [63]	Fe_2O_3	7	[303]	MWCNT-Fe_2O_3/water	0.50		27.75
		Water	0.613	[4]				
		MWCNT	~3000	[4]				
58	Sundar et al. [64]	Fe_2O_3	7	[303]	MWCNT-Fe_2O_3/water	0.30	60	29.00
		Water	0.613	[4]				
		MWCNTs	3000–6000	[61]				
59	Munkhbayar et al. [61]	Ag	429	[3]	MWCNTs-Ag/water	0.05	40	14.50
		Distilled water (DW)	0.597	[112]				
		MWNT	~3000	[4]				
60	Amiri et al. [137]	Ag	429	[3]	MWNT-Ag/water			
		Water	0.613	[4]				
		MWNTs	~3000	[4]				
61	Chen et al. [138]	Ag	429	[3]	MWNT-Ag/water		65	24.00
		Water	0.613	[4]				
		MWCNTs	~3000	[4]				
62	Farbod and Ahangarpour [139]	Ag	429	[3]	MWCNT-Ag/water	4.00	40	20.40
		Water	0.613	[4]				
		Ag	429	[3]				
63	Sinz et al. [140]	f-HEG	~10.9	[310]	Ag-f-HEG/water			
		Water	0.613	[4]				
		GNP	~2200	[311]				
64	Yarmand et al. [141]	Pt	71.5	[306]	GNP-Pt/water	0.10	40	17.77
		Water	0.613	[4]				
		Graphene (Gr)	5000	[142]				
65	Ahammed et al. [142]	Al_2O_3	46	[142]	Gr-Al_2O_3/water	0.10	50	13.84
		Water	0.613	[4]				
		Graphene (Gr)	5000	[142]				
66	Bakhtiari et al. [239]	TiO_2	8.4	[265]	Gr-TiO_3/water	0.50	75	27.84
		Water	0.613	[4]				
		Fe	80.4	[143]				
67	Okonkwo et al. [143]	Al_2O_3	40	[4]	Fe-Al_2O_3/water	0.20		14.00
		Water	0.613	[4]				
		Si	148	[296]				
68	Huminic et al. [144]	Fe	80.2	[296]	Si-Fe/water	1.00	50	12.60
		Water	0.613	[4]				
		Go	2–1000	[5]				
69	Mahyari et al. [145]	SiC	490	[296]	Go-SiC/water	1.00	50	33.20
		Water	0.606	[145]				
		COOH–MWCNT	1500–3000	[121]				
70	Pourrajab et al. [146]	Cu	401	[4]	MWCNT-Cu/water		50	47.30
		Water	0.613	[4]				

Table 5: Continued.

S/N	References authors	Thermal conductivity (TC) of hybrid composite element (W m^{-1} K^{-1})			Observation summary			
		Material/base fluid	TC (K (W/m K))	Source	hnf with increased TC	ϕ (%)	T (°C)	Max % rise
		Cu	400	[147]				
71	Kanti et al. [147]	Fly ash (Indonesia)	1.7	[147]	Cu-fly ash/water	0.50	60	14.00
		Water	0.613	[4]				
		Cu	400	Cu				
72	Kanti et al. [148]	Fly ash (Indian)	1.7	[147]	Cu-fly ash/water	0.50	60	11.90
		Water	0.613	[4]				
		Cu	400	[147]				
73	Kanti et al. [149]	Fly ash	1.7	[147]	Cu-fly ash/water	0.50	60	19.00
		Water	0.613	[4]				
		Ag	429	[3]				
74	Esfahani et al. [150]	ZnO	29	[303]	Ag-ZnO/water	2.00	50	
		Water	0.613	[4]				
		rGO	1000	[301]				
75	Said et al. [301]	Co_3O_4	69	[156]	ND-Co_3O_4/water	0.20	60	19.14
		Distilled water (DW)	0.602	[301]				
		Nanodiamond (ND)	3300	[265]				
76	Sundar et al. [151]	Co_3O_4	69	[156]	ND-Co_3O_4/water	0.15	60	16.00
		Water	0.613	[4]				
		Ethylene glycol (EG)	0.253	[4]				
		Nanodiamond (ND)	3300	[265]				
77	Sundar et al. [152]	Fe_3O_4	9.7	[236]	ND-Co_3O_4EG/water	0.20	60	17.80
		Water	0.613	[4]				
		Ethylene glycol (EG)	0.253	[4]				
		Nanodiamond (ND)	1000	[153]				
78	Sundar et al. [153]	Fe_3O_4	80.2	[153]	ND-Fe_3O_4EG/water	0.20	60	12.70
		Water	0.404	[153]				
		Ethylene glycol (EG)	0.253	[4]				
		Nanodiamond (ND)	3300	[4]				
79	Sundar et al. [154]	Ni	53.3	[306]	ND-NiEG/water	3.03	60	21.00
		Water	0.613	[4]				
		Ethylene glycol (EG)	0.253	[4]				
		Nanodiamond (ND)	3300	[265]				
80	de Oliveira et al. [155]	Ag	429	[3]	ND-AgEG	0.10		6.92
		Ethylene glycol (EG)	0.253	[4]				
		GO	1000	[156]				
81	Sundar et al. [156]	Co_3O_4	697	[156]	GO-Co_3O_4/water	0.20	60	19.14
		Ethylene glycol (EG)	0.253	[4]				
		Water	0.613	[4]				
		GO	2–1000	[5]				
82	Rostami et al. [157]	CuO	401 (cu)	[157]	GO-Co_3O_4EG/water	1.60		43.40
		Water	0.606	[157]				
		Ethylene glycol (EG)	0.26	[157]				
		Ag	418.69	[96]				
		Cu	386.11	[96]				
83	Chopkar et al. [96]	Al_2	237	[4]	$CuAl_2$EG/water	1.00		>70.00
		Deionized (DI) water	0.621	[96]				
		Ethylene glycol (EG)	0.246	[96]				
		MWCNTs	~3000	[4]				
84	Jha and Ramaprabhu [53]	Cu	401	[4]	MWCNT-CuEG/ water	0.03		35.00
		Deionized (DI) water	0.62	[54]				
		Ethylene glycol (EG)	0.253	[4]				
		MWCNT	3000	[54]				
		Ag	429	[54]				
85	Jha and Ramaprabhu [54]	Au	317	[54]	MWCNT-Ag/water	0.03		37.30
		Palladium (Pd)	71.8	[54]				
		Deionized (DI) water	0.62	[54]				
		Ethylene glycol (EG)	0.248	[54]				

Table 5: Continued.

S/N	References authors	Thermal conductivity (TC) of hybrid composite element (W m^{-1} K^{-1})			Observation summary			
		Material/base fluid	TC (K (W/m K))	Source	hnf with increased TC	ϕ (%)	T (°C)	Max % rise
86	Baby and Ramaprabhu [159]	f-MWNT	~3000	[4]	MWNT-Ag/water	0.05	25	20.00
		Ag	429	[3]				
		f-HEG	~10.9	[310]				
		Deionized (DI) water	0.606	[219]				
		Ethylene glycol (EG)	0.253	[4]				
87	Baby and Ramaprabhu [160]	Ag	429	[3]	Ag-HEGEG/water	0.05	25	25.00
		f-HEG	~10.9	[310]				
		Deionized (DI) water	0.606	[219]				
		Ethylene glycol (EG)	0.253	[4]				
88	Baby and Sundara [161]	CuO	76.5	[4]	CuO-HEGEG/water	0.05	25	28.00
		f-HEG	~10.9	[310]				
		Deionized (DI) water	0.606	[219]				
		Ethylene glycol (EG)	0.253	[4]				
89	Jyothirmayee Aravind and Ramaprabhu [94]	MWNT	~3000	[4]	MWNT-GrEG/water	0.04	25	13.70
		Graphene (Gr)	~3000	[4]				
		Deionized (DI) water	0.606	[219]				
		Ethylene glycol (EG)	0.253	[4]				
90	Aravind and Ramaprabhu [162]	Graphene (Gr)	~3000	[4]	Gr-MWNT/water	0.04	50	87.90
		MWNTs	~3000	[4]				
		Deionized (DI) water	0.606	[219]				
		Ethylene glycol (EG)	0.253	[4]				
91	Shankara et al. [278]	MWCNT	1500–3000	[278]	MWCNT/CuO/water	0.10	80	30.00
		Graphene (Gr)	2500	[278]				
		CuO	33	[278]				
		Deionized (DI) water	0.606	[219]				
92	Kazemi et al. [312]	Graphene (G)	2500	[278]	G-SiO_2/water	1.00	50	36.10
		SiO_2	1.4–12	[88, 302]				
		Water	0.613	[4]				
93	Shende and Sundara [163]	MWNTs	~3000	[4]	MWNT-N-rGO/ water	0.02	50	17.70
		N-rGO	2–1000	[5]				
		Deionized (DI) water	0.606	[219]				
		Ethylene glycol (EG)	0.253	[4]				
94	Esfe et al. [164]	DWCNT	>2000	[313]	DWCNT-ZnOEG/ water	1.00	50	32.00
		ZnO	29	[303]				
		Water	0.613	[4]				
		Ethylene glycol (EG)	0.253	[4]				
95	Esfe et al. [165]	DWCNT	>2000	[313]	DWCNT-ZnO/water	1.90	50	24.90
		ZnO	29	[303]				
		Ethylene glycol (EG)	0.253	[4]				
96	Sati et al. [166]	GC	5500	[166]	DI water-EGZnO (CuO)/graphene	0.02	50	26.00
		CuO	76.5	[4]				
		ZnO	29	[303]				
		Deionized (DI) water	0.606	[219]				
		Ethylene glycol	0.253	[4]				
97	Naiman et al. [167]	Al_2O_3	40	[4]	Al_2O_3/CNC-water/EG	0.90	70	
		Cellulose nanocrystal (CNC)	1.45	[167]				
		Water	0.613	[4]				
		Ethylene glycol (EG)	0.253	[4]				
98	Benedict et al. [168]	Al_2O_3	40	[4]	Al_2O_3/CNC-water/EG	0.90		
		TiO_2	8.4	[265]				
		Cellulose nanocrystal (CNC)	1.45	[314]				
		Distilled water (DW)	0.597	[112]	TiO_2/CNC-water/EG			
		Ethylene glycol (EG)	0.253	[4]				

Table 5: Continued.

S/N	References authors	Thermal conductivity (TC) of hybrid composite element (W m^{-1} K^{-1})			Observation summary			
		Material/base fluid	TC (K (W/m K))	Source	hnf with increased TC	ϕ (%)	T (°C)	Max % rise
99	Urmi et al. [71]	Al_2O_3	40	[4]	Al_2O_3/TiO_2-water/EG	0.10	80	40.86
		TiO_2	8.4	[265]				
		Water	0.6	[71]				
		Ethylene glycol (EG)	0.254	[71]				
100	Ramadhan et al. [315]	Al_2O_3	40	[45]	Al_2O_3-TiO_2-SiO_2/water/EG	3.00	70	27.00
		TiO_2	8.4	[45]				
		SiO_2	1.4	[45]				
		Water	0.613	[4]				
		Ethylene glycol (EG)	0.253	[4]				
101	Palanisamy et al. [316]	Al_2O_3	40	[45]	Al_2O_3-TiO_2-SiO_2/water	0.10	50	18.33
		TiO_2	8.4	[45]				
		SiO_2	1.4	[45]				
		Water	0.613	[4]				
102	Xian et al. [169]	GnP	~2200	[311]	GnP-TiO_2/water/EG	0.10	60	23.74
		TiO_2	8.4	[265]				
		Distilled water (DW)	0.597	[112]				
		Ethylene glycol (EG)	0.253	[4]				
103	Hamid et al. [170]	TiO_2	8.4	[265]	TiO_2-SiO_2/EG/water	3.00	70	22.10
		SiO_2	1.4–12	[88, 302]				
		Water	0.613	[4]				
		Ethylene glycol (EG)	0.253	[4]				
104	Hamid et al. [171]	TiO_2	8.4	[265]	TiO_2-SiO_2/EG/water	1.00	70	13.80
		SiO_2	1.4–12	[88, 302]				
		Water	0.613	[4]				
		Ethylene glycol (EG)	0.253	[4]				
105	Nabil et al. [172]	TiO_2	8.4	[265]	TiO_2-SiO_2/EG/water	3.00	30	3.70
		SiO_2	1.4–12	[88, 302]				
		Water	0.613	[4]				
		Ethylene glycol (EG)	0.253	[4]				
106	Nabil et al. [173]	TiO_2	8.4	[265]	TiO_2-SiO_2/EG/water	3.00	80	22.80
		SiO_2	1.4–12	[88, 302]				
		Water	0.613	[4]				
		Ethylene glycol (EG)	0.253	[4]				
107	Akhgar and Toghraie [32]	MWCNT	~3000	[4]	MWCNT-TiO_2/EG/water			38.70
		TiO_2	8.4	[88]				
		Water	0.613	[4]				
		Ethylene glycol (EG)	0.253	[4]				
108	Moradi et al. [174]	MWCNT	~3000	[4]	MWCNT-TiO_2/EG/water	1.00	60	34.31
		TiO_2	8.4	[265]				
		Water	0.613	[4]				
		Ethylene glycol (EG)	0.253	[4]				
109	Li et al. [175]	MWCNT	~3000	[4]	MWCNT-TiO_2/EG/water	1.00	50	56.48
		TiO_2	8.4	[265]				
		Water	0.613	[4]				
		Ethylene glycol (EG)	0.253	[4]				
110	Leong et al. [176]	Cu	401	[4]	Cu-TiO_2/EG/water			9.80
		TiO_2	8.4	[265]				
		Water	0.613	[4]				
		Ethylene glycol (EG)	0.253	[4]				
111	Amiri et al. [178]	Cu	401	[4]	MWCNT-SiO_2/EG/water			
		SiO_2	1.4–12	[88, 302]				
		Water	0.613	[4]				
		Ethylene glycol (EG)	0.253	[4]				
112	Tahat and Benim [179]	CuO	76.5	[4]	CuO-Al_2O_3/EG/water			
		Al_2O_3	40	[4]				
		Water	0.613	[4]				
		Ethylene glycol (EG)	0.253	[4]				

Table 5: Continued.

S/N	References authors	Thermal conductivity (TC) of hybrid composite element (W m^{-1} K^{-1})			Observation summary			
		Material/base fluid	TC (K (W/m K))	Source	hnf with increased TC	ϕ (%)	T (°C)	Max % rise
113	Bagheri and Nadooshan [180]	MWCNTs	1500	[180]	ZnO-MWCNT/EG-water			30.00
		ZnO	29	[180]				
		Water	0.6	[180]				
		Ethylene glycol (EG)	0.224	[180]				
114	Kakavandi and Akbari [181]	MWCNT	~3000	[4]	MWCNT-SiC/EG-water	0.75	50	33.00
		SiC	270	[4]				
		Water	0.613	[4]				
		Ethylene glycol (EG)	0.253	[4]				
115	Nikkam et al. [69]	SiC	270	[4]	SiC/SiO_2-water/EG	9.00		20.00
		SiO_2	1.4–12	[88, 302]				
		Water	0.613	[4]				
		Ethylene glycol (EG)	0.253	[4]				
116	Giwa et al. [72]	MgO	48	[237]	MgO-ZnO/water	0.10	50	22.33
		ZnO	29	[180]				
		Deionized (DI) water	0.606	[219]				
117	Vidhya et al. [182]	MgO	48	[237]	MgO-ZnO/EG-water	0.10	50	17.40
		ZnO	29	[180]				
		Water	0.613	[4]				
		Ethylene glycol (EG)	0.253	[4]				
118	Safaei et al. [183]	Co	96.4	[317]	$CoFe_2O_4$/SiO_2/EG-water			37.70
		Fe_2O_4	9.7	[297]				
		SiO_2	1.4–12	[88, 302]				
		Water	0.613	[4]				
		Ethylene glycol (EG)	0.253	[4]				
119	Sahoo and Sarkar [184]	Ag	429	[184]	Ag + Al_2O_3/EG/brine			4.00
		Cu	401	[184]				
		SiC	350	[184]				
		Al_2O_3	40	[184]				
		CuO	18	[184]				
		TiO_2	8.4	[184]				
		Water/brine (salt water)	0.6	[318]				
		Ethylene glycol (EG)	0.253	[4]				
120	Paul et al. [185]	Al	237	[4]	Al-Zn/EG	0.10	70	16.00
		Zn	116	[296]				
		Ethylene glycol (EG)	0.253	[4]				
121	Shirazi et al. [186]	MWNTs	~3000	[4]	MWNT-N-rGO/EG			10.16
		N-rGO	2–1000	[5]				
		Ethylene glycol (EG)	0.253	[4]				
122	Theres Baby and Sundara [187]	MWNT	~3000	[4]	Ag/MWNT-f-HEG/EG	0.08	25	8.00
		Ag	429	[3]				
		f-HEG	~10.9	[310]				
		Ethylene glycol (EG)	0.253	[4]				
123	Van Trinh et al. [97]	MWCNT	~3000	[4]	Gr-MWCNT/Cu	0.04	60	41.00
		Graphene (Gr)	~3000	[4]				
		Cu	401	[4]				
		Ethylene glycol (EG)	0.253	[4]				
124	Mbambo et al. [319]	Graphene (Gr)	3000–5000	[319]	GNs-AgNPs/EG		25–45	32.30
		Ag	429	[3]				
		Ethylene glycol (EG)	0.253	[4]				
125	Mbambo et al. [293]	Graphene (Gr)	3000–5000	[319]	GNs-AuNPs/EG		25–45	26.00
		Au	318	[52]				
		Ethylene glycol (EG)	0.253	[4]				
126	Parsian and Akbari [188]	Cu	401	[4]	Cu-Al_2O_3/EG	2.00	50	28.00
		Al_2O_3	40	[4]				
		Ethylene glycol (EG)	0.253	[4]				

Table 5: Continued.

S/N	References authors	Thermal conductivity (TC) of hybrid composite element (W m^{-1} K^{-1})			Observation summary			
		Material/base fluid	TC (K (W/m K))	Source	hnf with increased TC	ϕ (%)	T (°C)	Max % rise
		MWCNTs	1500–3000	[189]				
127	Harandi et al. [189]	Fe_3O_4	9.7	[236]	MWCNT-Fe_3O_4/EG	2.30	50	3.00
		Ethylene glycol (EG)	0.249	[189]				
		MWCNT	~3000	[4]				
128	Vafaei and Afrand [190]	MgO	48	[237]	MWCNT-MgO/EG			23.30
		Ethylene glycol (EG)	0.253	[4]				
		MWCNT	~3000	[4]				
129	Vafaei et al. [191]	MgO	48	[237]	MWCNT-MgO/EG			
		Ethylene glycol (EG)	0.253	[4]				
		FMWCNTs	~3000	[4]				
130	Afrand [192]	MgO	~50	[192]	FMWCNT-MgO/EG	0.60	25	21.30
		Ethylene glycol (EG)	~0.25	[192]				
		SWCNTs	3000–6000	[4]				
131	Esfe et al. [193]	MgO	48	[237]	SWCNT-MgO/EG			1.00
		Ethylene glycol (EG)	0.253	[4]				
		SWCNT	50–200	[194]				
132	Esfe et al. [194]	MgO	54.9	[296]	MWCNT-MgO/EG	0.55	50	>35
		Ethylene glycol (EG)	0.252	[296]				
		DWCNT	>2000	[313]				
133	Esfe et al. [195]	SiO_2	1.4–12	[88, 302]	DWCNT-SiO_2/EG	1.71	50	38.00
		Ethylene glycol (EG)	0.253	[4]				
		MWCNT	1500	[196]				
134	Esfe et al. [196]	SiO_2	1.4–12	[88, 302]	MWCNT-SiO_2/EG	0.86	50	20.10
		Ethylene glycol (EG)	0.253	[4]				
		MWCNT	1500	[196]				
135	Rostami et al. [260]	TiO_2	8.4	[265]	MWCNT-TiO_2/EG	1.00	50	25.18
		Ethylene glycol (EG)	0.253	[4]				
		MWCNTs	~3000	[4]				
136	Li et al. [197]	SiC	490	[296]	DWCNT-SiC/EG	0.40	50	32.01
		Ethylene glycol (EG)	0.256	[197]				
		MWCNT	~3000	[4]				
137	Arani and Pourmoghadam [198]	Al_2O_3	40	[4]	MWCNT-Al_2O_3/EG	0.80	50	17.00
		Ethylene glycol (EG)	0.253	[4]				
		MWCNT	~3000	[4]				
138	Esfe et al. [199]	ZnO	29	[303]	MWCNT-ZnO/EG	1.00	50	
		Ethylene glycol (EG)	0.253	[4]				
		ZnO	29	[303]				
139	Toghraie et al. [200]	TiO_2	8.4	[265]	ZnO-TiO_2/EG	3.50	50	32.00
		Ethylene glycol (EG)	0.253	[4]				
		ZnO	29	[303]				
140	Rubasingh et al. [201]	TiO_2	8.4	[265]	ZnO-TiO_2/EG	08.00	90	34.00
		Ethylene glycol (EG)	0.253	[4]				
		TiO_2	8.4	[265]				
141	Hamid et al. [202]	SiO_2	1.4–12	[88, 302]	TiO_2-SiO_2/EG	1.00		16.00
		Ethylene glycol (EG)	0.253	[4]				
		GO	2–1000	[5]				
142	Yarmand et al. [203]	Activated C	0.63	[320]	ACG/EG	0.06	40	6.47
		Ethylene glycol (EG)	0.253	[4]				
		CuO	76.5	[4]				
143	Akilu et al. [204]	TiO_2	8.4	[265]	TiO_2-CuO/CEG	2.00	60.1	16.70
		C	1.7	[263]				
		Ethylene glycol (EG)	0.253	[4]				
144	Hussein [205]	AIN	8.4	[205]	AIN/EG	4.00	50	
		Pure EG	0.26	[205]				
		CuO	76.5	[4]				
145	Kannaiyan et al. [206]	Al_2O_3	40	[4]	CuO-Al_2O_3/EG			45.00
		Ethylene glycol (EG)	0.253	[4]				

Table 5: Continued.

S/N	References authors	Thermal conductivity (TC) of hybrid composite element (W m^{-1} K^{-1})			Observation summary			
		Material/base fluid	TC (K (W/m K))	Source	hnf with increased TC	ϕ (%)	T (°C)	Max % rise
146	Mehrali a et al. [207]	GO	1000	[156]	GO-Fe_3O_4/EG			
		Fe_3O_4	9.7	[236]				
		Ethylene glycol (EG)	0.253	[4]				
147	Sadeghinezhad et al. [208]	GO	1000	[156]	GO-Fe_3O_4/EG			11.00
		Fe_3O_4	9.7	[236]				
		Ethylene glycol (EG)	0.253	[4]				
148	Van Trinh et al. [209]	Graphene (Gr)	~3000	[4]	Gr-CNT/EG		30–50	18.00
		CNT	~2000–4000	[6]				
		Ethylene glycol (EG)	0.253	[4]				
149	Amini et al. [210]	MWCNT	1500	[210]	MWCNT-SiO_2/glycerol	2.00	50	16.70
		SiO_2	1.3	[210]				
		Glycerol	0.275	[210]				
150	Han et al. [211]	CNT	~2000–4000	[6]	CNT-Al_2O_3/PAO	0.20	10	20.50
		Al_2O_3	40	[4]				
		Poly-alpha-olefins (PAO)	0.1434	[211]				
151	Chandran et al. [212]	ZnO	29	[303]	ZnO-paraffin wax/propylene gylcol/water	0.613		10.40
		Encapsulated paraffin wax	0.15	[55]				
		Propylene glycol	0.1962	[321]				
		Water	0.613	[4]				
152	Zawawi et al. [213]	Al_2O_3	40	[4]	Al_2O_3-SiO_2/polyalkylene glycol	0.10	30	2.41
		SiO_2	1.4–12	[88, 302]				
		Polyalkylene glycol	0.156	[322]				
153	Botha et al. [214]	Ag	429	[3]	Ag-SiO_2/oil			15.00
		SiO_2	1.4	[214]				
		Transformer oil	0.136	[214]				
154	Choi et al. [215]	AIN	285	[214]	AIN-Al_2O_3/oil	0.50		8.00
		Al_2O_3	40	[4]				
		Transformer oil	0.11	[214]				
155	Aberoumand and Jafarimoghaddam [221]	Ag	429	[3]	Ag-WO_3/oil	4.00	100	41.00
		WO_3	1.6	[235]				
		Transformer oil	0.11	[214]				
156	Asadi et al. [223]	MWCNT	1500	[224]	MWCNT-Al_2O_3/oil	1.50	50	45.00
		Al_2O_3	36	[224]				
		Thermal oil (TO)	0.1891	[220]				
157	Asadi et al. [224]	MWCNT	3000	[4]	MWCNT-MgO/oil	2.00	50	65.00
		MgO	48	[323]				
		Thermal oil (TO)	0.1891	[220]				
158	Asadi et al. [225]	MWCNT	~3000	[4]	MWCNT-$Mg(OH)_2$/oil	2.00	60	50.00
		$Mg(OH)_2$	0.16	[323]				
		Engine oil	0.145	[4]				
159	Soltani et al. [226]	MWcNTs	~3000	[4]	MWcNT-WO_3/oil	0.60	60	19.85
		WO_3	1.6	[235]				
		Engine oil	0.145	[4]				
160	Tian et al. [227]	MWCNT	~3000	[4]	MWCNT-Al_2O_3/oil	1.00	65	30.53
		Al_2O_3	40	[4]				
		Engine oil	0.145	[4]				
161	Sulgani and Karimipour [228]	Al_2O_3	40	[4]	MWCNT-Al_2O_3/oil	4.00	65	33.00
		Fe_2O_3	7	[303]				
		Engine oil	0.145	[4]				
162	Qing et al. [229]	Graphene (Gr)	~3000	[4]	Gr-SiO_2/oil	0.04	100	80.00
		SiO_2	1.4–12	[302]				
		Naphthenic oil	0.133	[218]				
163	Askari et al. [230]	Graphene (Gr)	~3000	[4]	Gr-Fe_3O_4/kerosene		50	
		Fe_3O_4	9.7	[236]				
		Kerosene	0.15	[236]				

Table 5: Continued.

S/N	References authors	Thermal conductivity (TC) of hybrid composite element (W m^{-1} K^{-1})			Observation summary			
		Material/base fluid	TC (K (W/m K))	Source	hnf with increased TC	ϕ (%)	T (°C)	Max % rise
164	Wei et al. [222]	SiC	220	[222]	SiC-TiO_2/diathermic oil	1.00	20	8.39
		TiO_2	8.4	[222]				
		Diathermic oil (DO)	0.119	[219]				
165	Gulzar et al. [231]	Al_2O_3	40	[4]	Al_2O_3-TiO_2/ Therminol-55	0.50	158.07	33.50
		TiO_2	8.4	[265]				
		Therminol-55	0.135	[324]				
166	Mechiri et al. [233]	Cu	401	[4]	Cu-Zn/vegetable oil		30	
		Zn	116	[296]				
		Vegetable oil	0.162	[216]				
167	Kumar et al. [216]	Cu	401	[4]	Cu-SiO_2/vegetable Oil	0.50	30	48.00
		Zn	116	[296]				
		Vegetable oil	0.162	[216]				
		Paraffin oil	0.136	[216]				
		SAE oil	0.133	[216]				
168	Parameshwaran et al. [234]	Ag	429	[4]	Ag-TiO_2/PCM			52.00
		TiO_2	8.4	[265]				
		PCM	0.257	[234]				
169	Jaiswal et al. [68]	Cu	401	[4]	Cu-Pd		80	18.79
		Palladium (Pd)	71.8	[54]				

Note. Bold cells indicate possible active material(s) in the blend, attachment nanoparticles to core nanoparticles, that are likely to influence the TC enhancement of the hybrid nanofluids.

carried out similar studies with Al_2O_3/deionized (DI) water and registered 79.36% for 0.1 wt.%. Yarmand et al. [91], in their trial, considered thermal conductivity of functionalized graphene nanoplatelets (GNP-Ag). They observed that the boost in GNP's effective thermal conductivity-Ag/water was uniform with increasing weight concentration of GNP-Ag nanoparticles and rise in temperature. Analogous thermal conductivity enhancement results were obtained using distilled water (DW) and CNT-TiO_2 [125], CNT-SiO_2 [126], ND-Ni [127], and also with MgO-TiO_2 ceramic matrix [128]. Esfe et al. [66] investigated Ag-MgO/water hybrid nanofluid for a range of 0.5–2.0% (50% Ag and 50% MgO) by volume concentrations of nanoparticles. Findings from the author's report indicated a rise in the thermal conductivity of nanofluid with an increase in nanoparticles. Batmunkh et al. [129] experimented with TiO_2 nanoparticles based on aqueous nanofluids by adding silver (Ag) nanoparticles as a modifier. The results obtained indicated that the thermal conductivity of TiO_2-based solutions could be enhanced by introducing the flattened "Ag" particles. Madhesh and Kalaiselvam [59] experimentally dissolved copper-titania hybrid nanocomposite in pure fluid (Cu-TiO_2/water) for use as a coolant. The result showed that the thermal conductivity of hybrid nanofluid increased with the nanocomposite volume concentration and the nanofluid temperature. The copper nanoparticles on the titania surface acted as the thermal boundary between the host liquid and the wall surfaces, which prompted the nanofluid's thermal conductivity enrichment. Madhesh et al. [130] also recorded the thermal conductivity of (Cu-TiO_2/water) hybrid nanofluid in a counterflow heat exchanger as a function of temperature and solid volume concentration. Authors credited this phenomenon to the configuration of Cu nanoparticles on the face of Al_2O_3 nanoparticles, hence forming a thermal interfacial synchronization between the nanoparticles and fluid, which promotes heat transfer. Nine et al. [62] dispersed Cu_2O and Cu/Cu_2O nanoparticles with water. The result shows that the thermal conductivity of hybridized nanofluids (containing both Cu and Cu_2O) nanoparticles exhibited maximum thermal enhancement compared to nanofluids containing Cu nanoparticles or Cu_2O nanoparticles separately. This implies that Cu-Cu_2O nanoparticles enhance collisions amid nanoparticles during Brownian motion. A similar report was presented by Ranga Babu et al. [131] using Cu and Cu_2O nanoparticles. Theres Baby and Sundara [65] achieved comparable results for trihybrid nanofluids of $Fe_2O_3 + SiO_2$-MWCNT/water. Shahsavar et al. [132] emulsified and dispersed Fe_3O_4-CNT particles using gum arabic and tetramethylammonium hydroxide. However, they observed that the addition of gum arabic (GA) coated with CNT nanofluid enhanced the thermal conductivity of the aqueous nanofluid containing tetramethylammonium hydroxide- (TMAH-) coated Fe_3O_4 nanoparticles. Enrichment in thermal conductivity was also reported in repeated work by Shahsavar et al. [67, 133] and Shahsavar and Bahiraei [134]. Similarly, Syam Sundar et al. [135] attained a 13.88% augmentation in the thermal conductivity of hybrid nanofluid at 0.3% solid volume fraction (ϕ) and 20°C, which further improved to 28.46% at 60°C. Chen et al. [63] studied the thermal conductivity of hybrid nanofluid by changing the solid volume fraction of iron oxide in the solid-liquid composite employing water as the host fluid. The result showed 27.7% augmentation in thermal conductivity. This was, however, attained with 0.02 wt.%

Fe_2O_3 and 0.05% MWCNTs. Furthermore, at an increase in volume concentration of Fe_2O_3 nanoparticles above 0.02%, the thermal conductivity decreased, resulting from excess clustering of nanoparticles [136]. Sundar et al. [64] reported a similar experiment and results with MWCNT-Fe_3O_4/water hybrid nanofluids and confirmed that thermal conductivity was thus enhanced by 29% with 0.3% particle concentration in the base fluid at a temperature of 60°C. Munkhbayar et al. [61] noticed the highest thermal conductivity enrichment of 14.5% at 40°C for 0.05 wt.% of MWCNTs and 3 wt% of Ag composite water blend. MWCNTs functionalized with gum arabic (MWCNT-GA), functionalized with cysteine (MWCNT-Cys), and blended with Ag (MWCNT-Ag) nanoparticles were studied by Amiri et al. [137]. Studies show higher thermal conductivity for MWCNT-Ag because of the higher thermal conductivity of silver nanoparticles (Figure 4). Chen et al. [138] looked at the effect of reducing time on the thermal conductivity of a water-based hybrid nanofluid containing MWCNTs adorned with Ag nanoparticles during formation. As the times are reduced by 0.5, 1, and 1.5 h, a maximum enrichment in thermal conductivity of about 24% was then obtained for 65°C at a 1.5 h reducing time. Farbod and Ahangarpour [139] obtained a similar result. Sinz et al. [140] likewise reported a rise in thermal conductivity for hybridized silver (Ag) and hydrogen exfoliated graphene (HEG) in water (i.e., Ag-HEG/water). A comparable experimental result was also realized when Yarmand et al. [141] considered graphene/nanoplatelet/platinum (GNP-Pt) hybridized nanofluids. Ahammed et al. [142] investigated graphene-alumina-Gr-Al_2O_3 streaming in a two-pass multiport minichannel. At 50°C, for 0.1 vol% graphene nanofluid and hybrid nanofluid, a better enhancement in thermal conductivity of 26.92% was observed for graphene nanofluids than that of hybrid nanofluid, which was 13.84%. However, a better result was obtained in later work when Taherialekouhi et al. [108] activated GO-Al_2O_3 nanoparticles in distilled water. Similar study reports were also given for water and Cu-Al_2O_3 [107]. Table 5 [143–150] provides more extensions of other analogous works. Sundar et al. [151] in their experiment to verify the thermal conductivity of nanodiamond ND-Co_3O_4/water, ND-Co_3O_4/ethylene glycol (EG), and dispersed synthesized ND-Co_3O_4 nanocomposite in water-ethylene glycol (EG/water) mixtures. The mixture ratio was 20 : 80, 40 : 60, and 60 : 40, and volume concentrations of ND-Co_3O_4 nanoparticles were 0.05%, 0.10%, and 0.15% correspondingly and then tested at a varying temperature range of 20–60°C. According to trial results, thermal conductivity enhancements for water, EG, 20 : 80%, 40 : 60%, and 60 : 40% EG/W-based nanofluids at 0.15 wt.% concentrations and 60°C are approximately 16%, 9%, 14%, and 10%, respectively. Sundar et al. [152] and Sundar et al. [153] reported comparable experimental results using ND + Fe_3O_4 hybrid nanofluid. Sundar et al. [154] presented a stable magnetic hybrid nanofluid composed of carboxylated nanodiamond (c-ND) and nickel (Ni) nanoparticles in ethylene glycol (EG) and water blend. However, with water at 60°C and 3.03% weight, a maximum thermal conductivity augmentation of 21% was achieved. In their study, Oliveira et al. [155] also looked at ND-Ag/EG. They recorded a significant increment in the thermal conductivity of hybridized nanofluid. In their investigations, some other authors [156, 157] also looked at carbonaceous materials blended with ceramics. Chopkar et al. [96] synthesized Al_2Cu and Ag_2Al water hybrid nanofluids for investigation. They observed that at a 1% volume concentration of Al_2Cu/water base nanofluid, a 70% augmentation in thermal conductivity was then attained compared to pure liquid. More so, cylindrical and platelet-shaped hybrid nanoparticles gave higher augmentation than those of spherical nanoparticles. However, a high augmentation was registered for Ag_2Al water-based nanofluid compared with Al_2Cu nanofluid. This enhancement is due to silver's higher thermal conductivity property (Figure 4) compared to copper. Jha and Ramaprabhu [53] synthesized copper nanoparticle-stacked multiwalled carbon nanotubes-(Cu/MWCNTs-) based nanofluids by scattering Cu/MWCNTs in deionized (DI) water and ethylene glycol (EG) polar base fluids without surfactant. The outcomes indicated that all properly suspended Cu/MWCNTs nanofluids with a change in concentration of Cu/MWCNTs could be blended using the present technique. However, most thermal conductivity at a shallow volume concentration of Cu/MWCNTs was nevertheless recorded due to the homogeneous scattering of Cu laced with MWCNTs in building-based liquid and the arrangement of increasing hydrophilic MWCNTs. Jha and Ramaprabhu [54] again considered MWCNTs laced with silver, gold, and palladium and dispersed separately in EG and DI water. Since silver's thermal conductivity was the highest among the chosen metals, Ag-MWCNTs exhibited an optimum enhancement in thermal conductivity of about 37.3% for DI water and 11.3% for EG. DI water-based nanofluid displayed more enhancement than EG-based nanofluid. This was due to the fact that thermal energy is transferred more easily in water than in EG [158]. Baby and Ramaprabhu [159] completed investigations of carbon nanohybrid-dispersed thermal transport properties in deionized (DI) water and ethylene glycol (EG) separately. The resultant blend's thermal conductivity was measured at different temperatures for various volume concentrations of functionalized multiwalled carbon nanotubes and functionalized hydrogen exfoliated graphene (f-MWCNT + f-HEG). The hybrid nanostructure spread in deionized (DI) water-based nanofluid displays a good thermal conductivity improvement of 20% for volume fractions not greater than 0.05%. Baby and Ramaprabhu [160] synthesized silver with functionalized (Ag/HEG) nanofluids in deionized (DI) water and ethylene glycol (EG). The results of the thermal properties studied showed an enhancement in the corresponding values compared to host liquid. At 25°C, hybridized fluid showed an 25% increase in thermal conductivity for a 0.05% volume fraction (ϕ). Munkhbayar et al. [61] noticed the highest thermal conductivity enrichment of 14.5% at 40°C for 0.05 wt.% of MWCNTs and 3wt% of Ag composite water blend. Baby and Sundara [161] synthesized copper oxide decorated hydrogen-induced exfoliated graphene (CuO/HEG) scattered in deionized (DI) water and ethylene glycol (EG) in a solid volume fraction of 0.05% and 0.01%. The study results show

that at 0.05% volume concentration, there is a 28% and 90% increase in thermal conductivity at 25°C and 50°C, respectively. Jyothirmayee Aravind and Ramaprabhu [94] blended graphene- (Gr-) enfolded multiwalled carbon nanotubes (Gr-MWNT) dispersed nanofluids for heat transfer applications using deionized (DI) water and ethylene glycol (EG) as the building base fluid. They obtained an enhancement in thermal conductivity of 11.3% and 13.7% with a 0.04% volume fraction of hybrid composite based on deionized (DI) water and EG nanofluids at 25°C. Aravind and Ramaprabhu [162] studied the thermal conductivity augmentation of synthesized graphene-multiwalled carbon nanotube (MWCNT) composites. For deionized (DI) water-based nanofluid, they obtained 10.5% and 87.9% enhancement for the solid volume fraction of 0.04 at temperatures between 25°C and 50°C, respectively, for deionized (DI) water-based nanofluid. For the ethylene glycol (EG) base fluid, 13.7% and 24% were also reported at the same volume concentration and temperature. Because MWCNTs retain a high aspect ratio, they can be firmly attached to graphene to limit the interfacial resistance, and so, hybrids (Gr/MWCNT) show better thermal conductivity than single mono (Gr) nanofluid. Shende and Sundara [163] investigated the use of nitrogen-doped hybrid carbon-based composites, N-(rGO-MWNTs), dispersed in nanofluids as a working fluid for low-temperature direct absorption solar collectors (DASC). They achieved a substantial augmentation in thermal conductivity of 17.7% with a 0.02% volume fraction in deionized (DI) water and 15.1% with a 0.03% volume fraction in ethylene glycol (EG). Esfe et al. [164] established that the thermal conductivity of functionalized DWCNT-ZnO/water-EG (60 : 40) hybridized nanofluids was nevertheless enhanced by 32% with 1.0 wt.% at 50°C. Esfe et al. [165] measured enhanced thermal conductivity of 24.9% for 1.90wt% at 50°C in another trial using DWCNT-ZnO/water. Other authors also undertook other analogous works, as given in Table 5 [166–177]. Amiri et al. [178] prepared SiO_2-Cu/water and SiO_2-Cu/EG nanofluids and then measured them in three volume concentrations of 1.0, 0.50, and 0.25% of the SiO_2-Cu nanoparticles and analyzed them at a varying temperature range of 20–40°C. The resultant outcome was the chemical deposition of a small quantity of Cu (approximately 8 percent) on the SiO_2 surface, bringing about a significant increase in the hybrid nanofluid's thermal conductivity. Several other researchers [179–184] looked at various works based on binary base liquid (EG/water).

Paul et al. [185] synthesized Al-5wt% Zn nanoparticles in ethylene glycol (EG) base fluid. The results showed a thermal conductivity enhancement of 16% at 0.1% volume concentration, which was comparable with results presented by Chakraborty et al. [46] with Cu-Au nanoparticles in water. Seyed Shirazi et al. [186] also synthesized nitrogen-doped activated carbon/graphene with a high nitrogen level, yielding nitrogen-activated carbon graphene (NACG), and recorded a significant augmentation in thermal conductivity of 10.16%. Compared with the result reported by Shende and Sundara [163] in a similar experiment with deionized (DI) water, this result showed that thermal conductivity enrichment was better with water. Theres Baby and Sundara [187] synthesized a hybrid nanostructure with silver (Ag) nanoparticles, multiwalled carbon nanotubes (MWCNT), and hydrogen exfoliated graphene (HEG)-Ag/(MWNT-HEG), dispersed in ethylene glycol (EG). The result shows an augmentation of 8% in thermal conductivity attained for a solid volume fraction (ϕ) of 0.04% at 25°C. Other authors [188–210] also attempted similar research.

Han et al. [211] considered the thermal conductivity of a multilayered hybrid sphere/carbon nanotube (CNT), consisting of various 2 μm CNTs affixed to a 70 nm alumina/iron oxide sphere with poly-alpha-olefin (PAO) oil nanofluids as the building base fluid at a temperature range of 10–90°C. They noticed a 21% enhancement in thermal conductivity in PAO oil-based hybrid sphere/CNT nanofluids, with a solid volume fraction (ϕ) of 0.2% at room temperature. Furthermore, they mentioned that the Brownian motion effect was evident in the case of the spherical type of nanoparticles. As for the comparison with other nanoparticles, it was thus observed that the effective thermal conductivity augmentation of the solid-liquid composite is higher than specimens containing spherical nanoparticles. Chandran et al. [212] experimented with ceramics in propylene glycol/water base liquid, and Zawawi et al. [213] looked at double ceramics in polyalkylene glycol as the host fluid. Botha et al. [214] blended transformer oil-based nanofluid with silica and silver upheld on silica (Ag-SiO_2/Oil). Thermal conductivity was observed to increase with silica concentration as 0.60 wt.% of silver (Ag) nanoparticles deposited on 0.07 wt.% of silica (SiO_2), causing a shorter phonon passage distance amid the nanoparticles. Choi et al. [215] prepared three types of nanofluids by dispersing aluminium oxide (Al_2O_3) and aluminium nitride (AlN) nanoparticles in transformer oil. The thermal conductivity of Al_2O_3/AIN hybrid nanofluid increases with particle volume fraction. The result also states that AlN nanoparticles at 0.5% volume concentration can increase the thermal conductivity of the transformer oil (Figure 10) by 8%. Furthermore, the overall heat transfer coefficient has been increased by 20%. In another study, improvement in the thermal conductivity of hybrid nanofluid was also registered by Aberoumand and Jafarimoghaddam [221], with Ag-WO_3/transformer oil. Another similar research with engine oil, naphthenic oil, kerosene, diathermic oil (DO), Therminol-55, paraffin oil, and SAE oil as host fluids was also considered by other authors [222–231], as given in Table 5. Mechiri et al. [232] completed an experimental work on Cu-Zn hybrid nanoparticles using the following formations (0 : 100, 75 : 25, 50 : 50, 25 : 75, and 100 : 0) to prepare nanofluids by spreading them into vegetable oils as accommodating fluid. Experimentally, the thermal conductivity of the host liquid and nanofluids with different nanoparticle loadings at varying temperatures was measured. The products showed an increase in the thermal conductivity of nanofluids with an increase in hybrid nanoparticle concentration with a temperature rise. Modified work was repeated by Mechiri et al. [233] using Cu-Zn hybrid nanoparticles. Analogous research was also carried out by Kumar et al. [216]. They compared Cu-Zn in

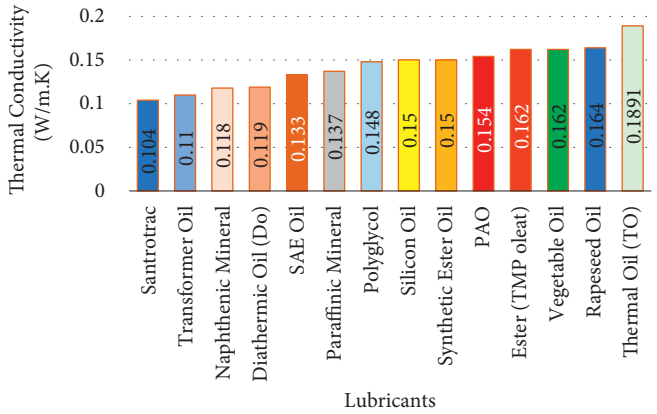

Figure 10: Thermal conductivities of various lubricants at 300 K [4, 214, 216–220].

vegetable oil, paraffin oil, and SAE oil hybridized nanofluids separately and reported that Cu-Zu/vegetable oil gave more thermal conductivity.

Parameshwaran et al. [234] in their work on new organic ester phase change material (PCM) embedded with silver-titania hybrid nanocomposite (Ag-TiO_2 HyNC) concluded that HyNPCM embedded with the surface-functionalized HyNC exhibited improved thermal conductivity by up to 52%. Moreover, the thermal conductivity of hybrid nanofluids was also investigated experimentally by Esfe et al. [90] after dispersing Cu and TiO_2 nanoparticles of a mean diameter of 70 and 40 nm in a dual blend of water and EG (60 : 40), measured at several particle loadings (0.1, 0.2, 0.4, 0.8, 1, 1.5, and 2%) and temperatures varying from 30 to 60°C. The results showed that the blend's thermal conductivity increased with an increase in nanoparticles and temperature concentration. Similar research has also been presented in the literature (Table 5). However, Zhao et al. [235] synthesized $CoSb_3/WO_3$ nanocomposites and observed decreased thermal conductivity of composites which resulted from phonon dispersion by WO_3. This showed that the thermal conductivity of nanofluids depends upon the suspension of solid particles and the choice of carrier fluids [236].

Generally, another research on the thermal conductivity of hybrid nanofluids (in the form of binary/dual and ternary/trihybrid nanofluids) within the last decade has nevertheless been very revealing. Their findings are given in Table 5. The results tabulated in Table 5 follow this order: water-based hybrid nanofluids and analogous experimental works (rows 1–74), water/EG-based hybrid nanofluids and comparable experimental works (rows 75–117), EG-based hybrid nanofluids, similar experimental works (rows 118–147), and finally, oil-based hybrid nanofluids and comparable experimental results (rows 148–168). However, recently, several aqueous, nonaqueous, and organic/oleic nanofluids have been tentatively contemplated [237]. These nanofluids have been explored with diverse particle shapes and sizes [238], volume fractions, sundry surfactants, and production approaches [237]. Most of the studies have demonstrated that hybrid nanofluids have the same trend of behavior as nanofluids in terms of the effect of changes in temperature and volume concentration. Therefore, using these nanocomposite and carrier fluid combinations can improve the thermal conductivity of hybrid nanofluids by increasing the concentration of hybrid nanoparticles and raising the temperature. However, temperature, according to some researchers [150, 164, 189, 239], has a greater influence on thermal conductivity than volume fraction.

4. Thermophysical Properties of Hybrid Nanofluids

4.1. Density and Specific Heat. Researchers have developed a model for determining some thermophysical properties of mono nanofluids that have been extrapolated to cover hybrid nanofluids. For example, the density of nanofluids depends on the physical principle of the mixture rule. This is thus denoted as [240]

$$\rho_{\text{eff}} = \left(\frac{m}{V}\right)_{\text{eff}} \frac{m_f + m_{\text{np}}}{V_f + V_{\text{np}}} = \frac{\rho_f V_f + \rho_{\text{np}} V_{\text{np}}}{V_f + V_{\text{np}}},$$

$$\rho_{\text{eff}} = 1 - \left(\frac{V_{\text{np}}}{V_f + V_{\text{np}}}\right)\rho_f + \left(\frac{V_{\text{np}}}{V_f + V_{\text{np}}}\right)\rho_{\text{np}}, \quad (1)$$

$$\rho_{\text{eff}} = (1 - \phi)\rho_f + (\phi)\rho_{\text{np}}.$$

For hybrid nanofluid (ρ_{hnf}) of two nanoparticles np1 and np2,

$$\rho_{\text{hnf}} = \left(\frac{m}{V}\right)_{\text{hnf}} = \frac{m_f + m_{\text{np1}} + m_{\text{np2}}}{V_f + V_{\text{np1}} + V_{\text{np2}}} = \frac{\rho_f V_f + \rho_{\text{np1}} V_{\text{np1}} + \rho_{\text{np2}} V_{\text{np2}}}{V_f + V_{\text{np1}} + V_{\text{np2}}},$$

$$\rho_{\text{hnf}} = 1 - \left(\frac{V_{\text{np1}} + V_{\text{np2}}}{V_f + V_{\text{np1}} + V_{\text{np2}}}\right)\rho_f + \left(\frac{V_{\text{np1}}}{V_f + V_{\text{np1}} + V_{\text{np2}}}\right)\rho_{\text{np1}} + \left(\frac{V_{\text{np2}}}{V_f + V_{\text{np1}} + V_{\text{np2}}}\right)\rho_{\text{np2}}, \quad (2)$$

$$\rho_{\text{hnf}} = \left(1 - \phi_{\text{np1}} - \phi_{\text{np2}}\right)\rho_f + \phi_{\text{np1}}\rho_{\text{np1}} + \phi_{\text{np2}}\rho_{\text{np2}},$$

where f and np refer to the fluid and nanoparticle, respectively, and $\phi_{\text{np}} = (V_{\text{np}}/V_f + V_{\text{np}})$ is the volume fraction of the nanoparticles [87]. While, ϕ_{np1} and ϕ_{np2} are the volume fractions of first and second nanoparticle. Ho et al. [55] tested a hybrid nanofluid made up of MEPCM and Al_2O_3 and found that the density could be accurately determined, with the aid of a mixing model.

The specific heat capacity is given as [87, 240]

$$\left(\rho C_p\right)_{\text{eff}} = \rho_{\text{nf}} \frac{\left(mC_p\right)_f \Delta T + \left(mC_p\right)_{\text{np}} \Delta T}{m_f \Delta T + \left(mC_p\right)_{\text{np}} \Delta T},$$

$$\left(\rho C_p\right)_{\text{nf}} = \rho_{\text{nf}} \frac{\left(mC_p\right)_f + \left(mC_p\right)_{\text{np}}}{m_f + m_{np}},$$

$$\left(\rho C_p\right)_{\text{nf}} = \rho_{\text{nf}} \frac{\left(\rho VC_p\right)_f + \left(\rho VC_p\right)_{np}}{\left(\left(m_f + m_{\text{np}}\right)/\left(V_f + V_{\text{np}}\right)\right) \times \left(V_f + V_{\text{np}}\right)}, \quad (3)$$

$$\left(\rho C_p\right)_{\text{hnf}} = \phi\left(\rho C_p\right)_{\text{np}} + (1 - \phi)\left(\rho C_p\right)_f,$$

where ρ_P is the density of the nanoparticle, ρ_f is the density of the base fluid, ρ_{eff} is the density of the nanofluid, and C_p and C_f are the heat capacities of the nanoparticle and the base fluid, respectively. For hybrid nanofluid of two nanoparticles np1 and np2,

$$\left(\rho C_p\right)_{\text{hnf}} = \rho_{\text{hnf}} \frac{\left(mC_p\right)_f \Delta T + \left(mC_p\right)_{\text{np1}} \Delta T + \left(mC_p\right)_{\text{np2}} \Delta T}{m_f \Delta T + \left(mC_p\right)_{\text{np1}} \Delta T + \left(mC_p\right)_{\text{np2}} \Delta T}, \quad (4)$$

$$\left(\rho C_p\right)_{\text{hnf}} = \rho_{\text{hnf}} \frac{\left(mC_p\right)_f + \left(mC_p\right)_{\text{np1}} + \left(mC_p\right)_{\text{np2}}}{m_f + \left(mC_p\right)_{\text{np1}} + \left(mC_p\right)_{\text{np2}}}, \quad (5)$$

$$\left(\rho C_p\right)_{\text{hnf}} = \rho_{\text{hnf}} \frac{\left(\rho VC_p\right)_f + \left(\rho VC_p\right)_{\text{np1}} + \left(\rho VC_p\right)_{\text{np2}}}{\left(\left(m_f + m_{\text{np1}} + m_{\text{np2}}\right)/\left(V_f + V_{\text{np1}} + V_{\text{np2}}\right)\right) \times \left(V_f + V_{\text{np1}} + V_{\text{np2}}\right)}, \quad (6)$$

$$\left(\rho C_p\right)_{\text{hnf}} = \phi_{\text{np1}}\left(\rho C_p\right)_{\text{np1}} + \phi_{\text{np2}}\left(\rho C_p\right)_{\text{np2}} + \left(1 - \phi_{\text{np1}} - \phi_{\text{np2}}\right)\left(\rho VC_p\right)_f, \quad (7)$$

where $(C_p)_f$ and $(C_p)_{\text{np}}$ are the heat capacities of the host liquid and nanofillers, respectively.

4.2. Viscosity. In 1906, Einstein considered a diluted solution of substances, a rigid sphere that does not dissociate in solution. Using hydrodynamic conditions, he expressed the viscosity as

$$\frac{k^*}{k} = 1 + 2.5\phi, \quad (8)$$

where k^* is the viscosity of the solution and k is the viscosity of the pure solvent.

Reexpressed at present as

$$\mu_{\text{eff}} = 1 + 25\phi\mu_f. \quad (9)$$

Since Einstein investigated the viscosity of a dilute suspension of rigid spheres in a viscous liquid, several equations (Table 6) have been established with the end goal of extending Einstein's formula to suspensions of higher concentrations, including the effect of nonspherical particle concentrations [87, 240].

The viscosity model formulated by Brinkman (equation (10)) [241], Krieger-Dougherty (equation (11)) [242], and others for higher particle volume fraction is thus also applicable for hybrid nanofluid.

$$\mu_{\text{hnf}} = \frac{\mu_f}{\left(1 - \phi_{\text{np1}}\right)^{2.5}\left(1 - \phi_{\text{np2}}\right)^{2.5}}, \tag{10}$$

$$\mu_{\text{hnf}} = \frac{\mu_f}{\left(1 - \phi_{\text{np1}} - \phi_{\text{np2}}\right)^{2.5}}. \tag{11}$$

The total volume fraction of the two different sorts of nanoparticles suspended in base fluid, denoted by ϕ, is computed using the following equation:

$$\phi = \phi_{\text{np1}} + \phi_{\text{np2}}. \tag{12}$$

To be effective in heat transfer applications, a base fluid must have high thermal conductivity and low viscosity. This is to avert pressure loss. Botha et al. [214] also recorded, after their investigation, that the viscosity of mixture nanofluid was lower than individual nanofluids. Dispersed particles in host liquid incorporate the advantages of increased thermal conductivity of both mono and composite fluids to keep viscosity low.

4.3. Thermal Conductivity. Currently, no consolidated or dependable theories or models consider all the core mechanisms and influence factors for the thermal conductivity of nanofluids (mono or hybrid). As reported by experiments, the important parameters that can influence the thermal conductivity of mono/hybrid nanofluid are as follows:

(i) Additives
(ii) Base fluid material
(iii) Nanoparticle concentration
(iv) Particle material
(v) Particle shape
(vi) Particle size
(vii) Acidity/pH value and
(viii) Temperature

Nonetheless, there exist a few semiempirical correlations for computing the apparent conductivity of two-phase mixtures. For example, Maxwell [248] proposed one of the first, most famous, and widely used models (effective medium theory, EMT) for solid-liquid mixtures with relatively large particles. However, it was based on the solution of the heat conduction equation through an arbitrary stationary suspension of spheres. As a result, the effective thermal conductivity was given by

$$\frac{k_{\text{nf}}}{k_f} = \frac{k_{\text{np}} + 2k_f + 2\phi\left(k_{\text{np}} - k_f\right)}{k_{\text{np}} + 2k_f - \phi\left(k_{\text{np}} - k_f\right)}, \tag{13}$$

where K_p is the thermal conductivity of the particles, K_f is the fluid thermal conductivity, and the modified Maxwell model for hybrid nanofluid is presented as

$$k_{\text{hnf}} = \frac{\left(\phi_{\text{np1}}k_{\text{np1+}}\phi_{\text{np2}}k_{\text{np2}}/\phi_{\text{np1}} + \phi_{\text{np2}}\right) + 2k_f + 2\left(\phi_{\text{np1}}k_{\text{np1+}}\phi_{\text{np2}}k_{\text{np2}}\right) - 2\left(\phi_{\text{np1}} + \phi_{\text{np2}}\right)k_f}{\left(\phi_{\text{np1}}k_{\text{np1+}}\phi_{\text{np2}}k_{\text{np2}}/\phi_{\text{np1}} + \phi_{\text{np2}}\right) + 2k_f - \left(\phi_{\text{np1}}k_{\text{np1+}}\phi_{\text{np2}}k_{\text{np2}}\right) - \left(\phi_{\text{np1}} + \phi_{\text{np2}}\right)k_f}, \tag{14}$$

where np1 k and np2 k are the thermal conductivities of primary and secondary nanoparticles.

4.4. Electrical Conductivity. Crystalline structure, electron mobility, and physical state (whether solid or liquid, single, or multiple phases) play a role in determining conductivity. Under a temperature difference, thermal conductivity evaluates how easily heat (thermal energy in motion) can travel through a substance. On the other hand, electrical conductivity measures how well electrical current (charge in motion) can travel through a substance when a voltage or electric field is applied. Electrons are the primary carriers of both electromotive force (flow of charge) and heat transfer (flow of thermal energy) in metals. Metal conductivities are thus determined by the number of loose electrons available to flow through the metal. Valence electrons that are not paired are known as "free or loose electrons." They are only loosely connected with the atomic nucleus in conductive metals. They are free to wander around within the metal. Metals' thermal and electrical conductivities share the same relative magnitude, determined by the number of free electrons available. It also depends on how tightly they are bound to the nucleus. As a result, if the electrical conductivity is high, so will the heat conductivity. This will enhance effective cooling. The crystalline structure of nonmetals plays a more significant role in determining thermal conductivity. Temperature evaluates the average kinetic energy of the vibrations of the individual atoms in the crystalline lattice. As an elastic wave of vibration (phonon waves), thermal energy can thus travel through the material. Some atomic configurations allow phonon waves to flow more easily than others. This is why the heat conductivity of nonmetals varies greatly depending on the crystalline structure. Pure carbon compounds, for example (Table 7), have variable degrees of conductivity. This varies by an order of magnitude

Table 6: Some of the models found in the literature.

Researchers	Viscosity of nanofluids	Remarks
Brinkman [241]	$(\mu_{\text{eff}}/\mu_f) = [1-\phi]^{2.5}$	Spherical particles
Krieger and Dougherty [242]	$(\mu_{\text{eff}}/\mu_f) = [\phi/\phi_m]^{-\eta\phi}$	Spherical particles
Lundgren [243]	$(\mu_{\text{eff}}/\mu_f) = [1 + 2.5\phi + (2.5/4)\phi^2 + f(\phi^3)]$	Moderate concentration
Batchelor [244]	$(\mu_{\text{eff}}/\mu_f) = [1 + 2.5\phi + 6.5\phi^2]$	Spherical particles
Bicerano et al. [245]	$(\mu_{\text{eff}}/\mu_f) = 1 + \eta\phi + k_h\phi^2$	
Nguyen et al. [246]	$(\mu_{\text{eff}}/\mu_f) = (2.1275 - 0.0215T + 0.00027T)$	Nonspherical particle concentrations
Sahu and Sarkar [247]	$\mu_{\text{hnf}} = ((\mu_{\text{nf1}}\phi_1 + \mu_{\text{nf2}}\phi_2/\phi))$	Different shaped particles

Table 7: Electrical and thermal conductivities of some carbon-based materials at 300 K.

Form of carbon	Electrical conductivity	Thermal conductivity (W/m K)
Graphite	2×10^5–3×10^5	110–190
Graphene	1.00×10^8	2000–5300
Diamond	1×10^{-11}–1×10^{-18}	900–2300
Carbon nanotubes	2.5×10^4–2×10^7	1800–4000

depending on the atomic arrangement. It is also worth noting that, while diamond is a near-perfect electrical insulator, it has the highest heat conductivity of any metal. Also, although having an identical electron arrangement, carbon nanotubes have a fairer electrical conductivity. They demonstrated better electron mobility in that crystalline form than graphite or diamond.

Computing enhancement in electrical conductivity $(\sigma_{\text{nf}}/\sigma_{\text{bf}})$ for nanofluid is expressed by the following relationship presented:

$$\frac{\sigma_{\text{nf}}}{\sigma_{\text{bf}}} = 1 + \frac{3(\sigma-1)\phi}{(\sigma+2)-(\sigma-1)\phi}, \tag{15}$$

where σ_{nf} is the electrical conductivity of the particles, σ_{bf} is the fluid electrical conductivity, and the modified Maxwell model for hybrid nanofluid is presented as

$$\frac{\sigma_{\text{nf}}}{\sigma_{\text{bf}}} = 1 + \frac{3\phi(\sigma_1\phi_1 + \sigma_2\phi_2 - \sigma_{\text{bf}}(\phi_1+\phi_2))}{(\sigma_1\phi_1 + \sigma_2\phi_2 + 2\phi\sigma_{\text{bf}}) - \phi\sigma_{\text{bf}}(\sigma_1\phi_1 + \sigma_2\phi_2) - \sigma_{\text{bf}}(\phi_1+\phi_2))}. \tag{16}$$

4.5. Thermal Expansion Coefficient. The thermal expansion coefficient for nanofluid is represented as

$$(\beta)_{\text{nf}} = \frac{\phi(\rho\beta)_{\text{np}} + (1-\phi)(\rho\beta)_f}{\rho_{\text{nf}}}, \tag{17}$$

where β_{np} and β_f correspondingly are the thermal expansion coefficients for the nanoparticles and the base fluid. For hybrid nanofluid,

$$(\rho\beta)_{\text{hnf}} = \left(1 - \phi_{\text{np1}} - \phi_{\text{np2}}\right)(\rho\beta)_f + \phi_{\text{np1}}(\rho\beta)_{\text{np1}} + \phi_{\text{np2}}(\rho\beta)_{\text{np2}}. \tag{18}$$

Again, β_{np1} and β_{np2} are the thermal expansion coefficients of the initial and additional nanoparticles.

Keblinski et al. [249] explored the possible factors for enhancing thermal conductivity in nanofluids and projected that the size effect, the clustering of nanoparticles, and the nanolayer at the solid/liquid interface could be the major contributions to the enhancement. However, their work was referenced in 2004 by Eastman et al. [250] where they shed additional insight on the effect of nanoparticle Brownian motion (Figure 11).

Several extensions to Maxwell's equation have been recorded since Maxwell's initial investigation. Maxwell's equation and other thermal conductivity expressions, such as Rayleigh [251] and Hamilton and Crosser [252], predicts thermal conductivity reasonably well for dilute mixtures of relatively large particles in liquids with lower particle volume fractions [87, 253]. Rayleigh [251] and Jeffrey [254] grouped the thermal conductivity models based on nanoparticles' arrangement and discovered that the clustered path of particles conducts more heat, hence higher thermal conductivity. Table 8 provides some of these model expressions, strengths, and areas of limitation.

A couple of scholars have established and derived some correlations for the thermal conductivity of hybrid nanofluids (Table 9). This is to help reduce errors and enhance precision in their investigation. Hybrid nanofluids can thus be used for various systems requiring heat transfer eventually. Sahu and Sarkar [247] proposed a mixture model (equation (19)) for the thermal conductivity of hybrid nanofluids of different shaped nanoparticles by interpolating the individual particle equation. Other specific equations are given in Table 9.

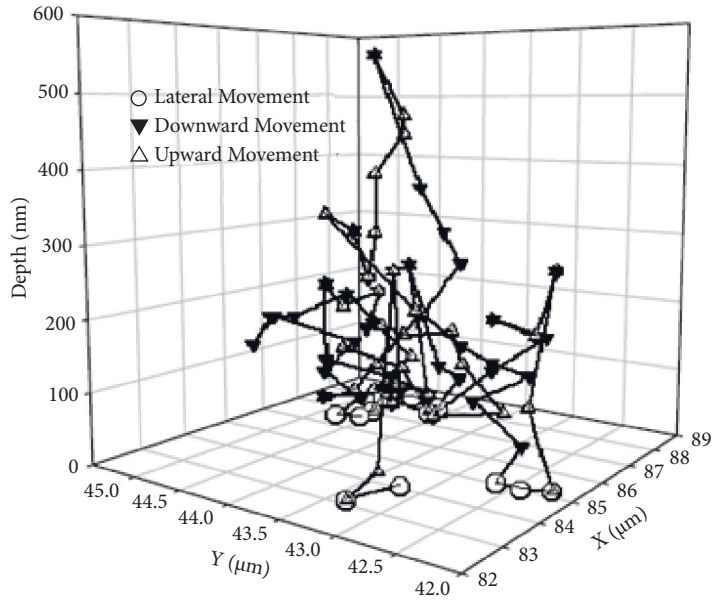

Brownian motion could have an important indirect rol in producing particle clustering, which could significantly enhance thermal conductivity.

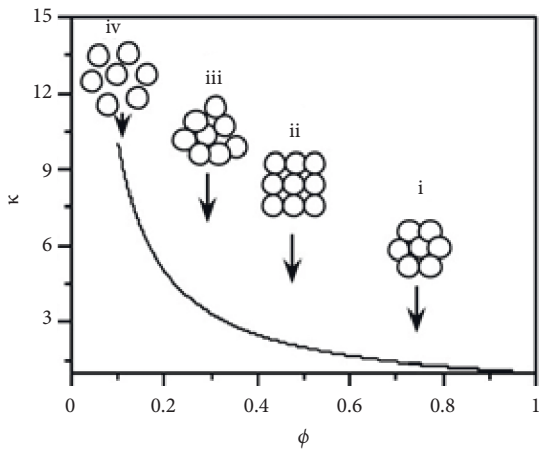

i (closely packed),
ii (simple cubic arrangement),
iii (loosely packed) and
iv (separated by layer thine enough).

Thermal conductivity k increases with decreasing parcking fraction ϕ as can be seen in iv.

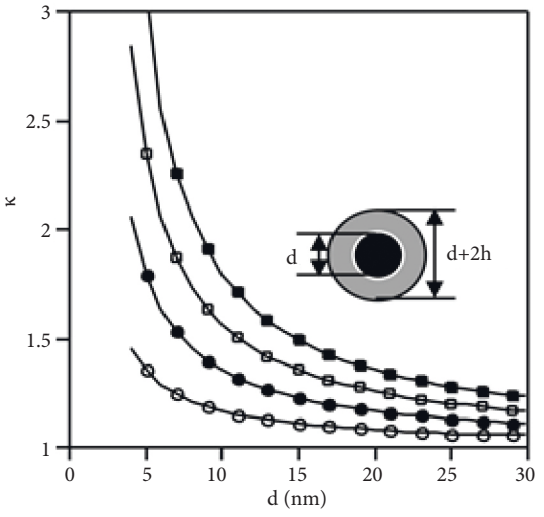

d= Nonoparticles Thermal Conductivity
(d+2h) - d = Base fluid Thermal Conductivity

Enhancement of k due to formation of highly conductive layer-liquid structure at the liquid/particle interface.

Figure 11: Schematic diagrams of the 3 significant possible mechanisms [249, 250].

$$\mu_{\text{hnf}} = \left(\frac{k_{\text{nf1}}\phi_1 + k_{\text{nf2}}\phi_2}{\phi} \right). \tag{19}$$

4.6. Relationships between Thermal Conductivity and Heat Transfer Performance. The thermal conductivity is directly proportional to its heat transmission performance. Convective heat transfer can be improved passively by changing boundary conditions, stream geometry, or by augmenting the thermal conductivity of the liquid. The influence of a property on heat transfer rates is frequently stated as a thermal conductivity value. Again, the most essential parameter responsible for the improved heat transfer is

Table 8: Established thermal conductivity of solid/liquid blends k_{eff}, thermal conductivity of base fluid k_f, thermal conductivity of particle k_p, thermal conductivity ratio $\alpha = k_p/k_f$, $\vartheta = (\alpha - 1)/(\alpha + 2)$, particle shape factor n, and particle volume fraction ϕ.

Models	Expressions	Remarks/limitations
Maxwell [248]	$(K_{\text{eff}}/K_f) = 1 + ((3(\alpha - 1)\phi)/(\alpha + 2) - (\alpha - 1)\phi)$	Accurate to order ϕ^1, uniformly sized spherical particles p is considered at low volume. Considerable deviation from measured experiment.
Rayleigh [251]	$(k_{\text{eff}}/k_f) = 1 + ((3\phi)/(((k_1 - 2k_f)/(k_1 - k_f)) - \phi + 1.569((k_1 - k_f)/(3k_1 - 4k_f))\phi^{10/3} + \cdots))$	Considered material in the form of spherical inclusions arranged in a simple cubic array. Far from reality for higher ϕ.
Hamilton and Crosser [252]	$(K_{\text{eff}}/K_f) = 1 + ((3(\alpha - 1)\phi)/((\alpha + 2) - (\alpha - 1)\phi))$, $(K_{\text{eff}}/K_f) = ((\alpha + (n - 1)(n - 1)((1 - \alpha)\phi)/(\alpha + (n = 1) + (1 - \alpha)\phi))$	Spherical and nonspherical particles p are considered: $n = 3$ for spheres and $n = 6$ for cylinders. Consider only shape and volume concentration.
Jeffrey [254]	$(k_{\text{eff}}/k_f) = 1 + 3\vartheta\phi(3\vartheta^2 + (3\vartheta^2/4) + (9\beta^2/16) + ((\alpha + 2)/(2\alpha + 3)) + \cdots)\phi^2$	Accurate to order ϕ^2, high-order terms represent pair interaction of randomly dispersed spheres
Davis [255]	$(K_{\text{eff}}/k_f) = ((3(\alpha - 1))/((\alpha + 2) - (\alpha - 1)\phi))[\phi + f(\alpha)\phi^2 + 0(\phi^3)]$	Accurate to order ϕ^2, high-order terms represent pair interaction of randomly dispersed spheres. $f(\alpha) = 2.5$ for $\alpha = 10$; $f(\alpha) = 0.5$ for $\alpha = \infty$
Lu and Lin [256]	$(k_{\text{eff}}/k_f) = 1 + \alpha.\phi + b.\phi^2$	Spherical and nonspherical particles p are considered. For spherical particles, $a = 2:25$, $b = 2:27$ for $\alpha = 10$; $a = 3:00$, $b = 4:51$ for $\alpha = \infty$
Bonnecaze and Brady [257, 258]	Numerical simulation	Near and far-field interactions among two or more particles p are considered. Numerical simulation, expressions not given.

thought to be thermal conductivity. Heat convention in the hybridized fluid matrix is one factor that leads to enhanced heat transmission. Knowing the thermal conductivities of the different materials that make up the hybridized fluids allows us to compare how well heat can be transferred. The higher the number for a given material, the faster heat will be transported through it. Metal-based nanofluids have better heat transfer performance than most fluids in ceramic make-up. Combining the two can significantly improve the thermal conductivity of ceramics. Effective heat transfer performance is a better indicator than effective thermal conductivity. Hence, it is the preferred marker for nanofluids used as coolants in transportation and other industries. The suspended nanoparticles alter the fluid's effective thermal conductivity (dependent on numerous elements such as shape, size, surfactant, pH, volume/weight fraction, and mass flow rate) and convective heat transfer coefficient, improving the nanofluid's heat transfer capability. When the heat transfer capacity of the working fluids is improved, the size of the heat exchanger is reduced, as is the fuel consumption rate, lowering CO_2 emissions.

5. Applications of Hybrid Nanofluids in Radiator Cooling Systems

Recently, the number of fields that have seen nanofluids' intrinsic potential and their demand for specific industrial applications seems to have grown [263]. Hybrid nanofluid has applications in diverse areas, which include but are not limited to the automobile industry (Figure 12) or heat transfer purposes only [265]. Thermal management is a significant factor in the automobile industry because it directly or indirectly impacts the general use of the automobile [266]. The efficiency with which a plethora of heat moves from the engine walls to the surrounding air is critical in enhancing engine performance and preserving the material

Table 9: Some empirical correlations for the thermal conductivity of hybrid nanofluids.

Model	Expression	Comment
Jana et al. [52]	$(k_{nf}/k_{bf}) = ((1-\phi + (4\phi/\pi)\sqrt{(k_p/k_{bf})}\arctan(\pi/4\sqrt{(k_p/k_{bf})}))/(1-\phi + (4\phi/\pi)\sqrt{(k_p/k_{bf})}\arctan(\pi/4\sqrt{k_{bf}/k_p})))$	CNTs-AuNP/water CNTs-CuNP/water
Esfe et al. [66]	$k_{nf} = k_{bf}((0.1747.10^5)/(0.1747.10^5 - 0.1498.10^6.\phi_P + 0.1117.10^7.\phi_P^2 + 0.1997.10^8.\phi_P^3))$	Ag + MgO/water (50% : 50%) $0 < \phi \leq 0:02$
Valan Arasu et al. [259]	$(k_{nf}/k_{bf}) = 1.146 - 0.852(\phi) - 0.0006T + 1.27538(\phi)^2 + 0.000007T^2 + 0.01422(\phi * T)$	TiO_2-Ag/water $0.1 < \phi \leq 0:4$, $35^\circ C \leq T \leq 60^\circ C$
Esfe et al. [90]	$(k_{nf}/k_{bf}) = 1.07 + 0.00589 \times T + (-0.000184/(T \times \phi)) + 4.44 \times T \times \phi \times \cos(6.11 + 0.00673 \times T + 4,41 \times T \times \phi - 0.0414\sin(T) - 32.5 \times \phi$	Cu-TiO_2/water-ethylene Glycol (60 : 40) $0 < \phi \leq 0:02$ $30^\circ C \leq T \leq 60^\circ C$
Esfe et al. [193]	$k_{nf} = k_{bf}(0.90844 - 0.6613\phi^{0.3}T^{0.7} + 0.01266\phi^{0.31}T)$	SWCNT-MgO/EG $0 < \phi \leq 0:02$ $30^\circ C \leq T \leq 50^\circ C$
Sarbolookzadeh Harandi et al. [189]	$k_{nf} = k_{bf}(1 + 0.0162\phi^{0.7038}T^{0.6009})$	MWCNTs-Fe_3O_4/ethylene glycol $0 < \phi \leq 0.023$ $25^\circ C \leq T \leq 50^\circ C$
Sundar et al. [152]	$k_{nf} = k_{bf}(a + b\phi)$ For $T = 20^\circ C$, $a = 1:0149$; $b = 0:2403$ $T = 30^\circ C$, $a = 1:0188$; $b = 0:3751$ $T = 40^\circ C$, $a = 1:0157$; $b = 0:4728$ $T = 50^\circ C$, $a = 1:0168$; $b = 0:5697$ $T = 60^\circ C$, $a = 1:0150$; $b = 0:6818$	ND-Fe_3O_4/water ND-Fe_3O_4/EG-water (20 : 80, 40 : 60, and 60 : 40) $0 < \phi \leq 0:002$ $20^\circ C \leq T \leq 60^\circ C$
Sundar et al. [151]	$k_{nf} = k_{bf}(0.9978(1+\phi)^{0.6556})$	ND-Co_3O_4/water ND-Co_3O_4/ethylene Glycol ND-Co_3O_4/EG-water (20 : 80, 40 : 60, and 60 : 40) $0 < \phi \leq 0:0015$ $20^\circ C \leq T \leq 60^\circ C$
Vafaei et al. [191]	$k_{nf} = k_{bf}(0.987 + \exp(0.3081\phi^{0.3097} - 0.2002T))$	MgO-MWCNTs/ethylene glycol $0 < \phi \leq 0:006$ $25^\circ C \leq T \leq 50^\circ C$
Afrand [192]	$k_{nf} = k_{bf}(0.8341 + 1.1\phi^{0.243}T^{-0.289})$	MgO-fMWCNT/ethylene Glycol $0 < \phi \leq 0:006$ $25^\circ C \leq T \leq 50^\circ C$

Table 9: Continued.

Model	Expression	Comment
Rostami et al. [260]	$(k_{nf}/k_{bf}) = 0.9969 - 0.001225T + 26.758\phi + 9.7434T\phi + 0.01505T^2 - 1157.438\phi^2$	MWCNTs-TiO_2/ethylene glycol $0.005 < \phi \leq 1$ $25^{\circ}C \leq T \leq 50^{\circ}C$
Esfahani et al. [150]	$(k_{nf}/k_{bf}) = 1 + 0.0008794\phi^{0.5899}T^{1.345}$	ZnO-Ag (50%–50%)/water for $25^{\circ}C \leq T \leq 50^{\circ}C$, $0\% \leq \phi \leq 2\%$
Bagheri and Ahmadi Nadooshan [180]	$(k_{nf}/k_{bf}) = ((0.8603 + 4.9806\phi^{0.2684} \cdot 0.0260.T^{0.3065})/(\exp(34.9071 \cdot \phi^2 \cdot t^{-17738}))$	ZnO-MWCNT/water-ethylene glycol (25%:75%) $0.1\% \leq \phi \leq 1.6\%$, $25^{\circ}C \leq t \leq 50^{\circ}C$
Moradi et al. [174]	$(k_{nf}/k_{bf}) = 1 + 0.0187\phi^{0.6717}T^{0.6913}$	TiO_2-MWCNTs (70–30)/EG-water $0.0625\% \leq \phi \leq 1:0\%$, $20^{\circ}C \leq t \leq 50^{\circ}C$
Moghadam et al. [261]	$(k_{nf}/k_{bf}) = 1.017 + 0.072 \times 1.029^T \times \phi^{0.773}$	GO-TiO_2/water $20^{\circ}C \leq T \leq 50^{\circ}C$ $0\% \leq \phi \leq 1.0\%$
Mahyari et al. [145]	$(k_{nf}/k_{bf}) = 0.015229T^{(0.52876+0.31508\phi)} + 0.92124$	GO-SiC (50% : 50%) $0.05\% \leq \phi \leq 1:0\%$ $25^{\circ}C \leq t \leq 50^{\circ}C$
Rostami et al. [157]	$(k_{nf}/k_{bf}) = 0.2051 \cdot (t/t_0)^{0.7083} \cdot \phi^{0.5059} + 0.9679$	CuO-GO/water-ethylene glycol (50% : 50%) $0.1\% \leq \phi \leq 1.6\%$ $25^{\circ}C \leq t \leq 50^{\circ}C$
Soltani et al. [226]	$(k_{nf}/k_{bf}) = ((0.9714 + (1.3974\phi^{0.3681})(0.0077T^{0.7787}))/(\exp((-310.0683\phi^2)(T^{-1.9772})))$	WO_3-MWCNTs/engine oil $0.05\% \leq \phi \leq 0:6\%$ $20^{\circ}C \leq t \leq 60^{\circ}C$
Tiwari et al. [89]	$k_{nf} = k_{bf}(1 + 0.580453) \times (T/T_0)^{1.54358} \times \phi^{0.356853}$	CeO_2+MWCNT (80:20)/water based for $30^{\circ}C \leq T \leq 50^{\circ}C$, $0\% \leq \phi \leq 1:50\%$
Kamel et al. [117]	$(k_{nf}/k_{bf}) = 1.21 - 0.009581T + 0.223\phi + 0.0001223T^2 + 0.006598T\phi$	Al_2O_3-CeO_2 (80 : 20)/water based $0.01\% \leq \phi \leq 0:50\%$ $35^{\circ}C \leq T \leq 50^{\circ}C$
Kanti et al. [262]	$(k_{hnf}/k_{bf}) = 1.77(T_{hnf}/T_{ref})^{0.354}(\phi_{hnf}/100)^{0.0915}$	Fly ash-Cu/water $0.5 < \phi < 4.0\%$ $30 < T < 60^{\circ}C$

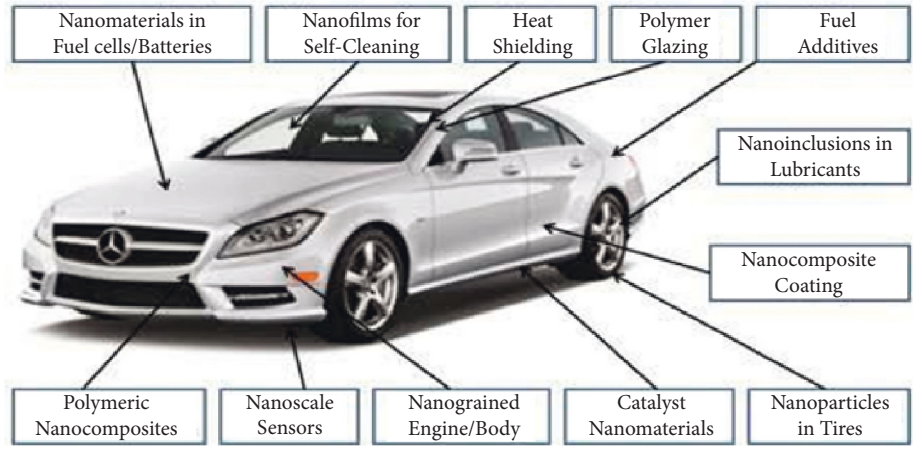

Figure 12: Current application areas of nanofluids in the automobile industry [264].

integrity of the engine [267]. This, therefore, means that an efficient and responsive thermal management system is key in the design and operation of an automobile [268]. The use of nanofluids has turned out to be a reasonable choice for improving the engine cooling rate and easing the complex nature of the thermal management system [269]. An automobile cooling network consists of six parts. They are the radiator, water pump, thermostat, radiator pressure-release cap, and electric cooling fan (Figure 13).

Generally, the coolant used in the automobile radiator is water or a mixture of water and an added liquid-like ethylene glycol (EG) (antifreezing fluid boil over protection), flowing inside the tubes. Another coolant (natural air) exiting outside the system flows through the fins to cool the water temperature inside the tubes [270]. Ethylene glycol (EG) and water have long been used as coolants in the automobile industry because they are cheap, readily available, and have worked well in achieving the cooling of the automobile system. Generally, in the heat exchanger, the thermal conductivity enhancement results in a higher heat transfer rate and thermal efficiency in nanofluid applications [223, 271]. Ho et al. [101] significantly improved cooling effectiveness with a hybrid suspension (Al_2O_3-MEPCM) in a circular tube. Sinz et al. [140] numerically looked at the convective heat transfer of silver (Ag) and graphene HEG nanoparticles spread in water (Ag-HEG/water) hybrid nanofluids streaming through a circular channel. However, the thermal conductivity was raised from 0.6006 to 0.6053 W/m·K by increasing the solid volume fraction (ϕ) ranged between 0.1 and 0.9%, enhancing the heat transfer performance of Ag-HEG/water as a working fluid.

Hong et al. [272] investigated the hydrothermal performance and erosion-corrosion effects of a new hybrid nanofluid in automobile cooling systems. They recommended the fluid for future cooling frameworks. Sahoo and Sarkar [184] completed a study dealing with the augmentation of convective heat transfer performance of an EG salt water-based mixture fluid. Several hybrid nanofluids, i.e., Ag, Cu, SiC, CuO, and TiO_2 in a 0-1% solid volume fraction (ϕ) of Al_2O_3 nanofluids, were used as coolants in a louvered-fin automobile radiator. Among all the hybrid nanofluids investigated, 1% Ag hybrid nanofluid (0.5% Ag and 0.5% Al_2O_3) recorded the highest effectiveness, heat transfer rate, and pumping power. Nonetheless, $SiC + Al_2O_3$ dispersed hybrid nanofluid recorded the best performance profile, indicating that it is the best coolant. Sahoo et al. [273] in another study used water-based (50/50) volume fraction for Fe_2O_3, CuO, TiO_2, Ag, and Cu in Al_2O_3 hybrid nanofluids as coolants for a louvered fin automobile radiator. For all considered hybrid nanofluids, Al_2O_3-Ag/water hybrid nanofluid exhibited higher effectiveness, heat transfer rate, pumping power, and pressure drop of 0.8%, 3%, 6%, and 5.6%, respectively, as compared to water as radiator coolant. Okello et al. [274] investigated three different samples of ethylene glycol (EG)-based hybridized nanocoolants. They are (Cu-Al_2O_3), (Cu-TiO_2), and (TiO_2-Al_2O_3) in that order. This was to decide their suitability as a possible coolant for use in a car radiator. They concluded that the (Cu-Al_2O_3)/EG hybridized solid-liquid blend showed a faster heat transfer rate compared to the other two ceramic matrices, and it is recommendable. Soylu et al. [275] examined the effects of using nanofluids on heat transfer performance in automobile radiators. Four different sorts of nanoparticles were then prepared in nanofluids, which included pure TiO_2, TiO_2 doped with 0.1% Ag, TiO_2 doped with 0.3% Ag, and TiO_2 doped with 0.1% Cu. Prepared nanoparticles were then introduced into the retaining fluid (50 : 50), ethylene glycol (EG)-water mixture by volume with a 0.3, 0.5, 1, and 2% ratio. The experimental results indicated a net change was then seen in the thermal conductivity of 0.3% Ag-doped nanofluids. Sandhya et al. [177] treated CNC-graphene-based hybrid nanofluids in a car radiator. However, a system investigation was performed by mulling a single tube unit in the radiator for pattern advancement. A CFD examination was then conducted using the ANSYS FLUENT module. The results indicate that graphene + CNC-based hybrid nanofluids will improve the performance of an auto radiator when compared with graphene nanofluid and base fluid. Benedict et al. [168] investigated mono and hybrid metal oxide performance of Al_2O_3 and TiO_2 with or without plant-based extracted nanocellulose (CNC) for various volume concentrations and an improved heat transmission

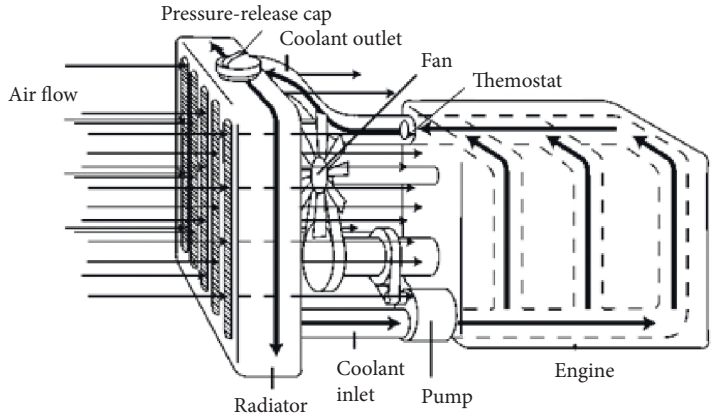

Figure 13: Components within an automotive cooling system.

nanofluid in comparison to distilled water (DW) as a radiator coolant. The thermal conductivity of nanofluids (mono and hybrid) improved significantly as the volume concentration of nanoparticles dispersed in the host fluid increased. A higher thermal conductivity was also exhibited by Al_2O_3/CNC and Al_2O_3/TiO_2 hybrid nanofluids. Naiman et al. [167] considered the thermophysical properties of alumina-cellulose nanocrystal (Al_2O_3/CNC) composite nanofluids in water/ethylene glycol (EG) (W/EG) as a new coolant for a radiator. The results obtained indicate that enhancement in Al_2O_3/CNC nanofluid's thermal conductivity increased compared to base fluid W/EG. This was so as the temperature increased and peaked at a volume concentration of 0.9% at a temperature of 70°C. Kumar and Sahoo [276] realized better results with $Al_2O_{3(\text{spherical})}$ and graphene $_{(\text{platelet})}$ in a water base. Sahoo [277] progressed the research with spherical (Al_2O_3), cylindrical (CNT), and platelet (graphene) based ternary hybrid nanofluid for an automotive radiator and reported the effectiveness of the combination in enhancing the thermohydraulic performance of an automobile cooling system. Shankara et al. [278] investigated a deionized (DI) water-built hybrid nanofluid of MWCNT-CuO and graphene as an automobile coolant, increasing the convective heat transfer coefficient in arrays of 65–87% at different coolant stream rates. Ramalingam et al. [279] used aluminium oxide (Al_2O_3) doped with unmilled silicon carbide (SiC_{UM}) nanoparticles and milled silicon carbide (SiC_M) nanoparticles dispersed in distilled water (DW) and ethylene glycol (EG) at 50 : 50 volumetric proportions and then employed in their experiment to assess the heat transfer characteristics and system physiognomies using it in an automotive radiator. The results show that both samples attained high thermal conductivity at a volume concentration of 0.4% and an optimum improvement regarding the overall thermal performance of 28.34% using Al_2O_3 doped with milled silicon carbide (SiC_M) at a volume loading of 0.8%. In their study, Li et al. [197] also looked at EG/SiC-MWCNTs hybrid nanofluids for car radiator systems. They reported that the heat transfer advantage of SiC-MWCNTs hybrid nanofluid showed its potential application in automobile cooling systems. Bharadwaj et al. [280] used carboxyl-graphene (CG) and graphene oxide (GO)/EG nanoparticles because of their high thermal conductivity to explore their effects in automobile radiators at 1%, 2%, and 3% volume concentrations for the nanoparticles and different flow rates of 4.5 and 6 LPM and investigated them through a numerical approach by assuming laminar flow. The results indicate that including graphene oxide and carboxyl graphene will augment the radiator's heat transfer performance by increasing the heat transfer. This hybrid nanofluid is ideal for the automotive radiator to deliver the best effect when used at the proper concentration. Karimi and Afrand [281] researched the efficiency of vertical and horizontal tube radiators. However, MgO-MWCNTs/ethylene glycol (EG) was nevertheless considered for their work. The results indicated a vertical tube radiator showed better performance and a 10% higher efficiency than a horizontal tube. Jadar et al. [282] compared forced convective heat transfer in aluminium functionalized-MWCNT (Al-*f*MWCNT)-water nanofluid to distilled water (DW) in an automobile radiator with conventional and composite fins. The results obtained prove that increasing the fluid streaming rate can enhance heat transfer performance. The *f*MWCNT nanofluid displayed an immense enhancement in heat transfer rate compared to DI water. Due to its prevalent thermal conductivity (0.92 W/m K at 80°C), the heat transfer performance of *f*MWCNT nanofluid was better than distilled water (DW). The present outcomes are valuable for use in designing a smaller size of automobile radiator. Abbas et al. [283] recently employed Fe_2O_3-TiO_2/water for convective heat transfer improvement in an aluminium tube automotive radiator, which confirmed an increase in heat transfer rate by 26.7% at a flow rate of 15 LPM for a 0.009 vol.% fraction.

Nanoparticles added to normal engine coolants have the potential to increase cooling rates in automobiles and heavy-duty engines. This advancement may be used to remove engine heat with a smaller coolant system, resulting in smaller and lighter radiators that improve nearly every element of automobile and truck performance while also increasing fuel economy. Improved cooling rates for car and truck engines, on the other hand, can be used to remove more heat from higher horsepower engines while maintaining the same coolant system size.

5.1. Applications of Nanofluidics. With so many accomplishments already under our belts, it is only natural to wonder, "Where is nanotechnology headed?" Nanotechnology is projected to lead to tiny robotic devices that monitor and detect electrooptic faults and malfunctions in human systems in real-time using nanoelectronics, sensors, microelectromechanical systems (MEMS), and nanoelectromechanical systems (NEMS). Manipulating small volumes of liquid is essential in fluidic digital display devices, optical gadgets, and microelectromechanical systems (MEMS), such as lab-on-chips analysis structures. However, this can be achieved by electrowetting or lowering the contact angle by an applied voltage to the little volumes of liquid. Nanofluidics habitually falls under nanoelectromechanical systems (NEMS), which are usually fabricated using complementary metal-oxide semiconductor (CMOS) technology. Following the advanced lab-on-a-chip gadgets for PCR and associated techniques, nanofluidics has significantly impacted biotechnology, clinical diagnostics, and medicine. Several researchers have made efforts [284, 285] to comprehend the conduct of stream fields around nanoparticles concerning liquid forces as a function of Reynolds and Knudsen's numbers using computational fluid dynamics. The correlation between drag, lift, and Reynolds numbers has thus been seen to differ significantly at the nanoscale compared to those at the macroscale. Therefore, nanofluidics has the potential to become a focus technology worthy of further investigation.

5.2. Recent Advances, Enhanced Values of Thermal Conductivity, and Stability. Cele et al. [286] synthesized platinum (Pt) nanoparticles of different sizes and shapes using a radiolysis technique. Pt nanoparticles were thus produced after gamma irradiation of solutions at 70, 90, and 120 kGy at room temperature. Maaza et al. [287] reported the stability of Pt, Ag, Au, and Cu nano-based dispersions (in three dissimilar dispersing liquid agents of acetonitrile, pentane, and water) produced by laser liquid-solid interaction (LLSI) with the fundamental Nd:YAG frequency. They observed the stability of these metals in the solution was due to their large polarizability index. Maaza et al. [288] also described in another report the production option of binary oxide nanoparticles in a nano-scaled form by the Nd:YAG laser liquid-solid interaction (LLSI) technique (irradiating laser source), using water and or hydrogen peroxide-based coating fluid layer. They had established the likely possibility of manipulating the electronic metal-oxygen valence through the nature of the coating liquid layer of pure H_2O and hydrogen peroxide H_2O_2, specifically for molybdenum oxide. Kana et al. [289] used the standard platinum wire technique at temperatures ranging from 25 to 45°C, obtaining a net increase in thermal conductivity (up to 44%) of molybdenum oxide-based nanosheets via direct dissolution of metallic Mo in water (MoO_3-H_2O). Molybdenum was also noticed in mainly 6^+ electronic valence. Riahi et al. [290] demonstrated the feasibility of fabricating Al_2O_3-water nanofluid with high thermal conductivity enhancement using pulsed laser ablation in liquid for temperatures ranging 25–45°C. Khamliche et al. [291] reported the fabrication of copper nanoparticles-ethylene glycol (CuNPs-EG) nanofluid by the one-step pulsed Nd:YAG laser ablation technique to ablate the surface of a polished copper target in EG base fluid in ambient conditions. The authors proposed that this medium can also be used to create highly efficient nanofluids. Mbambo et al. [292] formulated graphene nanosheets using nanosecond pulsed Nd:YAG laser ablation of pure graphite in water-based fluid under ambient conditions in a single-step formation process. Mbambo et al. [293] synthesized graphene nanosheets adorned with Au nanoparticles by ablating graphite targets trailed by Au in ethylene glycol as the accommodating liquid using an ultrafast pulsed Nd:YAG laser. They reported that GNs-AuNPs/EG hybridized nanofluid displays an improvement in thermal conductivity of about 26% for a temperature range of 25–45°C. The latter is higher when compared to studies on the thermal conductivity enhancement of equivalent nanoparticle-matrix with ethylene glycol (EG)-based nanofluids. Maaza et al. [288] reported an improved result in a similar experiment with pure EG, AgNPs-EG, GNs-EG, and AgNPs-GNs-EG separately for the same temperature range. The thermal conductivity measurement of the AgNPs-GNs-EG hybridized fluid temperature-based was thus estimated as 32.3% higher than that for pure EG. This result is the best so far when compared to other parallel studies reported earlier [163]. Khamliche et al. [294] conducted thermal conductivity measurements on nAgPs:EG nanofluids for sundry volume fractions (ϕ) of nAgPs. The study considers the effect of ageing time on the shape of nAgPs spread. However, this was done at a temperature range of $25 < T < 50$°C, exploiting a guarded hot plate (GHP) technique. The thermal conductivity revealed a monotonic increment with temperature and a circa linear relationship with the volume fraction (ϕ) of nAgPs. An enhancement of about 23% was obtained by ageing the nanofluid for 5 h, and AgNWs were predominant. In another trial, Chen et al. [295] looked at the thermal conductivity and stability of composites of carbon black filled polydimethylsiloxane (PDMS-CB) as temperature and filler fraction functions from the perspective of fuel cells. The study also showed good thermal stability under ambient conditions. Composite materials maintained thermal stability at the fuel cells' high operating temperatures (90–180°C). Thermal conductivity generally intensifies as the filling fraction increases. Significantly, when compared with other composites such as epoxy resin-CB, it was observed that little CB loading for PDMS is required to realize the same thermal conductivity as an epoxy resin-CB composite.

5.3. Future of Prediction of Nanofluid in New Technological Systems. Today, work on nanoparticles (NPs) is ubiquitous. Considering the present state of nanotechnology in terms of research achievement, it is easy to say that the near future will be a remarkable period for technological convergence in numerous spaces aside from the automobile industry (Figure 12), such as biotechnology, machine learning, the web of things, material science, semiconductors, and 3D

printing. Silicon nanoparticles made of silicon dioxide are a superb example of the wide range of industrial applications for NPs (SiNPS). SiNPs are currently used in construction (for example, concrete or rubber), electronics, polishing agents, catalysis, paints and coatings, polymers, and agriculture. The MWCNTs, which are coaxial nanotubes found unequivocally inside one another, have endorsed renowned properties to such an extent that a nanotube in the focal center can slip into the external one with no force of friction, prompting the formation of an ideal nuclear rotational bearing. This is one of the principal genuine models of subatomic nanotechnology. This property is presently being used to assemble the minutest rotary engine and oscillator. Future applications incorporate fascinating possibilities, such as GHz mechanical oscillators. The conceivable effect that these and other advances will have on the more extensive meaning of nanotechnology will be almost unfathomable. Furthermore, much more work is needed before the theories of nanofluids can be fully developed, accepted, and used with confidence. Researchers are yet making progress in this field for better futuristic possibilities for industrial applications. Hence, we are just a few steps closer to realizing their use. This will cover various new technological systems.

5.4. Reliability of Future Prediction of Research Results. Many scholars have proposed various correlations for evaluating the effective thermophysical properties of nanofluids, and these correlations are consistent with experimental results. Hence, the predicted results of the investigated work of nanofluid's application for new technological systems can be trusted. This, which denotes the consistency of a measure of a particular construct over time, has been demonstrated based on several reports presented by researchers. So far, it is clear from proposed correlations that the theoretical predictions based on the modified liquid mixture rule have good conformity with the experimental outcomes. For instance, the proposed theoretic predictions based on liquid mixture theory for the density and heat capacity of hybridized nanofluid at diverse volume concentrations agree with the experimental conclusions of Ho et al. [55]. Also, the trial results of Syam Sundar et al. [153] for the specific heat of nanodiamond-Fe_3O_4/water hybrid nanofluid compared with the findings obtained using the proposed theoretical prediction (equation (7)) were in fact in good agreement. Esfe et al. [66], having numerically compared and validated measured values of thermal conductivity and dynamic viscosity ratio with predicted values by different proposed dynamic viscosity and thermal conductivity ratio models, observed similar ranges in the values of obtained results for various nanoparticle volume fractions and, in their concluding statement, claimed that nanofluids would offer engineers a better option for their use in electronics, automotive, and nuclear applications where heat transfer improvement or efficient heat dissipation is necessary. The validity of predicted results for future use has also been demonstrated using modern artificial intelligence (AI) methods such as ANN (Peng et al. [21]), SVM, and others. Several results of modeling data using AI are in very good conformity with the predicted data. Vafaei et al. [191], used ANN modeling to account for the thermal conductivity of MgO-MWCNTs/EG. On the other hand, the authors compared the results obtained to the outcomes of 36 previous analogous experimental works. It was found that the experimental and smart modeling results were convergent, proving the validity of ANN modeling. Similar accounts were also presented by Esfe et al. [195].

6. Conclusion and Prospects

This work, however, steered a critical overview of the improving thermal conductivity for the latest nanofluids research for their heat transfer applications (Table 5), which also covered the heat transfer applications of mixture nanofluids for automobile cooling in one space. The study entails extracting and comparing information obtained from recent analytical, artificial intelligence/machine learning approaches, and experimental examinations with mixture nanofluids, describing hybrid nanofluids in terms of thermal conductivity enhancement and heating performance. There are a number of challenges confronting mixed nanofluid society today, ranging from formulation and functional application to mechanism understanding. Although, there has been a significant advancement in the preparation methods for hybrid nanoparticles, resulting in many ultramodern combinations and innovations of nanoparticles in the process. The lack of long-term stability, the manufacturing process, the selection of appropriate nanomaterial blends to achieve the synergistic effect, and the high cost of nanofluids may all pose significant challenges in their actual applications. The following significant, complex, and fascinating phenomena involving mixtures of nanofluids have subsequently been archived in the reviewed work of literature from which the accompanying outcomes were nevertheless deduced:

(i) When two or more than two nanoparticle types are combined to form a composite in a base fluid, one plays the role of the core and the others attach to the core to enhance thermal conductivity. Although there are a few discrepancies in the percentage of augmentation and the ideal measure of nanoparticles, significant thermal conductivity enhancement of nanofluids has been reported in both experimental and theoretical studies. Carbon-based hybridized nanofluids revealed superior enhancement. The solid volume fraction of nanoparticles was nevertheless reported as the key factor (most significant effect) responsible for the enhancement.

(ii) Water-based nanofluids give better enhancement concerning heat transfer when compared with EG-based nanofluids. Oil-based hybrid nanofluids perform the least (fairly) as heat transfer mediums. They are chosen for applications where the pumping capacity is not considered important.

(iii) With the exception of four cases [52, 56, 142, 299], hybrid nanofluids produce a noticeable thermal conductivity enhancement and a relatively higher

heat transfer coefficient when compared to regular nanofluids

(iv) Through the uniform dispersion and stable suspension of nanoparticles in the host liquids, the maximum possible thermal augmentation can be obtained at the lowest possible concentrations (by < 0.1% by volume)

(v) Mainly, cylindrical, spherical, or platelet-shaped nanoparticles were mentioned in experimental studies. However, it could not be ascertained if other nanoparticle shapes such as blades, bricks, dendritic, pyramids, and icosahedrons were used as they were barely mentioned.

(vi) It also demonstrates that a clear understanding of the major mechanism(s) involved in the behavior of hybrid nanofluids has yet to be established

(vii) It has additionally been seen that hybrid nanofluids can thus be considered as a likely possibility for several applications requiring improved thermal performance

Other factors, the mechanisms that are effective in the motion analysis of nanoparticles such as Brownian, thermophoresis, and inertia, which could affect the thermal conductivity of hybrid nanofluid were not covered in this review work as our cardinal interest did not include these areas.

A top-to-bottom understanding of the diverse shapes, sizes, and amalgamations of particles, communications between particles, stabilizers, accommodating fluid, and the heating surface will nevertheless be significant for applications of nanofluid. Recently, researchers have employed hybrid nanofluids as nanocoolants in automobile radiators with the enduring aim of further broadly considering these hybrid nanofluids in real industrial applications. Clearly, hybrid nanofluids can work efficiently as conventional coolants for auto radiators, including a variety of thermal applications in light of different perspectives, especially compatibility, thermal conductivity, stability, and viscosity. Nevertheless, multidisciplinary teamwork among various (colloid science, engineering, nanomaterials, and physics) researchers will thus be required to better comprehend and design suitable nanofluids and models to accelerate their real applications.

Nomenclature

ACG: Activated carbon graphene
AgNWs: Silver (Ag) nanowires
AI: Artificial intelligence
ANFIS: Adaptive neurofuzzy inference system
ANN: Artificial neural network
C: Specific heat capacity
CB: Carbon black
CMOS: Complementary metal oxide semiconductor
CNC: Cellulose nanocrystal
CNTs: Carbon nanotubes
COOH: Carboxyl group
CTAB: Cetyltrimethylammonium bromide
DASC: Direct absorption solar collectors
DW: Distilled water
DWCNT: Double-walled carbon nanotubes
DI: Deionized water
EANN: Enhanced artificial neural network
EG: Ethylene glycol
Eq: Equation
FF: Ferrofluid
FHEG: Functionalized hydrogen exfoliated graphene
FMWCNTs: Functionalized multiwalled carbon nanotubes
GA: Gum arabic
GHP: Guarded hot plate
GMDH: Group method of data handling
GNP: Graphene nanoparticle
GO: Graphene oxide
Gr: Graphene
HEG: Hydrogen exfoliated graphene
HTC: Heat transfer coefficient
HyNC: Hybrid nanophase change material
HyNPCM: Hybrid nanocomposite
K: Thermal conductivity (TC)
LLSI: Laser liquid-solid interaction
LPM: Liter per minute
LS-SVM: Least-square support vector machines
MARS: Multivariate adaptive regression spline
MEPCM: Micro encapsulated phase change material
MEMS: Microelectromechanical systems
MHD: Magnetohydrodynamics
MWCNTs: Multiwalled carbon nanotubes
ND: Nanodiamond
NACG: Nitrogen activated carbon graphene
NEMS: Nanoelectromechanical systems
NM: Noble metals
NPs: Nanoparticles
N-rGO: Nitrogen reduced graphene oxide
n: Particle shape factor
nAgPs: Nanosilver particles
PAO: Poly-alpha-olefins
PCM: Phase change materials
PCR: Polymerase chain reaction
PDMS: Polydimethylsiloxane
PVA: Polyvinyl alcohol
PPY-CNT: Polypyrene-carbon nanotube
SAB-15: Mesoporous silica
SANSS: Submerged arc nanoparticle synthesis system
SWCNTs: Single-walled carbon nanotubes
SVM: Support vector machines
T: Temperature
TMAH: Tetramethylammonium hydroxide
VEROS: Vacuum evaporation on running oil substrate
Vol.: Volume
W: Water
Wt.: Weight concentration

Symbol
α: Thermal conductivity ratio
β: Thermal expansion coefficient ($1/K$)
γ: Functionalized group

ϑ: Thermal constant
μ: Dynamic viscosity (N/sm^2)
ρ: Density (kg/m^3)
σ: Electrical conductivity ($S{\cdot}m^{-1}$)
ϕ: Volume fraction (%)
ω: Mass fraction (%)

Subscripts
bf: Base fluid
eff: Effective
f: Fluid
hnf: Hybrid nanofluid
nf: Nanofluid
np: Nanoparticles
p: Particles
ref: Reference.

Conflicts of Interest

The authors declare that they have no conflicts of interest.

References

[1] J. E. Hulla, S. C. Sahu, and A. W. Hayes, "Nanotechnology: history and future," *Human & Experimental Toxicology*, vol. 34, no. 12, pp. 1318–1321, 2015.

[2] M. C. Ndukwu, C. E. Ikechukwu–Edeh, N. R. Nwakuba, I. Okosa, I. T. Horsefall, and F. N. Orji, "Nanomaterials application in greenhouse structures, crop processing machinery, packaging materials and agro–biomass conversion," *Materials Science for Energy Technologies*, vol. 3, pp. 690–699, 2020.

[3] S. U. Choi and J. A. Eastman, *Enhancing Thermal Conductivity of Fluids with Nanoparticles*, Argonne National Laboratory, Illinois, IL, USA, 1995.

[4] Y. Li, J. Zhou, E. Schneider, and S. Xi, "A review on development of nanofluid preparation and characterization," *Powder Technology*, vol. 196, no. 2, pp. 89–101, 2009.

[5] Y. Yang, J. Cao, N. Wei et al., "Thermal conductivity of defective graphene oxide: a molecular dynamic study," *Molecules*, vol. 24, no. 6, p. 1103, 2019.

[6] M. Akhilesh, K. Santarao, and M. V. S. Babu, "Thermal conductivity of CNT–wated nanofluids: a review," *Mechanics and Mechanical Engineering*, vol. 22, no. 1, pp. 207–220, 2018.

[7] F. D. S. Marquis and L. P. F. Chibante, "Improving the heat transfer of nanofluids and nano–lubricants with carbon nanotubes," *Journal of Occupational Medicine*, vol. 57, no. 12, pp. 32–43, 2005.

[8] G. Huminic and A. Huminic, "The heat transfer performances and entropy generation analysis of hybrid nanofluids in a flattened tube," *International Journal of Heat and Mass Transfer*, vol. 119, pp. 813–827, 2018.

[9] H. Babar and H. M. Ali, "Towards hybrid nanofluids: preparation, thermophysical properties, applications, and challenges," *Journal of Molecular Liquids*, vol. 281, pp. 598–633, 2019.

[10] R. Turcu, A. L. Darabont, A. Nan et al., "New polypyrrole-multiwall carbon nanotubes hybrid materials," *Journal of Optoelectronics and Advanced Materials*, vol. 8, no. 2, pp. 643–647, 2006.

[11] A. Akhgar, D. Toghraie, N. Sina, and M. Afrand, "Developing dissimilar artificial neural networks (ANNs) to prediction the thermal conductivity of MWCNT-TiO_2/Water-ethylene glycol hybrid nanofluid," *Powder Technology*, vol. 355, pp. 602–610, 2019.

[12] A. Shahsavar, S. Khanmohammadi, D. Toghraie, and H. Salihepour, "Experimental investigation and develop ANNs by introducing the suitable architectures and training algorithms supported by sensitivity analysis: measure thermal conductivity and viscosity for liquid paraffin based nanofluid containing Al_2O_3 nanoparticles," *Journal of Molecular Liquids*, vol. 276, pp. 850–860, 2019.

[13] S. H. Rostamian, M. Biglari, S. Saedodin, and M. Hemmat Esfe, "An inspection of thermal conductivity of CuO-SWCNTs hybrid nanofluid versus temperature and concentration using experimental data, ANN modeling and new correlation," *Journal of Molecular Liquids*, vol. 231, pp. 364–369, 2017.

[14] S. Rostami, D. Toghraie, B. Shabani, N. Sina, and P. Barnoon, "Measurement of the thermal conductivity of MWCNT-CuO/water hybrid nanofluid using artificial neural networks (ANNs)," *Journal of Thermal Analysis and Calorimetry*, vol. 143, no. 2, pp. 1097–1105, 2021.

[15] M. R. Safaei, A. Hajizadeh, M. Afrand, C. Qi, H. Yarmand, and N. W. B. M. Zulkifli, "Evaluating the effect of temperature and concentration on the thermal conductivity of ZnO-TiO_2/EG hybrid nanofluid using artificial neural network and curve fitting on experimental data," *Physica A: Statistical Mechanics and its Applications*, vol. 519, pp. 209–216, 2019.

[16] S. Tian, N. I. Arshad, D. Toghraie, S. A. Eftekhari, and M. Hekmatifar, "Using perception feed-forward Artificial Neural Network (ANN) for predicting the thermal conductivity of graphene oxide-Al_2O_3/water-ethylene glycol hybrid nanofluid," *Case Studies in Thermal Engineering*, vol. 26, Article ID 101055, 2021.

[17] W. Ji, L. Yang, Z. Chen, M. Mao, and J. N. Huang, "Experimental studies and ANN predictions on the thermal properties of TiO_2-Ag hybrid nanofluids: consideration of temperature, particle loading, ultrasonication and storage time," *Powder Technology*, vol. 388, pp. 212–232, 2021.

[18] D. Toghraie, N. Sina, N. A. Jolfaei, M. Hajian, and M. Afrand, "Designing an artificial neural network (ANN) to predict the viscosity of silver/ethylene glycol nanofluid at different temperatures and volume fraction of nanoparticles," *Physica A: Statistical Mechanics and its Applications*, vol. 534, Article ID 122142, 2019.

[19] A. Komeilibirjandi, A. H. Raffiee, A. Maleki, M. Alhuyi Nazari, and M. Safdari Shadloo, "Thermal conductivity prediction of nanofluids containing CuO nanoparticles by using correlation and artificial neural network," *Journal of Thermal Analysis and Calorimetry*, vol. 139, no. 4, pp. 2679–2689, 2020.

[20] A. Maleki, M. Elahi, M. E. H. Assad, M. Alhuyi Nazari, M. Safdari Shadloo, and N. Nabipour, "Thermal conductivity modeling of nanofluids with ZnO particles by using approaches based on artificial neural network and MARS," *Journal of Thermal Analysis and Calorimetry*, vol. 143, no. 6, pp. 4261–4272, 2021.

[21] Y. Peng, A. Parsian, H. Khodadadi et al., "Develop optimal network topology of artificial neural network (AONN) to predict the hybrid nanofluids thermal conductivity according to the empirical data of Al_2O_3–Cu nanoparticles dispersed in ethylene glycol," *Physica A: Statistical Mechanics and its Applications*, vol. 549, Article ID 124015, 2020.

[22] S. O. Giwa, M. Sharifpur, M. Goodarzi, H. Alsulami, and J. P. Meyer, "Influence of base fluid, temperature, and concentration on the thermophysical properties of hybrid nanofluids of alumina–ferrofluid: experimental data, modeling through enhanced ANN, ANFIS, and curve fitting," *Journal of Thermal Analysis and Calorimetry*, vol. 143, no. 6, pp. 4149–4167, 2021.

[23] S. A. Bagherzadeh, A. D'Orazio, A. Karimipour, M. Goodarzi, and Q. V. Bach, "A novel sensitivity analysis model of EANN for F-MWCNTs–Fe_3O_4/EG nanofluid thermal conductivity: outputs predicted analytically instead of numerically to more accuracy and less costs," *Physica A: Statistical Mechanics and its Applications*, vol. 521, pp. 406–415, 2019.

[24] M. Safdari Shadloo, "Application of support vector machines for accurate prediction of convection heat transfer coefficient of nanofluids through circular pipes," *International Journal of Numerical Methods for Heat and Fluid Flow*, vol. 31, no. 8, pp. 2660–2679, 2020.

[25] A. H. Saeedi, M. Akbari, and D. Toghraie, "An experimental study on rheological behavior of a nanofluid containing oxide nanoparticle and proposing a new correlation," *Physica E: Low-dimensional Systems and Nanostructures*, vol. 99, pp. 285–293, 2018.

[26] M. Goodarzi, D. Toghraie, M. Reiszadeh, and M. Afrand, "Experimental evaluation of dynamic viscosity of ZnO–MWCNTs/engine oil hybrid nanolubricant based on changes in temperature and concentration," *Journal of Thermal Analysis and Calorimetry*, vol. 136, no. 2, pp. 513–525, 2019.

[27] H. Khodadadi, D. Toghraie, and A. Karimipour, "Effects of nanoparticles to present a statistical model for the viscosity of MgO-Water nanofluid," *Powder Technology*, vol. 342, pp. 166–180, 2019.

[28] B. Ruhani, D. Toghraie, M. Hekmatifar, and M. Hadian, "Statistical investigation for developing a new model for rheological behavior of ZnO–Ag (50%–50%)/water hybrid Newtonian nanofluid using experimental data," *Physica A: Statistical Mechanics and its Applications*, vol. 525, pp. 741–751, 2019.

[29] A. Afshari, M. Akbari, D. Toghraie, and M. E. Yazdi, "Experimental investigation of rheological behavior of the hybrid nanofluid of MWCNT–alumina/water (80%)–ethylene-glycol (20%)," *Journal of Thermal Analysis and Calorimetry*, vol. 132, no. 2, pp. 1001–1015, 2018.

[30] A. D. Zadeh and D. Toghraie, "Experimental investigation for developing a new model for the dynamic viscosity of silver/ethylene glycol nanofluid at different temperatures and solid volume fractions," *Journal of Thermal Analysis and Calorimetry*, vol. 131, no. 2, pp. 1449–1461, 2018.

[31] M. Keyvani, M. Afrand, D. Toghraie, and M. Reiszadeh, "An experimental study on the thermal conductivity of cerium oxide/ethylene glycol nanofluid: developing a new correlation," *Journal of Molecular Liquids*, vol. 266, pp. 211–217, 2018.

[32] A. Akhgar and D. Toghraie, "An experimental study on the stability and thermal conductivity of water–ethylene glycol/TiO_2–MWCNTs hybrid nanofluid: developing a new correlation," *Powder Technology*, vol. 338, pp. 806–818, 2018.

[33] A. Moradi, D. Toghraie, A. H. M. Isfahani, and A. Hosseinian, "An experimental study on MWCNT–water nanofluids flow and heat transfer in double-pipe heat exchanger using porous media," *Journal of Thermal Analysis and Calorimetry*, vol. 137, no. 5, pp. 1797–1807, 2019.

[34] H. Arasteh, R. Mashayekhi, D. Toghraie, A. Karimipour, M. Bahiraei, and A. Rahbari, "Optimal arrangements of a heat sink partially filled with multilayered porous media employing hybrid nanofluid," *Journal of Thermal Analysis and Calorimetry*, vol. 137, no. 3, pp. 1045–1058, 2019.

[35] M. R. Gholami, O. A. Akbari, A. Marzban, D. Toghraie, G. A. S. Shabani, and M. Zarringhalam, "The effect of rib shape on the behavior of laminar flow of oil/MWCNT nanofluid in a rectangular microchannel," *Journal of Thermal Analysis and Calorimetry*, vol. 134, no. 3, pp. 1611–1628, 2018.

[36] P. Barnoon, D. Toghraie, R. B. Dehkordi, and H. Abed, "MHD mixed convection and entropy generation in a lid-driven cavity with rotating cylinders filled by a nanofluid using two phase mixture model," *Journal of Magnetism and Magnetic Materials*, vol. 483, pp. 224–248, 2019.

[37] D. K. Lee and Y. S. Kang, "Synthesis of silver nanocrystallites by a new thermal decomposition method and their characterization," *ETRI Journal*, vol. 26, no. 3, pp. 252–256, 2004.

[38] H. T. Zhu, Y. S. Lin, and Y. S. Yin, "A novel one–step chemical method for preparation of copper nanofluids," *Journal of Colloid and Interface Science*, vol. 277, no. 1, pp. 100–103, 2004.

[39] H. E. Patel, S. K. Das, T. Sundararajan, A. Sreekumaran Nair, B. George, and T. Pradeep, "Thermal conductivities of naked and monolayer protected metal nanoparticle based nanofluids: manifestation of anomalous enhancement and chemical effects," *Applied Physics Letters*, vol. 83, no. 14, pp. 2931–2933, 2003.

[40] J. P. Abid, A. W. Wark, P. F. Brevet, and H. H. Girault, "Preparation of silver nanoparticles in solution from a silver salt by laser irradiation," *Chemical Communications*, vol. 7, pp. 792-793, 2002.

[41] S. Yatsuya, Y. Tsukasaki, K. Mihama, and R. Uyeda, "Preparation of extremely fine particles by vacuum evaporation onto a running oil substrate," *Journal of Crystal Growth*, vol. 45, pp. 490–494, 1978.

[42] P. K. Das, "A review based on the effect and mechanism of thermal conductivity of normal nanofluids and hybrid nanofluids," *Journal of Molecular Liquids*, vol. 240, pp. 420–446, 2017.

[43] S. Suresh, K. P. Venkitaraj, M. S. Hameed, and J. Sarangan, "Turbulent heat transfer and pressure drop characteristics of dilute water based Al_2O_3–Cu hybrid nanofluids," *Journal of Nanoscience and Nanotechnology*, vol. 14, no. 3, pp. 2563–2572, 2014.

[44] F. R. Siddiqui, C. Y. Tso, K. C. Chan, S. C. Fu, and C. Y. Chao, "On trade–off for dispersion stability and thermal transport of Cu–Al_2O_3 hybrid nanofluid for various mixing ratios," *International Journal of Heat and Mass Transfer*, vol. 132, pp. 1200–1216, 2019.

[45] A. I. Ramadhan, W. H. Azmi, and R. Mamat, "Heat transfer characteristics of car radiator using tri-hybrid nanocoolant," *IOP Conference Series: Materials Science and Engineering*, vol. 863, no. 1, Article ID 012054, 2020.

[46] S. Chakraborty, I. Sarkar, K. Haldar, S. K. Pal, and S. Chakraborty, "Synthesis of Cu–Al layered double hydroxide nanofluid and characterization of its thermal properties," *Applied Clay Science*, vol. 107, pp. 98–108, 2015.

[47] M. F. Nabil, W. H. Azmi, K. A. Hamid, N. N. Zawawi, G. Priyandoko, and R. Mamat, "Thermo–physical properties of hybrid nanofluids and hybrid nanolubricants: a comprehensive review on performance," *International Communications in Heat and Mass Transfer*, vol. 83, pp. 30–39, 2017.

[48] R. Parameshwaran, R. Jayavel, and S. Kalaiselvam, "Study on thermal properties of organic ester phase–change material embedded with silver nanoparticles," *Journal of Thermal Analysis and Calorimetry*, vol. 114, no. 2, pp. 845–858, 2013.

[49] S. U. S. Choi and J. A. Eastman, "Enhanced heat transfer using nanofluids," UChicago Argonne LLC, Chicago, IL, USA, U.S. Patent. 6221275, 2001.

[50] W. S. Han and S. H. Rhi, "Thermal characteristics of grooved heat pipe with hybrid nanofluids," *Thermal Science*, vol. 15, no. 1, pp. 195–206, 2011.

[51] G. H. Bhosale and S. L. Borse, "Pool boiling CHF enhancement with Al_2O_3–CuO/H_2O hybrid nanofluid," *International Journal of Engineering Research and Technology*, vol. 2, no. 10, pp. 946–950, 2013.

[52] S. Jana, A. Salehi–Khojin, and W. H. Zhong, "Enhancement of fluid thermal conductivity by the addition of single and hybrid nano–additives," *Thermochimica Acta*, vol. 462, no. 1-2, pp. 45–55, 2007.

[53] N. Jha and S. Ramaprabhu, "Synthesis and thermal conductivity of copper nanoparticle decorated multiwalled carbon nanotubes based nanofluids," *Journal of Physical Chemistry C*, vol. 112, no. 25, pp. 9315–9319, 2008.

[54] N. Jha and S. Ramaprabhu, "Thermal conductivity studies of metal dispersed multiwalled carbon nanotubes in water and ethylene glycol based nanofluids," *Journal of Applied Physics*, vol. 106, no. 8, Article ID 084317, 2009.

[55] C. J. Ho, J. B. Huang, P. S. Tsai, and Y. M. Yang, "Preparation and properties of hybrid water–based suspension of Al_2O_3 nanoparticles and MEPCM particles as functional forced convection fluid," *International Communications in Heat and Mass Transfer*, vol. 37, no. 5, pp. 490–494, 2010.

[56] M. Baghbanzadeh, A. Rashidi, D. Rashtchian, R. Lotfi, and A. Amrollahi, "Synthesis of spherical silica/multiwall carbon nanotubes hybrid nanostructures and investigation of thermal conductivity of related nanofluids," *Thermochimica Acta*, vol. 549, pp. 87–94, 2012.

[57] S. Suresh, K. P. Venkitaraj, P. Selvakumar, and M. Chandrasekar, "Synthesis of Al_2O_3–Cu/water hybrid nanofluids using two step method and its thermo physical properties," *Colloids and Surfaces A: Physicochemical and Engineering Aspects*, vol. 388, no. 1–3, pp. 41–48, 2011.

[58] G. G. Momin, "Experimental investigation of mixed convection with water–Al_2O_3 & hybrid nanofluid in inclined tube for laminar flow," *International Journal of Scientific & Technology Research*, vol. 2, pp. 195–202, 2013.

[59] D. Madhesh and S. Kalaiselvam, "Experimental analysis of hybrid nanofluid as a coolant," *Procedia Engineering*, vol. 97, pp. 1667–1675, 2014.

[60] S. M. Abbasi, A. Rashidi, A. Nemati, and K. Arzani, "The effect of functionalisation method on the stability and the thermal conductivity of nanofluid hybrids of carbon nanotubes/gamma alumina," *Ceramics International*, vol. 39, no. 4, pp. 3885–3891, 2013.

[61] B. Munkhbayar, M. R. Tanshen, J. Jeoun, H. Chung, and H. Jeong, "Surfactant–free dispersion of silver nanoparticles into MWCNT–aqueous nanofluids prepared by one–step technique and their thermal characteristics," *Ceramics International*, vol. 39, no. 6, pp. 6415–6425, 2013.

[62] M. J. Nine, B. Munkhbayar, M. S. Rahman, H. Chung, and H. Jeong, "Highly productive synthesis process of well dispersed Cu_2O and Cu/Cu_2O nanoparticles and its thermal characterization," *Materials Chemistry and Physics*, vol. 141, no. 2–3, pp. 636–642, 2013.

[63] L. F. Chen, M. Cheng, D. J. Yang, and L. Yang, "Enhanced thermal conductivity of nanofluid by synergistic effect of multi–walled carbon nanotubes and Fe_2O_3 nanoparticles," in *Applied Mechanics and Materials*vol. 548, pp. 118–123, Trans Tech Publications Limited, 2014.

[64] L. S. Sundar, M. K. Singh, and A. C. Sousa, "Enhanced heat transfer and friction factor of MWCNT–Fe_3O_4/water hybrid nanofluids," *International Communications in Heat and Mass Transfer*, vol. 52, pp. 73–83, 2014.

[65] T. Theres Baby and R. Sundara, "Surfactant free magnetic nanofluids based on core–shell type nanoparticle decorated multiwalled carbon nanotubes," *Journal of Applied Physics*, vol. 110, no. 6, Article ID 064325, 2011.

[66] M. H. Esfe, A. A. Abbasian Arani, M. Rezaie, W. M. Yan, and A. Karimipour, "Experimental determination of thermal conductivity and dynamic viscosity of Ag–MgO/water hybrid nanofluid," *International Communications in Heat and Mass Transfer*, vol. 66, pp. 189–195, 2015.

[67] A. Shahsavar, M. R. Salimpour, M. Saghafian, and M. B. Shafii, "Effect of magnetic field on thermal conductivity and viscosity of a magnetic nanofluid loaded with carbon nanotubes," *Journal of Mechanical Science and Technology*, vol. 30, no. 2, pp. 809–815, 2016.

[68] A. K. Jaiswal, M. Wan, S. Singh et al., "Experimental investigation of thermal conduction in copper-palladium nanofluids," *Journal of Nanofluids*, vol. 5, no. 4, pp. 496–501, 2016.

[69] N. Nikkam, M. Saleemi, M. Behi, R. Khodabandeh, and M. S. Toprak, "Experimental investigation on the effect of SiO_2 secondary phase on thermo-physical properties of SiC nanofluids," *International Communications in Heat and Mass Transfer*, vol. 87, pp. 164–168, 2017.

[70] W. N. Septiadi, I. A. Trisnadewi, N. Putra, and I. Setyawan, "Synthesis of hybrid nanofluid with two–step method," in *Proceedings of the 3rd International Tropical Renewable Energy Conference "Sustainable Development of Tropical Renewable Energy" (i-TREC 2018)*, vol. 67, p. 03057p. 03057, EDP Sciences, November 2018.

[71] W. Urmi, M. M. Rahman, and W. A. Hamzah, "An experimental investigation on the thermophysical properties of 40% ethylene glycol based TiO_2-Al_2O_3 hybrid nanofluids," *International Communications in Heat and Mass Transfer*, vol. 116, Article ID 104663, 2020.

[72] S. O. Giwa, M. Momin, C. N. Nwaokocha, M. Sharifpur, and J. P. Meyer, "Influence of nanoparticles size, per cent mass ratio, and temperature on the thermal properties of water-based MgO–ZnO nanofluid: an experimental approach," *Journal of Thermal Analysis and Calorimetry*, vol. 143, no. 2, pp. 1063–1079, 2021.

[73] N. Gupta, S. M. Gupta, and S. K. Sharma, "Preparation of stable metal/COOH–MWCNT hybrid nanofluid," *Materials Today Proceedings*, vol. 36, pp. 649–656, 2021.

[74] H. Akoh, Y. Tsukasaki, S. Yatsuya, and A. Tasaki, "Magnetic properties of ferromagnetic ultrafine particles prepared by vacuum evaporation on running oil substrate," *Journal of Crystal Growth*, vol. 45, pp. 495–500, 1978.

[75] V. Singh and P. Chauhan, "Structural and optical characterization of CdS nanoparticles prepared by chemical precipitation method," *Journal of Physics and Chemistry of Solids*, vol. 70, no. 7, pp. 1074–1079, 2009.

[76] M. Nazari, N. Ghasemi, H. Maddah, and M. M. Motlagh, "Synthesis and characterization of maghemite nanopowders by chemical precipitation method," *Journal of Nanostructure in Chemistry*, vol. 4, no. 2, p. 99, 2014.

[77] B. Gnana Sundara Raj, A. M. Asiri, J. J. Wu, and S. Anandan, "Synthesis of Mn_3O_4 nanoparticles via chemical precipitation approach for supercapacitor application," *Journal of Alloys and Compounds*, vol. 636, pp. 234–240, 2015.

[78] G. H. Lee, J. H. Park, C. K. Rhee, and W. W. Kim, "Fabrication of Al nano powders by pulsed wire evaporation (PWE) method," *Journal of Industrial and Engineering Chemistry*, vol. 9, no. 1, pp. 71–75, 2003.

[79] J. Ranga Babu, K. K. Kumar, and S. Srinivasa Rao, "State–of–art review on hybrid nanofluids," *Renewable and Sustainable Energy Reviews*, vol. 77, pp. 551–565, 2017.

[80] S. A. Angayarkanni and J. Philip, "Review on thermal properties of nanofluids: recent developments," *Advances in Colloid and Interface Science*, vol. 225, pp. 146–176, 2015.

[81] T. X. Phuoc, Y. Soong, and M. K. Chyu, "Synthesis of Ag–deionized water nanofluids using multi–beam laser ablation in liquids," *Optics and Lasers in Engineering*, vol. 45, no. 12, pp. 1099–1106, 2007.

[82] H. J. Kim, I. C. Bang, and J. Onoe, "Characteristic stability of bare Au–water nanofluids fabricated by pulsed laser ablation in liquids," *Optics and Lasers in Engineering*, vol. 47, no. 5, pp. 532–538, 2009.

[83] C. H. Lo, T. T. Tsung, and L. C. Chen, "Shape–controlled synthesis of Cu–based nanofluid using submerged arc nanoparticle synthesis system (SANSS)," *Journal of Crystal Growth*, vol. 277, no. 1–4, pp. 636–642, 2005.

[84] C. H. Lo, T. T. Tsung, L. C. Chen, C. H. Su, and H. M. Lin, "Fabrication of copper oxide nanofluid using submerged arc nanoparticle synthesis system (SANSS)," *Journal of Nanoparticle Research*, vol. 7, no. 2-3, pp. 313–320, 2005.

[85] C. H. Lo, T. T. Tsung, and H. M. Lin, "Preparation of silver nanofluid by the submerged arc nanoparticle synthesis system (SANSS)," *Journal of Alloys and Compounds*, vol. 434-435, pp. 659–662, 2007.

[86] C. G. Granqvist and R. A. Buhrman, "Ultrafine metal particles," *Journal of Applied Physics*, vol. 47, no. 5, pp. 2200–2219, 1976.

[87] W. Yu, D. M. France, S. U. Choi, and J. L. Routbort, *Review and Assessment of Nanofluid Technology for Transportation and Other Applications*, Argonne National Laboratory (ANL), Argonne, IL, USA, 2007.

[88] Y. Hwang, H. S. Park, J. K. Lee, and W. H. Jung, "Thermal conductivity and lubrication characteristics of nanofluids," *Current Applied Physics*, vol. 6, pp. e67–e71, 2006.

[89] A. K. Tiwari, N. S. Pandya, Z. Said, H. F. Öztop, and N. Abu-Hamdeh, "4S consideration (synthesis, sonication, surfactant, stability) for the thermal conductivity of CeO_2 with MWCNT and water-based hybrid nanofluid: an experimental assessment," *Colloids and Surfaces A: Physicochemical and Engineering Aspects*, vol. 610, Article ID 125918, 2021.

[90] M. H. Esfe, S. Wongwises, A. Naderi et al., "Thermal conductivity of Cu/TiO_2–water/EG hybrid nanofluid: experimental data and modeling using artificial neural network and correlation," *International Communications in Heat and Mass Transfer*, vol. 66, pp. 100–104, 2015.

[91] H. Yarmand, S. Gharehkhani, G. Ahmadi et al., "Graphene nanoplatelets–silver hybrid nanofluids for enhanced heat transfer," *Energy Conversion and Management*, vol. 100, pp. 419–428, 2015.

[92] S. Mohapatra, T. A. Nguyen, and P. Nguyen–Tri, *Noble Metal–Metal Oxide Hybrid Nanoparticles: Fundamentals and Applications*, Elsevier, Amsterdam, Netherlands, 2018.

[93] A. Ali, M. Z. Hira Zafar, M. Zia et al., "Synthesis, characterization, applications, and challenges of iron oxide nanoparticles," *Nanotechnology, Science and Applications*, vol. 9, pp. 49–67, 2016.

[94] S. S. Jyothirmayee Aravind and S. Ramaprabhu, "Graphene wrapped multiwalled carbon nanotubes dispersed nanofluids for heat transfer applications," *Journal of Applied Physics*, vol. 112, no. 12, p. 124304, 2012.

[95] B. Ma and D. Banerjee, "A review of nanofluid synthesis," *Advances in Nanomaterials*, Springer, Berlin, Germany, pp. 135–176, 2018.

[96] M. Chopkar, S. Kumar, D. R. Bhandari, P. K. Das, and I. Manna, "Development and characterization of Al_2Cu and Ag_2Al nanoparticle dispersed water and ethylene glycol based nanofluid," *Materials Science and Engineering: B*, vol. 139, no. 2-3, pp. 141–148, 2007.

[97] P. Van Trinh, N. N. Anh, B. H. Thang et al., "Enhanced thermal conductivity of nanofluid–based ethylene glycol containing Cu nanoparticles decorated on a Gr–MWCNT hybrid material," *RSC Advances*, vol. 7, no. 1, pp. 318–326, 2017.

[98] A. Aureen Albert, D. G. Harris Samuel, V. Parthasarathy, and K. Kiruthiga, "A facile one pot synthesis of highly stable PVA–CuO hybrid nanofluid for heat transfer application," *Chemical Engineering Communications*, vol. 207, no. 3, pp. 319–330, 2020.

[99] V. Kumar and J. Sarkar, "Research and development on composite nanofluids as next-generation heat transfer medium," *Journal of Thermal Analysis and Calorimetry*, vol. 137, no. 4, pp. 1133–1154, 2019.

[100] Ç Yıldız, M. Arıcı, and H. Karabay, "Comparison of a theoretical and experimental thermal conductivity model on the heat transfer performance of Al_2O_3-SiO_2/water hybrid-nanofluid," *International Journal of Heat and Mass Transfer*, vol. 140, pp. 598–605, 2019.

[101] C. J. Ho, J. B. Huang, P. S. Tsai, and Y. M. Yang, "On laminar convective cooling performance of hybrid water–based suspensions of Al_2O_3 nanoparticles and MEPCM particles in a circular tube," *International Journal of Heat and Mass Transfer*, vol. 54, no. 11-12, pp. 2397–2407, 2011.

[102] G. Huminic and A. Huminic, "Hybrid nanofluids for heat transfer applications–a state–of–the–art review," *International Journal of Heat and Mass Transfer*, vol. 125, pp. 82–103, 2018.

[103] J. Akram, N. S. Akbar, and D. Tripathi, "A theoretical investigation on the heat transfer ability of water-based hybrid (Ag–Au) nanofluids and Ag nanofluids flow driven by electroosmotic pumping through a microchannel," *Arabian Journal for Science and Engineering*, vol. 46, no. 3, pp. 2911–2927, 2021.

[104] M. Gupta, V. Singh, and Z. Said, "Heat transfer analysis using zinc Ferrite/water (Hybrid) nanofluids in a circular tube: an experimental investigation and development of new correlations for thermophysical and heat transfer properties," *Sustainable Energy Technologies and Assessments*, vol. 39, Article ID 100720, 2020.

[105] R. Pourrajab, A. Noghrehabadi, E. Hajidavalloo, and M. Behbahani, "Investigation of thermal conductivity of a new hybrid nanofluids based on mesoporous silica modified with copper nanoparticles: synthesis, characterization and experimental study," *Journal of Molecular Liquids*, vol. 300, Article ID 112337, 2020.

[106] S. Suresh, K. P. Venkitaraj, P. Selvakumar, and M. Chandrasekar, "Effect of Al_2O_3–Cu/water hybrid nanofluid in heat transfer," *Experimental Thermal and Fluid Science*, vol. 38, pp. 54–60, 2012.

[107] S. A. Mehryan, F. M. Kashkooli, M. Ghalambaz, and A. J. Chamkha, "Free convection of hybrid Al_2O_3–Cu water nanofluid in a differentially heated porous cavity," *Advanced Powder Technology*, vol. 28, no. 9, pp. 2295–2305, 2017.

[108] R. Taherialekouhi, S. Rasouli, and A. Khosravi, "An experimental study on stability and thermal conductivity of water–graphene oxide/aluminum oxide nanoparticles as a cooling hybrid nanofluid," *International Journal of Heat and Mass Transfer*, vol. 145, Article ID 118751, 2019.

[109] M. J. Nine, M. Batmunkh, J. H. Kim, H. S. Chung, and H. M. Jeong, "Investigation of Al_2O_3–MWCNTs hybrid dispersion in water and their thermal characterization," *Journal of Nanoscience and Nanotechnology*, vol. 12, no. 6, pp. 4553–4559, 2012.

[110] M. H. Esfe, S. Saedodin, M. Biglari, and H. Rostamian, "Experimental investigation of thermal conductivity of CNTs–Al_2O_3/water: a statistical approach," *International Communications in Heat and Mass Transfer*, vol. 69, pp. 29–33, 2015.

[111] M. Devarajan, N. Parasumanna Krishnamurthy, M. Balasubramanian et al., "Thermophysical properties of CNT and CNT/Al_2O_3 hybrid nanofluid," *Micro & Nano Letters*, vol. 13, no. 5, pp. 617–621, 2018.

[112] G. M. Moldoveanu, G. Huminic, A. A. Minea, and A. Huminic, "Experimental study on thermal conductivity of stabilized Al_2O_3 and SiO_2 nanofluids and their hybrid," *International Journal of Heat and Mass Transfer*, vol. 127, pp. 450–457, 2018.

[113] G. M. Moldoveanu, A. A. Minea, G. Huminic, and A. Huminic, "Al_2O_3/TiO_2 hybrid nanofluids thermal conductivity: an experimental approach," *Journal of Thermal Analysis and Calorimetry*, vol. 137, no. 2, pp. 583–592, 2019.

[114] V. V. Wanatasanapan, M. Z. Abdullah, and P. Gunnasegaran, "Effect of TiO_2–Al_2O_3 nanoparticle mixing ratio on the thermal conductivity, rheological properties, and dynamic viscosity of water–based hybrid nanofluid," *Journal of Materials Research and Technology*, vol. 9, no. 6, pp. 13781–13792, 2020.

[115] A. A. Minea, "Hybrid nanofluids based on Al_2O_3, TiO_2 and SiO_2: numerical evaluation of different approaches," *International Journal of Heat and Mass Transfer*, vol. 104, pp. 852–860, 2017.

[116] I. Wole–Osho, E. C. Okonkwo, H. Adun, D. Kavaz, and S. Abbasoglu, "An intelligent approach to predicting the effect of nanoparticle mixture ratio, concentration and temperature on thermal conductivity of hybrid nanofluids," *Journal of Thermal Analysis and Calorimetry*, vol. 144, no. 3, pp. 671–688, 2020.

[117] M. S. Kamel, O. Al-Oran, and F. Lezsovits, "Thermal conductivity of Al_2O_3 and CeO_2 nanoparticles and their hybrid based water nanofluids: an experimental study," *Periodica Polytechnica Chemical Engineering*, vol. 65, 2020.

[118] Z. Aparna, M. Michael, S. K. Pabi, and S. Ghosh, "Thermal conductivity of aqueous Al_2O_3/Ag hybrid nanofluid at different temperatures and volume concentrations: an experimental investigation and development of new correlation function," *Powder Technology*, vol. 343, pp. 714–722, 2019.

[119] M. A. Safi, A. Ghozatloo, N. M. Shariaty, and A. A. Hamidi, "Preparation of MWNT/TiO_2 nanofluids and study of its thermal conductivity and stability," *Iranian Journal of Chemical Engineering (IJChE)*, vol. 11, pp. 3–9, 2014.

[120] A. Karimipour, O. Malekahmadi, A. Karimipour, M. Shahgholi, and Z. Li, "Thermal conductivity enhancement via synthesis produces a new hybrid mixture composed of copper oxide and multi–walled carbon nanotube dispersed in water: experimental characterization and artificial neural network modeling," *International Journal of Thermophysics*, vol. 41, no. 8, pp. 116–127, 2020.

[121] M. Zadkhast, D. Toghraie, and A. Karimipour, "Developing a new correlation to estimate the thermal conductivity of MWCNT–CuO/water hybrid nanofluid via an experimental investigation," *Journal of Thermal Analysis and Calorimetry*, vol. 129, no. 2, pp. 859–867, 2017.

[122] S. K. Verma, A. K. Tiwari, S. Tiwari, and D. S. Chauhan, "Performance analysis of hybrid nanofluids in flat plate solar collector as an advanced working fluid," *Solar Energy*, vol. 167, pp. 231–241, 2018.

[123] S. Senthilraja, K. Vijayakumar, and R. Gangadevi, "A comparative study on thermal conductivity of Al_2O_3/water, CuO/water and Al_2O_3–CuO/water nanofluids," *Digest Journal of Nanomaterials and Biostructures*, vol. 10, no. 4, pp. 1449–1458, 2015.

[124] R. N. Ramachandran, K. Ganesan, and L. G. Asirvatham, "The role of hybrid nanofluids in improving the thermal characteristics of screen mesh cylindrical heat pipes," *Thermal Science*, vol. 20, no. 6, pp. 2027–2035, 2016.

[125] L. Megatif, A. Ghozatloo, A. Arimi, and M. Shariati–Niasar, "Investigation of laminar convective heat transfer of a novel TiO_2–carbon nanotube hybrid water–based nanofluid," *Experimental Heat Transfer*, vol. 29, no. 1, pp. 124–138.

[126] A. S. Dalkılıç, G. Yalçın, B. O. Küçükyıldırım et al., "Experimental study on the thermal conductivity of water–based CNT–SiO_2 hybrid nanofluids," *International Communications in Heat and Mass Transfer*, vol. 99, pp. 18–25, 2018.

[127] L. S. Sundar, M. K. Singh, and A. C. Sousa, "Turbulent heat transfer and friction factor of nanodiamond–nickel hybrid nanofluids flow in a tube: an experimental study," *International Journal of Heat and Mass Transfer*, vol. 117, pp. 223–234, 2018.

[128] S. M. Mousavi, F. Esmaeilzadeh, and X. P. Wang, "A detailed investigation on the thermo–physical and rheological behavior of MgO/TiO_2 aqueous dual hybrid nanofluid," *Journal of Molecular Liquids*, vol. 282, pp. 323–339, 2019.

[129] M. Batmunkh, M. R. Tanshen, M. J. Nine et al., "Thermal conductivity of TiO_2 nanoparticles based aqueous nanofluids with an addition of a modified silver particle," *Industrial & Engineering Chemistry Research*, vol. 53, no. 20, pp. 8445–8451, 2014.

[130] D. Madhesh, R. Parameshwaran, and S. Kalaiselvam, "Experimental investigation on convective heat transfer and rheological characteristics of Cu–TiO_2 hybrid nanofluids," *Experimental Thermal and Fluid Science*, vol. 52, pp. 104–115, 2014.

[131] J. A. Ranga Babu, K. Kumar, and S. Srinivasa Rao, "Thermodynamic analysis of hybrid nanofluid based solar flat plate collector," *World Journal of Engineering*, vol. 15, no. 1, pp. 27–39, 2018.

[132] A. Shahsavar, M. R. Salimpour, M. Saghafian, and M. B. Shafii, "An experimental study on the effect of ultrasonication on thermal conductivity of ferrofluid loaded with carbon nanotubes," *Thermochimica Acta*, vol. 617, pp. 102–110, 2015.

[133] A. Shahsavar, M. Saghafian, M. R. Salimpour, and M. B. Shafii, "Effect of temperature and concentration on thermal conductivity and viscosity of ferrofluid loaded with carbon nanotubes," *Heat and Mass Transfer*, vol. 52, no. 10, pp. 2293–2301, 2016.

[134] A. Shahsavar and M. Bahiraei, "Experimental investigation and modeling of thermal conductivity and viscosity for non–Newtonian hybrid nanofluid containing coated CNT/Fe_3O_4 nanoparticles," *Powder Technology*, vol. 318, pp. 441–450, 2017.

[135] L. Syam Sundar, A. C. M. Sousa, and M. K. Singh, "Heat transfer enhancement of low volume concentration of carbon nanotube–Fe_3O_4/water hybrid nanofluids in a tube with twisted tape inserts under turbulent flow," *Journal of Thermal Science and Engineering Applications*, vol. 7, no. 2, 2015.

[136] N. A. Che Sidik, M. Mahmud Jamil, W. M. A. Aziz Japar, and I. Muhammad Adamu, "A review on preparation methods, stability, and applications of hybrid nanofluids," *Renewable and Sustainable Energy Reviews*, vol. 80, pp. 1112–1122, 2017.

[137] A. Amiri, M. Shanbedi, H. Eshghi, S. Z. Heris, and M. Baniadam, "Highly dispersed multiwalled carbon nanotubes decorated with Ag nanoparticles in water and experimental investigation of the thermophysical properties," *Journal of Physical Chemistry C*, vol. 116, no. 5, pp. 3369–3375, 2012.

[138] L. Chen, W. Yu, and H. Xie, "Enhanced thermal conductivity of nanofluids containing Ag/MWNT composites," *Powder Technology*, vol. 231, pp. 18–20, 2012.

[139] M. Farbod and A. Ahangarpour, "Improved thermal conductivity of Ag decorated carbon nanotubes water–based nanofluids," *Physics Letters A*, vol. 380, no. 48, pp. 4044–4048, 2016.

[140] C. Sinz, H. Woei, M. Khalis, and S. A. Abbas, "Numerical study on turbulent force convective heat transfer of hybrid nanofluid, Ag/HEG in a circular channel with constant heat flux," *Journal of Advanced Research in Fluid Mechanics and Thermal Sciences*, vol. 24, no. 1, p. 1, 2016.

[141] H. Yarmand, S. Gharehkhani, S. F. S. Shirazi et al., "Study of synthesis, stability and thermo–physical properties of graphene nanoplatelet/platinum hybrid nanofluid," *International Communications in Heat and Mass Transfer*, vol. 77, pp. 15–21, 2016.

[142] N. Ahammed, L. G. Asirvatham, and S. Wongwises, "Entropy generation analysis of graphene–alumina hybrid nanofluid in multiport minichannel heat exchanger coupled with thermoelectric cooler," *International Journal of Heat and Mass Transfer*, vol. 103, pp. 1084–1097, 2016.

[143] E. C. Okonkwo, I. Wole–Osho, D. Kavaz, and M. Abid, "Comparison of experimental and theoretical methods of obtaining the thermal properties of alumina/iron mono and hybrid nanofluids," *Journal of Molecular Liquids*, vol. 292, Article ID 111377, 2019.

[144] G. Huminic, A. Huminic, F. Dumitrache, C. Fleacă, and I. Morjan, "Study of the thermal conductivity of hybrid nanofluids: recent research and experimental study," *Powder Technology*, vol. 367, pp. 347–357, 2020.

[145] A. A. Mahyari, A. Karimipour, and M. Afrand, "Effects of dispersed added graphene oxide–silicon carbide nanoparticles to present a statistical formulation for the mixture thermal properties," *Physica A: Statistical Mechanics and its Applications*, vol. 521, pp. 98–112, 2019.

[146] R. Pourrajab, A. Noghrehabadi, M. Behbahani, and E. Hajidavalloo, "An efficient enhancement in thermal conductivity of water–based hybrid nanofluid containing MWCNTs–COOH and Ag nanoparticles: experimental study," *Journal of Thermal Analysis and Calorimetry*, vol. 143, no. 5, pp. 3331–3343, 2020.

[147] P. Kanti, K. V. Sharma, R. Cg, and W. H. Azmi, "Experimental determination of thermophysical properties of Indonesian fly–ash nanofluid for heat transfer applications," *Particulate Science & Technology*, vol. 39, no. 5, pp. 597–606, 2020.

[148] P. Kanti, V. S. Korada, C. G. Ramachandra, and P. H. Sesha Talpa Sai, "Experimental study on density and thermal conductivity properties of Indian coal fly ash water-based nanofluid," *International Journal of Ambient Energy*, pp. 1–6, 2020.

[149] P. Kanti, K. V. Sharma, M. Revanasiddappa, C. G. Ramachandra, and S. Akilu, "Thermophysical properties of fly ash–Cu hybrid nanofluid for heat transfer applications," *Heat Transfer*, vol. 49, no. 8, pp. 4491–4510, 2020.

[150] N. N. Esfahani, D. Toghraie, and M. Afrand, "A new correlation for predicting the thermal conductivity of ZnO–Ag (50%–50%)/water hybrid nanofluid: an experimental study," *Powder Technology*, vol. 323, pp. 367–373, 2018.

[151] L. S. Sundar, G. O. Irurueta, E. Venkata Ramana, M. K. Singh, and A. C. Sousa, "Thermal conductivity, and viscosity of hybrid nanfluids prepared with magnetic nanodiamond–cobalt oxide (ND–Co_3O_4) nanocomposite," *Case Studies in Thermal Engineering*, vol. 7, pp. 66–77, 2016.

[152] L. S. Sundar, E. Venkata Ramana, M. P. Graça, M. K. Singh, and A. C. Sousa, "Nanodiamond–Fe_3O_4 nanofluids: preparation and measurement of viscosity, electrical and thermal conductivities," *International Communications in Heat and Mass Transfer*, vol. 73, pp. 62–74, 2016.

[153] L. Syam Sundar, S. Mesfin, E. Venkata Ramana, Z. Said, and A. C. Sousa, "Experimental investigation of thermo–physical properties, heat transfer, pumping power, entropy generation, and exergy efficiency of nanodiamond+ Fe_3O_4/60: 40% water–ethylene glycol hybrid nanofluid flow in a tube," *Thermal Science and Engineering Progress*, vol. 21, Article ID 100799, 2021.

[154] L. S. Sundar, M. K. Singh, E. V. Ramana, B. Singh, J. Grácio, and A. C. M. Sousa, "Enhanced thermal conductivity and viscosity of nanodiamond–nickel nanocomposite nanofluids," *Scientific Reports*, vol. 4, no. 1, p. 4039, 2014.

[155] L. R. d Oliveira, S. R. F. L. Ribeiro, M. H. M. Reis, V. L. Cardoso, and E. P. Bandarra Filho, "Experimental study on the thermal conductivity and viscosity of ethylene glycol –based nanofluid containing diamond–silver hybrid material," *Diamond and Related Materials*, vol. 96, pp. 216–230, 2019.

[156] L. Syam Sundar, M. K. Singh, M. C. Ferro, and A. C. Sousa, "Experimental investigation of the thermal transport properties of graphene oxide/Co_3O_4 hybrid nanofluids," *International Communications in Heat and Mass Transfer*, vol. 84, pp. 1–10, 2017.

[157] S. Rostami, A. A. Nadooshan, and A. Raisi, "An experimental study on the thermal conductivity of new antifreeze containing copper oxide and graphene oxide nano–additives," *Powder Technology*, vol. 345, pp. 658–667, 2019.

[158] M. U. Sajid and H. M. Ali, "Thermal conductivity of hybrid nanofluids: a critical review," *International Journal of Heat and Mass Transfer*, vol. 126, pp. 211–234, 2018.

[159] T. T. Baby and S. Ramaprabhu, "Experimental investigation of the thermal transport properties of a carbon nanohybrid dispersed nanofluid," *Nanoscale*, vol. 3, no. 5, pp. 2208–2214, 2011.

[160] T. T. Baby and S. Ramaprabhu, "Synthesis and nanofluid application of silver nanoparticles decorated graphene," *Journal of Materials Chemistry*, vol. 21, no. 26, pp. 9702–9709, 2011.

[161] T. T. Baby and R. Sundara, "Synthesis and transport properties of metal oxide decorated graphene dispersed nanofluids," *Journal of Physical Chemistry C*, vol. 115, no. 17, pp. 8527–8533, 2011.

[162] S. S. J. Aravind and S. Ramaprabhu, "Graphene–multiwalled carbon nanotube–based nanofluids for improved heat dissipation," *RSC Advances*, vol. 3, no. 13, pp. 4199–4206, 2013.

[163] R. Shende and R. Sundara, "Nitrogen doped hybrid carbon based composite dispersed nanofluids as working fluid for low–temperature direct absorption solar collectors," *Solar Energy Materials and Solar Cells*, vol. 140, pp. 9–16, 2015.

[164] M. H. Esfe, W. M. Yan, M. Akbari, A. Karimipour, and M. Hassani, "Experimental study on thermal conductivity of DWCNT–ZnO/water–EG nanofluids," *International Communications in Heat and Mass Transfer*, vol. 68, pp. 248–251, 2015.

[165] M. H. Esfe, S. Esfandeh, M. Afrand, M. Rejvani, and S. H. Rostamian, "Experimental evaluation, new correlation proposing and ANN modeling of thermal properties of EG based hybrid nanofluid containing ZnO–DWCNT nanoparticles for internal combustion engines applications," *Applied Thermal Engineering*, vol. 133, pp. 452–463, 2018.

[166] P. Sati, R. C. Shende, and S. Ramaprabhu, "An experimental study on thermal conductivity enhancement of DI water–EG based ZnO (CuO)/graphene wrapped carbon nanotubes nanofluids," *Thermochimica Acta*, vol. 666, pp. 75–81, 2018.

[167] I. Naiman, D. Ramasamy, and K. Kadirgama, "Experimental and one–dimensional investigation on nanocellulose and aluminium oxide hybrid nanofluid as a new coolant for radiator," *IOP Conference Series: Materials Science and Engineering*, vol. 469, no. 1, Article ID 012096, 2019.

[168] F. Benedict, A. Kumar, K. Kadirgama et al., "Thermal performance of hybrid–inspired coolant for radiator application," *Nanomaterials*, vol. 10, no. 6, p. 1100, 2020.

[169] H. W. Xian, N. A. C. Sidik, and R. Saidur, "Impact of different surfactants and ultrasonication time on the stability and thermophysical properties of hybrid nanofluids," *International Communications in Heat and Mass Transfer*, vol. 110, Article ID 104389, 2020.

[170] K. A. Hamid, W. H. Azmi, M. F. Nabil, and R. Mamat, "Improved thermal conductivity of TiO_2–SiO_2 hybrid nanofluid in ethylene glycol and water mixture," *IOP Conference Series: Materials Science and Engineering*, vol. 257, pp. 1–7, Article ID 012067, 2017.

[171] K. A. Hamid, W. H. Azmi, M. F. Nabil, and R. Mamat, "Experimental investigation of nanoparticle mixture ratios on TiO_2–SiO_2 nanofluids heat transfer performance under turbulent flow," *International Journal of Heat and Mass Transfer*, vol. 118, pp. 617–627, 2018.

[172] M. F. Nabil, W. H. Azmi, K. A. Hamid, and R. Mamat, "Heat transfer and friction factor of composite TiO_2–SiO_2 nanofluids in water–ethylene glycol (60: 40) mixture," *IOP Conference Series: Materials Science and Engineering*, vol. 257, no. 1, Article ID 012066, 2017.

[173] M. F. Nabil, W. H. Azmi, K. Abdul Hamid, R. Mamat, and F. Y. Hagos, "An experimental study on the thermal conductivity and dynamic viscosity of TiO_2–SiO_2 nanofluids in water: ethylene glycol mixture," *International Communications in Heat and Mass Transfer*, vol. 86, pp. 181–189, 2017.

[174] A. Moradi, M. Zareh, M. Afrand, and M. Khayat, "Effects of temperature and volume concentration on thermal conductivity of TiO_2–MWCNTs (70–30)/EG–water hybrid nano–fluid," *Powder Technology*, vol. 362, pp. 578–585, 2020.

[175] Y. Li, I. Moradi, M. Kalantar, E. Babadi, O. Malekahmadi, and A. Mosavi, "Synthesis of new dihybrid nanofluid of TiO_2/MWCNT in water–ethylene glycol to improve mixture thermal performance: preparation, characterization, and a novel correlation via ANN based on orthogonal distance regression algorithm," *Journal of Thermal Analysis and Calorimetry*, vol. 144, no. 6, pp. 2587–2603, 2021.

[176] K. Y. Leong, I. Razali, K. Ku Ahmad, H. C. Ong, M. J. Ghazali, and M. R. Abdul Rahman, "Thermal conductivity of an ethylene glycol/water–based nanofluid with copper–titanium dioxide nanoparticles: an experimental approach," *International Communications in Heat and Mass Transfer*, vol. 90, pp. 23–28, 2018.

[177] M. Sandhya, D. Ramasamy, K. Sudhakar, K. Kadirgama, and W. S. Harun, "Enhancement of the heat transfer in radiator with louvered fin by using Graphene-based hybrid nanofluids," *InIOP Conference Series: Materials Science and Engineering*, vol. 1062, no. 1, Article ID 012014, 2021.

[178] M. Amiri, S. Movahedirad, and F. Manteghi, "Thermal conductivity of water and ethylene glycol nanofluids containing new modified surface SiO_2–Cu nanoparticles: experimental and modeling," *Applied Thermal Engineering*, vol. 108, pp. 48–53, 2016.

[179] M. S. Tahat and A. C. Benim, "Experimental analysis on thermophysical properties of Al_2O_3/CuO hybrid nano fluid with its effects on flat plate solar collector," *Defect and Diffusion Forum*, vol. 374, pp. 148–156, 2017.

[180] H. Bagheri and A. Ahmadi Nadooshan, "The effects of hybrid nano–powder of zinc oxide and multi walled carbon nanotubes on the thermal conductivity of an antifreeze," *Physica E: Low-dimensional Systems and Nanostructures*, vol. 103, pp. 361–366, 2018.

[181] A. Kakavandi and M. Akbari, "Experimental investigation of thermal conductivity of nanofluids containing of hybrid nanoparticles suspended in binary base fluids and propose a new correlation," *International Journal of Heat and Mass Transfer*, vol. 124, pp. 742–751, 2018.

[182] R. Vidhya, T. Balakrishnan, and B. Suresh Kumar, "Investigation on thermophysical properties and heat transfer performance of heat pipe charged with binary mixture based ZnO-MgO hybrid nanofluids," *Materials Today Proceedings*, vol. 37, pp. 3423–3433, 2021.

[183] M. R. Safaei, R. Ranjbarzadeh, A. Hajizadeh, M. Bahiraei, M. Afrand, and A. Karimipour, "Simultaneous effects of cobalt ferrite and silica nanoparticles on the thermal conductivity of antifreeze: new hybrid nanofluid for refrigeration condensers," *International Journal of Refrigeration*, vol. 102, 2018.

[184] R. R. Sahoo and J. Sarkar, "Heat transfer performance characteristics of hybrid nanofluids as coolant in louvered fin automotive radiator," *Heat and Mass Transfer*, vol. 53, no. 6, pp. 1923–1931, 2017.

[185] G. Paul, J. Philip, B. Raj, P. K. Das, and I. Manna, "Synthesis, characterization, and thermal property measurement of nano–Al95Zn05 dispersed nanofluid prepared by a two–step process," *International Journal of Heat and Mass Transfer*, vol. 54, no. 15-16, pp. 3783–3788, 2011.

[186] S. F. Seyed Shirazi, S. Gharehkhani, H. Yarmand, A. Badarudin, H. S. Cornelis Metselaar, and S. N. Kazi, "Nitrogen doped activated carbon/graphene with high nitrogen level: green synthesis and thermo–electrical properties of its nanofluid," *Materials Letters*, vol. 152, pp. 192–195, 2015.

[187] T. Theres BabyR. Sundara, "Synthesis of silver nanoparticle decorated multiwalled carbon nanotubes–graphene mixture and its heat transfer studies in nanofluid," *AIP Advances*, vol. 3, no. 1, Article ID 012111, 2013.

[188] A. Parsian and M. Akbari, "New experimental correlation for the thermal conductivity of ethylene glycol containing Al_2O_3–Cu hybrid nanoparticles," *Journal of Thermal Analysis and Calorimetry*, vol. 131, no. 2, pp. 1605–1613, 2018.

[189] S. Sarboolookzadeh Harandi, A. Karimipour, M. Afrand, M. Akbari, and A. D'Orazio, "An experimental study on thermal conductivity of F–MWCNTs–Fe_3O_4/EG hybrid nanofluid: effects of temperature and concentration," *International Communications in Heat and Mass Transfer*, vol. 76, pp. 171–177, 2016.

[190] M. Vafaie and M. Afrand, "An experimental investigation on effect of hybrid solid MWCNTs and MgO on thermal conductivity of ethylene glycol," *Journal of Simulation and Analysis of Novel Technologies in Mechanical Engineering*, vol. 9, no. 3, pp. 431–440, 2016.

[191] M. Vafaei, M. Afrand, N. Sina, R. Kalbasi, F. Sourani, and H. Teimouri, "Evaluation of thermal conductivity of MgO–MWCNTs/EG hybrid nanofluids based on experimental data by selecting optimal artificial neural networks," *Physica E: Low-dimensional Systems and Nanostructures*, vol. 85, pp. 90–96, 2017.

[192] M. Afrand, "Experimental study on thermal conductivity of ethylene glycol containing hybrid nano–additives and development of a new correlation," *Applied Thermal Engineering*, vol. 110, pp. 1111–1119, 2017.

[193] M. H. Esfe, A. Alirezaie, and M. Rejvani, "An applicable study on the thermal conductivity of SWCNT–MgO hybrid nanofluid and price–performance analysis for energy management," *Applied Thermal Engineering*, vol. 111, pp. 1202–1210, 2017.

[194] M. H. Esfe, S. Esfandeh, M. K. Amiri, and M. Afrand, "A novel applicable experimental study on the thermal behavior of SWCNTs (60%)–MgO (40%)/EG hybrid nanofluid by focusing on the thermal conductivity," *Powder Technology*, vol. 342, pp. 998–1007, 2019.

[195] M. H. Esfe, A. A. Abbasian Arani, R. Shafiei Badi, and M. Rejvani, "ANN modeling, cost performance and sensitivity analyzing of thermal conductivity of DWCNT–SiO_2/EG hybrid nanofluid for higher heat transfer," *Journal of Thermal Analysis and Calorimetry*, vol. 131, no. 3, pp. 2381–2393, 2018.

[196] M. Hemmat Esfe, S. Esfandeh, and M. Rejvani, "Modeling of thermal conductivity of MWCNT–SiO_2 (30:70%)/EG hybrid nanofluid, sensitivity analyzing and cost performance for industrial applications," *Journal of Thermal Analysis and Calorimetry*, vol. 131, no. 2, pp. 1437–1447, 2018.

[197] X. Li, H. Wang, and B. Luo, "The thermophysical properties and enhanced heat transfer performance of SiC–MWCNTs hybrid nanofluids for car radiator system," *Colloids and Surfaces A: Physicochemical and Engineering Aspects*, vol. 612, Article ID 125968, 2021.

[198] A. A. A. Arani and F. Pourmoghadam, "Experimental investigation of thermal conductivity behavior of MWCNTS–Al_2O_3/ethylene glycol hybrid nanofluid: providing new thermal conductivity correlation," *Heat and Mass Transfer*, vol. 55, no. 8, pp. 2329–2339, 2019.

[199] M. Hemmat Esfe, S. Esfandeh, S. Saedodin, and H. Rostamian, "Experimental evaluation, sensitivity analyzation and ANN modeling of thermal conductivity of ZnO–MWCNT/EG–water hybrid nanofluid for engineering applications," *Applied Thermal Engineering*, vol. 125, pp. 673–685, 2017.

[200] D. Toghraie, V. A. Chaharsoghi, and M. Afrand, "Measurement of thermal conductivity of ZnO–TiO_2/EG hybrid nanofluid," *Journal of Thermal Analysis and Calorimetry*, vol. 125, no. 1, pp. 527–535, 2016.

[201] B. Jacob Rubasingh, P. Selvakumar, and R. S. Sanjay Raja, "Predicting thermal conductivity behaviour of ZnO, TiO_2 and ball milled TiO_2/ZnO based nanofluids with ethylene glycol as base fluid," *Materials Research Express*, vol. 6, no. 9, Article ID 095702, 2019.

[202] K. A. Hamid, W. H. Azmi, M. F. Nabil, R. Mamat, and K. V. Sharma, "Experimental investigation of thermal conductivity and dynamic viscosity on nanoparticle mixture ratios of TiO_2–SiO_2 nanofluids," *International Journal of Heat and Mass Transfer*, vol. 116, pp. 1143–1152, 2018.

[203] H. Yarmand, S. Gharehkhani, S. F. S. Shirazi et al., "Nanofluid based on activated hybrid of biomass carbon/graphene oxide: synthesis, thermo–physical and electrical properties," *International Communications in Heat and Mass Transfer*, vol. 72, pp. 10–15, 2016.

[204] S. Akilu, A. T. Baheta, and K. V. Sharma, "Experimental measurements of thermal conductivity and viscosity of ethylene glycol –based hybrid nanofluid with TiO_2–CuO/C inclusions," *Journal of Molecular Liquids*, vol. 246, pp. 396–405, 2017.

[205] A. M. Hussein, "Thermal performance and thermal properties of hybrid nanofluid laminar flow in a double pipe heat exchanger," *Experimental Thermal and Fluid Science*, vol. 88, pp. 37–45, 2017.

[206] S. Kannaiyan, C. Boobalan, A. Umasankaran, A. Ravirajan, S. Sathyan, and T. Thomas, "Comparison of experimental and calculated thermophysical properties of alumina/cupric oxide hybrid nanofluids," *Journal of Molecular Liquids*, vol. 244, pp. 469–477, 2017.

[207] M. Mehrali, E. Sadeghinezhad, A. R. Akhiani et al., "Heat transfer and entropy generation analysis of hybrid graphene/Fe_3O_4 ferro–nanofluid flow under the influence of a magnetic field," *Powder Technology*, vol. 308, pp. 149–157, 2017.

[208] E. Sadeghinezhad, M. Mehrali, A. R. Akhiani et al., "Experimental study on heat transfer augmentation of graphene based ferrofluids in presence of magnetic field," *Applied Thermal Engineering*, vol. 114, pp. 415–427, 2017.

[209] P. Van Trinh, N. N. Anh, N. T. Hong, P. N. Hong, P. N. Minh, and B. H. Thang, "Experimental study on the thermal conductivity of ethylene glycol –based nanofluid containing Gr–CNT hybrid material," *Journal of Molecular Liquids*, vol. 269, pp. 344–353, 2018.

[210] F. Amini, S. Z. Miry, A. Karimi, and M. Ashjaee, "Experimental investigation of thermal conductivity and viscosity of SiO_2/multiwalled carbon nanotube hybrid nanofluids," *Journal of Nanoscience and Nanotechnology*, vol. 19, no. 6, pp. 3398–3407, 2019.

[211] Z. H. Han, B. Yang, S. H. Kim, and M. R. Zachariah, "Application of hybrid sphere/carbon nanotube particles in nanofluids," *Nanotechnology*, vol. 18, no. 10, Article ID 105701, 2007.

[212] M. N. Chandran, S. Manikandan, K. S. Suganthi, and K. S. Rajan, "Novel hybrid nanofluid with tunable specific heat and thermal conductivity: characterization and performance assessment for energy related applications," *Energy*, vol. 140, pp. 27–39, 2017.

[213] N. N. Zawawi, W. H. Azmi, A. A. Redhwan, M. Z. Sharif, and K. V. Sharma, "Thermo–physical properties of Al_2O_3–SiO_2/PAG composite nanolubricant for refrigeration system," *international Journal of Refrigeration*, vol. 80, pp. 1–10, 2017.

[214] S. S. Botha, P. Ndungu, and B. J. Bladergroen, "Physicochemical properties of oil–based nanofluids containing hybrid structures of silver nanoparticles supported on silica," *Industrial & Engineering Chemistry Research*, vol. 50, no. 6, pp. 3071–3077, 2011.

[215] C. Choi, H. S. Yoo, and J. M. Oh, "Preparation and heat transfer properties of nanoparticle–in–transformer oil dispersions as advanced energy–efficient coolants," *Current Applied Physics*, vol. 8, no. 6, pp. 710–712, 2008.

[216] M. S. Kumar, V. Vasu, and A. V. Gopal, "Thermal conductivity and rheological studies for Cu–Zn hybrid nanofluids with various base fluids," *Journal of the Taiwan Institute of Chemical Engineers*, vol. 66, pp. 321–327, 2016.

[217] R. Larsson and O. Andersson, "Lubricant thermal conductivity and heat capacity under high pressure," *Proceedings of the Institution of Mechanical Engineers - Part J: Journal of Engineering Tribology*, vol. 214, no. 4, pp. 337–342, 2000.

[218] C. Perrier, A. Beroual, and J. L. Bessede, "Improvement of power transformers by using mixtures of mineral oil with synthetic esters," *IEEE Transactions on Dielectrics and Electrical Insulation*, vol. 13, no. 3, pp. 556–564, 2006.

[219] G. Colangelo, E. Favale, A. de Risi, and D. Laforgia, "Results of experimental investigations on the heat conductivity of nanofluids based on diathermic oil for high temperature applications," *Applied Energy*, vol. 97, pp. 828–833, 2012.

[220] B. Wu, R. G. Reddy, and R. D. Rogers, "Novel ionic liquid thermal storage for solar thermal electric power systems,"vol. 16702, pp. 445–451, in *Proceedings of the ASME 2001 Solar Engineering: International Solar Energy Conference (FORUM 2001: Solar Energy—The Power to Choose)*, vol. 16702, pp. 445–451, American Society of Mechanical Engineers (ASME), Washington, DC, USA, April 2001.

[221] S. Aberoumand and A. Jafarimoghaddam, "Tungsten (III) oxide (WO_3)–Silver/transformer oil hybrid nanofluid: preparation, stability, thermal conductivity and dielectric strength," *Alexandria Engineering Journal*, vol. 57, no. 1, pp. 169–174, 2018.

[222] B. Wei, C. Zou, X. Yuan, and X. Li, "Thermo–physical property evaluation of diathermic oil–based hybrid nanofluids for heat transfer applications," *International Journal of Heat and Mass Transfer*, vol. 107, pp. 281–287, 2017.

[223] A. Asadi, M. Asadi, A. Rezaniakolaei, L. A. Rosendahl, M. Afrand, and S. Wongwises, "Heat transfer efficiency of Al_2O_3–MWCNT/thermal oil hybrid nanofluid as a cooling fluid in thermal and energy management applications: an experimental and theoretical investigation," *International Journal of Heat and Mass Transfer*, vol. 117, pp. 474–486, 2018.

[224] A. Asadi, M. Asadi, A. Rezaniakolaei, L. A. Rosendahl, and S. Wongwises, "An experimental and theoretical investigation on heat transfer capability of Mg $(OH)_2$/MWCNT–engine oil hybrid nano–lubricant adopted as a coolant and lubricant fluid," *Applied Thermal Engineering*, vol. 129, pp. 577–586, 2018.

[225] M. Asadi, A. Asadi, and S. Aberoumand, "An experimental and theoretical investigation on the effects of adding hybrid nanoparticles on heat transfer efficiency and pumping power of an oil–based nanofluid as a coolant fluid," *International Journal of Refrigeration*, vol. 89, pp. 83–92, 2018.

[226] F. Soltani, D. Toghraie, and A. Karimipour, "Experimental measurements of thermal conductivity of engine oil–based hybrid and mono nanofluids with tungsten oxide (WO_3) and MWCNTs inclusions," *Powder Technology*, vol. 371, pp. 37–44, 2020.

[227] X. X. Tian, R. Kalbasi, C. Qi, A. Karimipour, and H. L. Huang, "Efficacy of hybrid nano–powder presence on the thermal conductivity of the engine oil: an experimental study," *Powder Technology*, vol. 369, pp. 261–269, 2020.

[228] M. Tahmasebi Sulgani and A. Karimipour, "Improve the thermal conductivity of 10w40-engine oil at various temperature by addition of Al_2O_3/Fe_2O_3 nanoparticles," *Journal of Molecular Liquids*, vol. 283, pp. 660–666, 2019.

[229] S. H. Qing, W. Rashmi, M. Khalid, T. C. S. M. Gupta, M. Nabipoor, and M. T. Hajibeigy, "Thermal conductivity and electrical properties of hybrid SiO_2–graphene naphthenic mineral oil nanofluid as potential transformer oil," *Materials Research Express*, vol. 4, no. 1, Article ID 015504, 2017.

[230] S. Askari, R. Lotfi, A. M. Rashidi, H. Koolivand, and M. Koolivand-Salooki, "Rheological and thermophysical properties of ultra–stable kerosene–based Fe_3O_4/Graphene nanofluids for energy conservation," *Energy Conversion and Management*, vol. 128, pp. 134–144, 2016.

[231] O. Gulzar, A. Qayoum, and R. Gupta, "Experimental study on thermal conductivity of mono and hybrid Al_2O_3– TiO_2 nanofluids for concentrating solar collectors," *International Journal of Energy Research*, vol. 45, no. 3, pp. 4370–4384, 2021.

[232] S. K. Mechiri, V. Vasu, S. B Babu, and A. Venu Gopal, "Thermal conductivity of Cu–Zn hybrid Newtonian nanofluids: experimental data and modeling using neural network," *Procedia Engineering*, vol. 127, pp. 561–567, 2015.

[233] S. K. Mechiri, V. Vasu, and A. Venu Gopal, "Investigation of thermal conductivity and rheological properties of vegetable oil-based hybrid nanofluids containing Cu–Zn hybrid nanoparticles," *Experimental Heat Transfer*, vol. 30, no. 3, pp. 205–217, 2017.

[234] R. Parameshwaran, K. Deepak, R. Saravanan, and S. Kalaiselvam, "Preparation, thermal and rheological properties of hybrid nanocomposite phase change material for thermal energy storage," *Applied Energy*, vol. 115, pp. 320–330, 2014.

[235] D. Zhao, M. Zuo, J. Leng, and H. Geng, "Synthesis and thermoelectric properties of $CoSb_3$/WO_3 thermoelectric composites," *Intermetallics*, vol. 40, pp. 71–75, 2013.

[236] J. Ramana Reddy, V. Sugunamma, and N. Sandeep, "Impact of nonlinear radiation on 3D magnetohydrodynamic flow of methanol and kerosene based ferrofluids with temperature dependent viscosity," *Journal of Molecular Liquids*, vol. 236, pp. 93–100, 2017.

[237] A. Alirezaie, M. H. Hajmohammad, M. R. Hassani Ahangar, and M. Hemmat Esfe, "Price–performance evaluation of thermal conductivity enhancement of nanofluids with different particle sizes," *Applied Thermal Engineering*, vol. 128, pp. 373–380, 2018.

[238] V. Kumar and R. R. Sahoo, "Viscosity and thermal conductivity comparative study for hybrid nanofluid in binary base fluids," *Heat Transfer-Asian Research*, vol. 48, no. 7, pp. 3144–3161, 2019.

[239] R. Bakhtiari, B. Kamkari, M. Afrand, and A. Abdollahi, "Preparation of stable TiO_2-Graphene/Water hybrid nanofluids and development of a new correlation for thermal conductivity," *Powder Technology*, vol. 385, pp. 466–477, 2021.

[240] K. Khanafer and K. Vafai, "A critical synthesis of thermophysical characteristics of nanofluids," *International Journal of Heat and Mass Transfer*, vol. 54, no. 19-20, pp. 4410–4428, 2011.

[241] H. C. Brinkman, "The viscosity of concentrated suspensions and solutions," *The Journal of Chemical Physics*, vol. 20, no. 4, p. 571, 1952.

[242] I. M. Krieger and T. J. Dougherty, "A mechanism for non-Newtonian flow in suspensions of rigid spheres," *Transactions of the Society of Rheology*, vol. 3, no. 1, pp. 137–152, 1959.

[243] T. S. Lundgren, "Slow flow through stationary random beds and suspensions of spheres," *Journal of Fluid Mechanics*, vol. 51, no. 2, pp. 273–299, 1972.

[244] G. K. Batchelor, "The effect of Brownian motion on the bulk stress in a suspension of spherical particles," *Journal of Fluid Mechanics*, vol. 83, no. 1, pp. 97–117, 1977.

[245] J. Bicerano, J. F. Douglas, and D. A. Brune, "Model for the viscosity of particle dispersions," *Journal of Macromolecular Science: Part C: Polymer Reviews*, vol. 39, no. 4, pp. 561–642, 1999.

[246] C. T. Nguyen, F. Desgranges, N. Galanis et al., "Viscosity data for Al_2O_3–water nanofluid—hysteresis: is heat transfer enhancement using nanofluids reliable?" *International Journal of Thermal Sciences*, vol. 47, no. 2, pp. 103–111, 2008.

[247] M. Sahu and J. Sarkar, "Steady-state energetic and exergetic performances of single-phase natural circulation loop with hybrid nanofluids," *Journal of Heat Transfer*, vol. 141, no. 8, 2019.

[248] J. C. Maxwell, *A Treatise on Electricity and Magnetism*, Clarendon Press, Oxford, UK, 1873.

[249] P. Keblinski, S. R. Phillpot, S. U. Choi, and J. A. Eastman, "Mechanisms of heat flow in suspensions of nano–sized particles (nanofluids)," *International Journal of Heat and Mass Transfer*, vol. 45, no. 4, pp. 855–863, 2002.

[250] J. A. Eastman, S. R. Phillpot, S. U. Choi, and P. Keblinski, "Thermal transport in nanofluids," *Annual Review of Materials Research*, vol. 34, no. 1, pp. 219–246, 2004.

[251] L. Rayleigh, "LVI. On the influence of obstacles arranged in rectangular order upon the properties of a medium," *The London, Edinburgh, and Dublin Philosophical Magazine and Journal of Science*, vol. 34, no. 211, pp. 481–502, 1892.

[252] R. L. Hamilton and O. K. Crosser, "Thermal conductivity of heterogeneous two–component systems," *Industrial & Engineering Chemistry Fundamentals*, vol. 1, no. 3, pp. 187–191, 1962.

[253] K. Pietrak and T. S. Wiśniewski, "A review of models for effective thermal conductivity of composite materials," *Journal of Power Technologies*, vol. 95, no. 1, pp. 14–24, 2014.

[254] D. J. Jeffrey, "Conduction through a random suspension of spheres," *Proceedings of the Royal Society of London. A. Mathematical and Physical Sciences*, vol. 335, no. 1602, pp. 355–367, 1973.

[255] R. H. Davis, "The effective thermal conductivity of a composite material with spherical inclusions," *International Journal of Thermophysics*, vol. 7, no. 3, pp. 609–620, 1986.

[256] S. Y. Lu and H. C. Lin, "Effective conductivity of composites containing aligned spheroidal inclusions of finite conductivity," *Journal of Applied Physics*, vol. 79, no. 9, pp. 6761–6769, 1996.

[257] R. T. Bonnecaze and J. F. Brady, "A method for determining the effective conductivity of dispersions of particles," *Proceedings of the Royal Society of London - Series A: Mathematical and Physical Sciences*, vol. 430, no. 1879, pp. 285–313, 1990.

[258] R. T. Bonnecaze and J. F. Brady, "The effective conductivity of random suspensions of spherical particles," *Proceedings of the Royal Society of London - Series A: Mathematical and Physical Sciences*, vol. 432, no. 1886, pp. 445–465, 1991.

[259] A. Valan Arasu, D. Dhinesh Kumar, and I. A. Khan, "Experimental validation of enhancement in thermal conductivity of titania/water nanofluid by the addition of silver nanoparticles," *International Communications in Heat and Mass Transfer*, vol. 120, Article ID 104910, 2021.

[260] S. Rostami, R. Kalbasi, M. Talebkeikhah, and A. S. Goldanlou, "Improving the thermal conductivity of ethylene glycol by addition of hybrid nano-materials containing multi-walled carbon nanotubes and titanium dioxide: applicable for cooling and heating," *Journal of Thermal Analysis and Calorimetry*, vol. 143, no. 2, pp. 1701–1712, 2021.

[261] I. P. Moghadam, M. Afrand, S. M. Hamad, A. A. Barzinjy, and P. Talebizadehsardari, "Curve-fitting on experimental data for predicting the thermal-conductivity of a new generated hybrid nanofluid of graphene oxide-titanium oxide/water," *Physica A: Statistical Mechanics and its Applications*, vol. 548, Article ID 122140, 2020.

[262] P. K. Kanti, K. V. Sharma, Z. Said, and M. Gupta, "Experimental investigation on thermo-hydraulic performance of water-based fly ash–Cu hybrid nanofluid flow in a pipe at various inlet fluid temperatures," *International Communications in Heat and Mass Transfer*, vol. 124, p. 105238, 2021.

[263] A. Kaggwa and J. K. Carson, "Developments and future insights of using nanofluids for heat transfer enhancements in thermal systems: a review of recent literature," *International Nano Letters*, vol. 9, no. 4, pp. 277–288, 2019.

[264] S. Yukta, P. Kunal, P. Rakesh, and C. Prathamesh, "Nanofluids with recent application & future trends," *International journal of innovations in engineering research and technology*, vol. 6, no. 8, pp. 458–468, 2021.

[265] A. Kamyar, R. Saidur, and M. Hasanuzzaman, "Application of computational fluid dynamics (CFD) for nanofluids," *International Journal of Heat and Mass Transfer*, vol. 55, no. 15-16, pp. 4104–4115, 2012.

[266] R. Saidur, K. Y. Leong, and H. A. Mohammed, "A review on applications and challenges of nanofluids," *Renewable and Sustainable Energy Reviews*, vol. 15, no. 3, pp. 1646–1668, 2011.

[267] S. D. Oduro, "Assessing the effect of blockage of dirt on engine radiator in the engine cooling system," *International Journal of Automotive Engineering*, vol. 2, no. 3, pp. 163–171, 2012.

[268] M. W. Wambsganss, "Thermal management concepts for higher–efficiency heavy vehicles," *Journal of Commercial Vehicles*, vol. 108, pp. 41–47, 1999.

[269] A. M. Hussein, R. A. Bakar, and K. Kadirgama, "Study of forced convection nanofluid heat transfer in the automotive cooling system," *Case Studies in Thermal Engineering*, vol. 2, pp. 50–61, 2014.

[270] S. A. Fadhilah, I. Hidayah, M. Z. Hilwa, H. N. Faizah, and R. S. Marhamah, "Thermophysical properties of Copper/Water nanofluid for automotive cooling system–Mathematical modeling," *Journal of Mechanical Engineering and Technology*, vol. 5, no. 2, 2013.

[271] F. Abbas, H. M. Ali, T. R. Shah et al., "Nanofluid: potential evaluation in automotive radiator," *Journal of Molecular Liquids*, vol. 297, Article ID 112014, 2020.

[272] W. X. Hong, N. C. Sidik, and M. Beriache, "Heat transfer performance of hybrid nanofluid as nanocoolant in automobile radiator system," *Journal of Advanced Research Design*, vol. 51, pp. 14–25, 2018.

[273] R. R. Sahoo, P. Ghosh, and J. Sarkar, "Performance analysis of a louvered fin automotive radiator using hybrid nanofluid as coolant," *Heat Transfer - Asian Research*, vol. 46, no. 7, pp. 978–995, 2017.

[274] J. A. Okello, W. N. Mutuku, and A. O. Oyem, "Analysis of ethylene glycol (EG)–based (($Cu–Al_2O_3$), ($Cu–TiO_2$), ($TiO_2–Al_2O_3$)) hybrid nanofluids for optimal car radiator coolant," *Journal of Engineering Research and Reports*, vol. 17, no. 2, pp. 34–50, 2020.

[275] S. K. Soylu, İ Atmaca, M. Asiltürk, and A. Doğan, "Improving heat transfer performance of an automobile radiator using Cu and Ag doped TiO_2 based nanofluids," *Applied Thermal Engineering*, vol. 157, Article ID 113743, 2019.

[276] V. Kumar and R. R. Sahoo, "Exergy and energy performance for wavy fin radiator with a new coolant of various shape nanoparticle–based hybrid nanofluids," *Journal of Thermal Analysis and Calorimetry*, vol. 143, no. 6, pp. 3911–3922, 2020.

[277] R. R. Sahoo, "Thermo–hydraulic characteristics of radiator with various shape nanoparticle–based ternary hybrid nanofluid," *Powder Technology*, vol. 370, pp. 19–28, 2020.

[278] R. P. Shankara, N. R. Banapurmath, A. D. Souza, and S. S. Dhaded, "Experimental investigation of enhanced cooling performance with the use of hybrid nanofluid for automotive application," *IOP Conference Series: Materials Science and Engineering*, vol. 872, no. 1, Article ID 012074, 2020.

[279] S. Ramalingam, R. Dhairiyasamy, and M. Govindasamy, "Assessment of heat transfer characteristics and system physiognomies using hybrid nanofluids in an automotive radiator," *Chemical Engineering and Processing–Process Intensification*, vol. 150, Article ID 107886, 2020.

[280] B. R. Bharadwaj, K. S. Mogeraya, D. M. Manjunath, B. R. Ponangi, K. R. Prasad, and V. Krishna, "CFD analysis of heat transfer performance of graphene–based hybrid nanofluid in radiators," *IOP Conference Series: Materials Science and Engineering*, vol. 346, no. 1, Article ID 012084, 2018.

[281] A. Karimi and M. Afrand, "Numerical study on thermal performance of an air–cooled heat exchanger: effects of hybrid nanofluid, pipe arrangement and cross section," *Energy Conversion and Management*, vol. 164, pp. 615–628, 2018.

[282] R. Jadar, K. S. Shashishekar, and S. R. Manohara, "Performance evaluation of Al–MWCNT based automobile radiator," *Materials Today Proceedings*, vol. 9, pp. 380–388, 2019.

[283] F. Abbas, H. M. Ali, M. Shaban et al., "Towards convective heat transfer optimization in aluminum tube automotive radiators: potential assessment of novel Fe_2O_3-TiO_2/water hybrid nanofluid," *Journal of the Taiwan Institute of Chemical Engineers*, vol. 124, pp. 424–436, 2021.

[284] B. Evans, "Nano-particle drag prediction at low Reynolds number using a direct Boltzmann–BGK solution approach," *Journal of Computational Physics*, vol. 352, pp. 123–141, 2018.

[285] S. Roy, R. Raju, H. F. Chuang, B. A. Cruden, and M. Meyyappan, "Modeling gas flow through microchannels and nanopores," *Journal of Applied Physics*, vol. 93, no. 8, pp. 4870–4879, 2003.

[286] T. Cele, M. Maaza, and A. Gibaud, "Synthesis of platinum nanoparticles by gamma radiolysis," *MRS Advances*, vol. 3, no. 42-43, pp. 2537–2557, 2018.

[287] M. Maaza, H. Chambalo, S. Ekambaram, O. Nemraoui, B. D. Ngom, and N. Manyala, "Pulsed laser liquid-solid interaction synthesis of Pt, Au, Ag and Cu nanosuspensions and their stability," *International Journal of Nanoparticles*, vol. 1, no. 3, pp. 212–223, 2008.

[288] M. Maaza, B. D. Ngom, S. Khamlich et al., "Valency control in MoO 3– δ nanoparticles generated by pulsed laser liquid solid interaction," *Journal of Nanoparticle Research*, vol. 14, no. 2, pp. 714–719, 2012.

[289] N. Kana, A. Galmed, T. Khamliche, K. Kaviyarasu, and M. Maaza, "Thermal conductivity enhancement in $MoO_3–H_2O$ nano-sheets based nano-fluids," *Materials Today Proceedings*, vol. 36, pp. 379–382, 2021.

[290] A. Riahi, S. Khamlich, M. Balghouthi et al., "Study of thermal conductivity of synthesized Al_2O_3-water nanofluid by pulsed laser ablation in liquid," *Journal of Molecular Liquids*, vol. 304, Article ID 112694, 2020.

[291] T. Khamliche, S. Khamlich, M. K. Moodley, B. M. Mothudi, M. Henini, and M. Maaza, "Laser fabrication of Cu nanoparticles based nanofluid with enhanced thermal conductivity: experimental and molecular dynamics studies," *Journal of Molecular Liquids*, vol. 323, Article ID 114975, 2021.

[292] M. C. Mbambo, S. Khamlich, T. Khamliche, B. M. Mothudi, and M. Maaza, "Pulsed Nd: YAG laser assisted fabrication of graphene nanosheets in water," *MRS Advances*, vol. 3, no. 42-43, pp. 2573–2580, 2018.

[293] M. C. Mbambo, M. J. Madito, T. Khamliche et al., "Thermal conductivity enhancement in gold decorated graphene nanosheets in ethylene glycol based nanofluid," *Scientific Reports*, vol. 10, no. 1, Article ID 14730, 2020.

[294] T. Khamliche, S. Khamlich, T. B. Doyle, D. Makinde, and M. Maaza, "Thermal conductivity enhancement of nanosilver particles dispersed ethylene glycol based nanofluids," *Materials Research Express*, vol. 5, no. 3, Article ID 035020, 2018.

[295] H. Chen, I. Botef, H. Zheng, M. Maaza, V. V. Rao, and V. V. Srinivasu, "Thermal conductivity and stability of nanosize carbon-black-filled PDMS: fuel cell perspective," *International Journal of Nanotechnology*, vol. 8, no. 6/7, pp. 437–445, 2011.

[296] H. M. Ali, *Hybrid Nanofluids for Convection Heat Transfer*, Academic Press, Cambridge, MA, USA, 2020.

[297] N. Muhammad, S. Nadeem, and M. T. Mustafa, "Analysis of ferrite nanoparticles in the flow of ferromagnetic nanofluid," *PLoS One*, vol. 13, no. 1, Article ID e0188460, 2018.

[298] T. Coquil, E. K. Richman, N. J. Hutchinson, S. H. Tolbert, and L. Pilon, "Thermal conductivity of cubic and hexagonal mesoporous silica thin films," *Volume 2: Theory and Fundamental Research; Aerospace Heat Transfer; Gas Turbine Heat Transfer; Computational Heat Transfer*, vol. 106, no. 3, Article ID 034910, 2009.

[299] J. Singh, R. Kumar, M. Gupta, and H. Kumar, "Thermal conductivity analysis of GO-CuO/DW hybrid nanofluid," *Materials Today Proceedings*, vol. 28, pp. 1714–1718, 2020.

[300] M. Zayan, A. K. Rasheed, A. John, S. Muniandi, and A. Faris, "Synthesis and characterization of novel ternary hybrid nanoparticles as thermal additives in H_2O," *Biological Science*, 2021.

[301] Z. Said, L. S. Sundar, H. Rezk, A. M. Nassef, H. M. Ali, and M. Sheikholeslami, "Optimizing density, dynamic viscosity, thermal conductivity, and specific heat of a hybrid nanofluid obtained experimentally via ANFIS-based model and modern optimization," *Journal of Molecular Liquids*, vol. 321, p. 114287, 2021.

[302] Z. L. Wang, D. W. Tang, S. Liu, X. H. Zheng, and N. Araki, "Thermal–conductivity and thermal–diffusivity measurements of nanofluids by 3ω method and mechanism analysis of heat transport," *International Journal of Thermophysics*, vol. 28, no. 4, pp. 1255–1268, 2007.

[303] T. Elango, A. Kannan, and K. Kalidasa Murugavel, "Performance study on single basin single slope solar still with different water nanofluids," *Desalination*, vol. 360, pp. 45–51, 2015.

[304] J. Roleček, Š Foral, K. Katovský, and D. Salamon, "A feasibility study of using CeO_2 as a surrogate material during the investigation of UO2 thermal conductivity enhancement," *Advances in applied ceramics*, vol. 116, no. 3, pp. 123–131, 2017.

[305] A. I. Khan, D. Dhinesh Kumar, and A. Valan Arasu, "Experimental investigation of thermal conductivity and stability of TiO_2-Ag/water nanocompositefluid with SDBS and SDS surfactants," *Thermochimica Acta*, vol. 678, Article ID 178308, 2019.

[306] B. Bakthavatchalam, K. Habib, R. Saidur, B. B. Saha, and K. Irshad, "Comprehensive study on nanofluid and ionanofluid for heat transfer enhancement: a review on current and future perspective," *Journal of Molecular Liquids*, vol. 305, Article ID 112787, 2020.

[307] S. M. Mousavi, F. Esmaeilzadeh, and X. P. Wang, "Effects of temperature and particles volume concentration on the thermophysical properties and the rheological behavior of $CuO/MgO/TiO_2$ aqueous ternary hybrid nanofluid," *Journal of Thermal Analysis and Calorimetry*, vol. 137, no. 3, pp. 879–901, 2019.

[308] X. Chen, D. Parker, M. H. Du, and D. J. Singh, "Potential thermoelectric performance of hole–doped Cu_2O," *New Journal of Physics*, vol. 15, no. 4, Article ID 043029, 2013.

[309] X. Xie, D. Li, T. H. Tsai, J. Liu, P. V. Braun, and D. G. Cahill, "Thermal conductivity, heat capacity, and elastic constants of water–soluble polymers and polymer blends," *Macromolecules*, vol. 49, no. 3, pp. 972–978, 2016.

[310] M. Kole and T. K. Dey, "Investigation of thermal conductivity, viscosity, and electrical conductivity of graphene based nanofluids," *Journal of Applied Physics*, vol. 113, no. 8, Article ID 084307, 2013.

[311] Z. Xing, W. Sun, L. Wang, Z. Yang, S. Wang, and G. Liu, "Size–controlled graphite nanoplatelets: thermal conductivity enhancers for epoxy resin," *Journal of Materials Science*, vol. 54, no. 13, pp. 10041–10054, 2019.

[312] I. Kazemi, M. Sefid, and M. Afrand, "Improving the thermal conductivity of water by adding mono & hybrid nano–additives containing graphene and silica: a comparative experimental study," *International Communications in Heat and Mass Transfer*, vol. 116, Article ID 104648, 2020.

[313] M. Shamaeil, M. Firouzi, and A. Fakhar, "The effects of temperature and volume fraction on the thermal conductivity of functionalized DWCNTs/ethylene glycol nanofluid," *Journal of Thermal Analysis and Calorimetry*, vol. 126, no. 3, pp. 1455–1462, 2016.

[314] X. Zeng, J. Sun, Y. Yao, R. Sun, J. B. Xu, and C. P. Wong, "A combination of boron nitride nanotubes and cellulose nanofibers for the preparation of a nanocomposite with high thermal conductivity," *ACS Nano*, vol. 11, no. 5, pp. 5167–5178, 2017.

[315] A. I. Ramadhan, W. H. Azmi, and R. Mamat, "Experimental investigation of thermo-physical properties of tri-hybrid nanoparticles in water-ethylene glycol mixture," *Walailak Journal of Science and Technology*, vol. 18, no. 8, pp. 9335–9415, 2021.

[316] R. Palanisamy, G. Parthipan, and S. Palani, "Study of synthesis, characterization and thermo physical properties of Al_2O_3-SiO_2-TiO_2/H_2O based tri-hybrid nanofluid," *Digest Journal of Nanomaterials & Biostructures (DJNB)*, vol. 16, no. 3, 2021.

[317] Y. Terada, K. Ohkubo, T. Mohri, and T. Suzuki, "Thermal conductivity of cobalt–base alloys," *Metallurgical and Materials Transactions A*, vol. 34, no. 9, pp. 2026–2028, 2003.

[318] M. H. Sharqawy, J. H. Lienhard, and S. M. Zubair, "Thermophysical properties of seawater: a review of existing correlations and data," *Desalination and Water Treatment*, vol. 16, no. 1–3, pp. 354–380, 2010.

[319] M. C. Mbambo, S. Khamlich, T. Khamliche et al., "Remarkable thermal conductivity enhancement in Ag—decorated graphene nanocomposites based nanofluid by laser liquid solid interaction in ethylene glycol," *Scientific Reports*, vol. 10, no. 1, pp. 10982–10984, 2020.

[320] R. Verma, H. N. Nagendra, S. Kasthurirengan, N. C. Shivaprakash, and U. Behera, "Thermal conductivity studies on activated carbon based cryopanel," *IOP Conference Series: Materials Science and Engineering*, vol. 502, no. 1, Article ID 012197, 2019.

[321] G. Sekrani and S. Poncet, "Ethylene- and propylene-glycol based nanofluids: a litterature review on their thermophysical properties and thermal performances," *Applied Sciences*, vol. 8, no. 11, p. 2311, 2018.

[322] C. Dang, K. Hoshika, and E. Hihara, "Effect of lubricating oil on the flow and heat–transfer characteristics of supercritical carbon dioxide," *International Journal of Refrigeration*, vol. 35, no. 5, pp. 1410–1417, 2012.

[323] M. Zamengo, J. Ryu, and Y. Kato, "Composite block of magnesium hydroxide–expanded graphite for chemical heat storage and heat pump," *Applied Thermal Engineering*, vol. 69, no. 1-2, pp. 29–38, 2014.

[324] S. Manikandan and K. S. Rajan, "MgO–Therminol 55 nanofluids for efficient energy management: analysis of transient heat transfer performance," *Energy*, vol. 88, pp. 408–416, 2015.